DOKUZ EYLÜL UNIVERSITY

GRADUATE SCHOOL OF NATURAL AND APPLIED SCIENCES

THE ROLE OF INTERFACES ON THE MECHANICAL PERFORMANCE OF FIBER REINFORCED POLYMER COMPOSITES

by

Kutlay SEVER

September, 2009

İZMİR

THE ROLE OF INTERFACES ON THE MECHANICAL PERFORMANCE OF FIBER REINFORCED POLYMER COMPOSITES

A Thesis Submitted to the
Graduate School of Natural and Applied Sciences of Dokuz Eylül University
In Partial Fulfilment of the Requirements for the Degree of Doctor of Philosophy in Mechanical Engineering, Design and Production Program

by

Kutlay SEVER

September, 2009

İZMİR

Ph.D. THESIS EXAMINATION RESULT FORM

We have read the thesis entitled **"THE ROLE OF INTERFACES ON THE MECHANICAL PERFORMANCE OF FIBER REINFORCED POLYMER COMPOSITES"** completed by **KUTLAY SEVER** under supervision of **Prof.Dr.İSMAİL HAKKI TAVMAN** and we certify that in our opinion it is fully adequate, in scope and in quality, as a thesis for the degree of Doctor of Philosophy.

Prof.Dr. İsmail Halkı TAVMAN

Supervisor

Assoc. Prof. Hasan YILDIZ	Assist. Prof. Aylin ALBAYRAK
Thesis Committee Member	Thesis Committee Member
Examining Committee Member	Examining Committee Member
Examining Committee Member	Examining Committee Member

Prof.Dr. Cahit HELVACI
Director
Graduate School of Natural and Applied Sciences

ACKNOWLEDGMENTS

First of all, I wish to express my deepest gratitude and thanks to Professor Dr. İsmail Hakkı Tavman, my major advisor professor, for providing the motivation of this study and for his guidance, patience and thoughtful opinions throughout the course of this study.

I would like to acknowledge all the contributions and invaluable advice Professor Dr. Mehmet Mutlu, my second advisor professor, provided during my research studies. I would like to thank Assoc. Prof. Dr. Hasan Yıldız and Assoc. Prof. Dr. İsmail Özdemir for their help with valuable suggestions and discussions during periodical meetings of this study.

I would like to thank Assistant Professor Dr. Mehmet Sarıkanat, Dr. Yoldaş Seki and Dr. Hacı Ali Güleç who provided valuable support, including use of equipment, discussion and encouragement during my study.

I would also like to express my appreciation for the financial support of Research Foundation of Dokuz Eylül University (project no: 2007.KB.FEN.007).

Finally, I wish to express sincere thanks to my family, my wife Kader Sever and my parents Şaban and Yadigar Sever for their endless love and support in enabling me to complete this study.

Kutlay SEVER

THE ROLE OF INTERFACES ON THE MECHANICAL PERFORMANCE OF FIBER REINFORCED POLYMER COMPOSITES

ABSTRACT

In this study, structure of -gamma-GPS (-gamma-glycidoxypropyltrimethoxysilane) on glass surfaces after fiber surface treatments was analyzed and effects of the treatments on mechanical properties of glass fiber/epoxy composites were investigated. Fiber surface treatments were used to create the beneficial interface between the fiber and the matrix. Glass fibers were treated using wet chemical and plasma polymerization processes to improve the interfacial adhesion between fiber and matrix.

The structure of -gamma-GPS on glass surfaces after wet chemical and plasma polymerization processes and the interaction between glass surface and -gamma-GPS were examined using Fourier Transform Infrared Spectroscopy (FT-IR), contact angle measurement device and Scanning Electron Microscopy (SEM). The influence of plasma power and exposure time on the properties of thin films prepared by plasma polymerization of -gamma-GPS on the glass surfaces was also investigated by X-ray Photo-electron Spectroscopy (XPS). XPS analyses were utilized to reveal the presence of functional groups in the films. Morphologies of the films on the glass surfaces were observed by Atomic Force Microscopy (AFM) and SEM.

The effects of fiber surface treatments on mechanical properties of glass fiber/epoxy composites were investigated. Mechanical properties of the composites were investigated by tensile tests, flexural tests and short beam shear tests. The fracture surfaces of the composites were observed with SEM. Mechanical properties of the composites were improved by wet chemical and plasma polymerization studies.

Keywords: Glass fiber, Plasma polymerization, Silane treatment, Interface, Interfacial adhesion, Interlaminar shear strength

FİBER TAKVİYELİ POLİMER KOMPOZİTLERİN MEKANİK PERFORMANSINDA ARAYÜZEYİN ROLÜ

ÖZ

Bu çalışmada, fiber yüzey işlemlerinden sonra cam yüzeylerindeki -gamma-GPS (-gamma-glycidoxypropyltrimethoxysilan)'ın yapısı analiz edildi ve cam elyaf/epoksi kompozitlerin mekanik özellikleri üzerinde yüzey işlemlerinin etkileri incelendi. Fiber yüzey işlemleri fiber ve matris arasında faydalı bir arayüzey oluşturmak için kullanıldı. Fiber ve matris arasındaki arayüzeysel yapışmayı geliştirmek için cam elyaflar kimyasal ve plazma polimerizasyon yöntemleri kullanılarak yüzey işlemine tabi tutuldu.

Kimyasal ve plazma polimerizasyon işlemlerinden sonra cam yüzeylerindeki -gamma-GPS'in yapısı ve cam yüzeyi ve -gamma-GPS arasındaki etkileşim Fourier Transform Infrared Spektrometre (FT-IR), temas açısı ölçüm cihazı ve taramalı elektron mikroskobu (SEM) kullanılarak incelendi. Cam yüzeylerinde -gamma-GPS'in plazma polimerizasyonu ile hazırlanan ince filmlerin özellikleri üstünde plazma gücünün ve maruz kalma zamanının etkisi X-ışını Fotoelektron Spektroskopisi (XPS) ile incelendi. Filmlerdeki fonksiyonel grupların varlığını ortaya çıkarmak için XPS analizlerinden yararlanıldı. Cam yüzeylerindeki filmlerin morfolojileri atomik kuvvet mikroskobu (AFM) ve SEM ile incelendi.

Cam elyaf/epoksi kompozitlerin mekanik özellikleri üzerinde fiber yüzey işlemlerinin etkisi incelendi. Kompozitlerin mekanik özellikleri çekme, eğilme ve kısa kirişle kayma testleri ile incelenmiştir. Kompozitlerin kırılma yüzeyleri ayrıca SEM ile incelendi. Kompozitlerin mekanik özellikleri kimyasal ve plazma polimerizasyon işlemleri ile geliştirildi.

Anahtar sözcükler: Cam elyaf, Plazma polimerizasyon, Silan yüzey işlemi, Arayüzey, Arayüzeysel yapışma, Tabakalar arası kayma mukavemeti

CONTENTS

Page

CHAPTER ONE
INTRODUCTION

1.1 Introduction

In recent years, the demand for fiber-reinforced polymeric composites in aircraft, automobiles, ships, and housing has been increasing. There is considerable interest in composite materials of plastics reinforced with high strength fibers such as glass. Glass is predominantly the most important and widely used fiber in reinforced plastics (Murphy, 2001). Approximately 95% of composites used today are fabricated from glass fibers, with epoxy resin being the preferred polymeric matrix because of the relatively good price-to-performance ratio, high availability, ease of processing, and dimensional stability (Feresenbet, Raghavan, & Holmes, 2003).

Composite materials are composed of two or more components that differ in physical and chemical properties to provide desirable characteristics (Park & Jin, 2003). Fiber reinforced polymer composites have three components: fiber, matrix, and interface (Rot, Huskić, Makarovič, Ljubič Mlakar, & Žigon, 2001). The interface presents a transition region of which properties vary continuously between the fiber and the matrix (Kim, Sham, & Wu, 2001). Interfaces in composites form in the vicinity of fiber surfaces and may exhibit significantly different material characteristics than the bulk resin properties. The chemical composition, as well as the microstructure, of the material at the interphase region mainly controls the properties of the interphase. The thickness of the interphase ranges from 1 to 1000 nanometers depending on materials, sizing and process conditions (Tanoglu, McKnight, Palmese, & Gillespie, 2001).

The properties of a composite material depend on the behavior of its constituent parts as well as that of the interfaces between reinforcement and matrix. Strength, toughness, fatigue resistance, and the life expectancy of the composite are particularly sensitive to the stability and strength of the interfaces (DiBenedetto, 1985). The properties of composites depend on the ability of the interface to transfer

stress from the matrix to the reinforcement (González-Benito, 2003). Since the fiber–matrix interface transfers stress between the fiber and matrix, the efficiency of this stress-transfer process and a composite's strength and durability are controlled by this region's properties (Feresenbet, Raghavan, & Holmes, 2003).

It is generally believed that the weakest portion of glass fiber reinforced plastics is the fiber/matrix interface, particularly as concerns water susceptibility (Ishida & Koenig, 1978). The fiber surface attracted water, resulting in much loss of strength for polymer composites. In severe cases, the water leached ions from the glass, and the ionic solutions created in the interface regions developed osmotic pressure. This pressure caused the spalling of surface layers, seriously damaging structures such as boat hulls (Piggott, 1997).

There is a need for appropriate methods to assess changes in the strength and stability of the interface. Surface treatments are used to create the beneficial interface between the composite constituents. Before being used as reinforcing elements of advanced composites, the fibers are subjected to surface treatment, undertaken to prevent any fiber damage under contact with processing equipment, to provide surface wetting when the fibers are combined with matrix materials and to improve the interface bond between fibers and matrices (Vasiliev &. Morozov, 2007).

When using surface modification techniques such as silane treatments or plasma techniques (plasma treatment, plasma polymerization), compatibility between inorganic fillers and polymer matrices can improve. In industry, silane coupling agents by wet-chemical process are applied for surface modification of glass reinforcements (fibers, particles) in order to form a functional interlayer. The silane molecule is a multifunctional one, which reacts at one end with the glass surface and at the other with the polymer matrix (Park & Jin, 2003; Zhao & Takeda, 2000; Wang, Blum, & Dharani, 1999; Saidpour & Richardson, 1997; Park & Jin, 2001; Prikryl, Cech, Kripal, & Vanek, 2005; Cech et al., 2006). Plasma surface treatment and plasma polymerization as an alternative coating techniques have been mainly

used for surface modification of fibers (Cech, Prikryl, Balkova, Vanek, & Grycova, 2003; Li , Ye, & Mai, 1997).

1.2 Background

1.2.1 Silane Treatments

Several researchers studied various silane coupling agents and sizing to understand their effects on the interface formation and composite mechanical behavior.

Kim, Sham, & Wu (2001) characterised the properties of the interphase formed between glass fiber and polymer resin. The variation of interphase thickness affected by differing silane coupling agents is specially evaluated. The effective interphase thickness values varied in the range between 0.8 and 1.5 μm depending on the type and concentration of silane agent. The effective interphase thickness increased with increasing silane concentration.

Park & Jin (2003) reported the effect of silane coupling agent concentration on the fiber-surface properties and the resulting mechanical interfacial behavior of the composites in terms of the surface energetics of fibers and the fracture toughness of composites. A silane coupling agent, γ-methacryloxypropyltrimethoxysilane (γ-MPS), was varied between 0.1 and 0.8 wt%. Both the surface free energy and mechanical interfacial properties are shown in a maximum value in the presence of 0.4 wt% silane coupling agent.

Park & Jin (2001) examined the surface treatment of glass fibers with different concentrations to improve the interfacial adhesion at interfaces between fibers and matrix. They used the γ-methacryloxypropyltrimethoxysilane (γ-MPS) (90%) containing γ-aminopropyltriethoxysilane (γ-APS) (10%) for the surface treatment of glass fibers. From the experimental results, the presence of coupling agent does lead to an increase of interlaminar shear strength (ILSS) of the composites, which can be

related to the effect of increasing the degree of adhesion at interfaces among the three elements, i.e., fiber, matrix, and silane coupling agent. On the basis of experimental results, it was also reported that the mechanical interfacial properties of the composites decrease due to excess silane layer physisorbed onto the glass fiber at a given higher silane coupling agent concentration.

Park & Jang (2004) investigated the effect of the surface treatment of the glass fiber on the mechanical properties of glass fiber/vinyl ester composites. They observed that the values of the flexural strength and the interlaminar shear strength (ILSS) of MPS-treated glass fiber/vinyl ester composites increase to a 0.3% silane concentration and then decrease smoothly after the maximum point. Their results indicate that physically sorbed MPS layers are formed on the chemisorbed layer by an excess amount above 0.3% concentration. This layer acts as a lubricant or deformable layer. In case of excess silane concentration, the silane coupling agent is not always formed in hydrogen bonding with the glass fiber, due to the thick layer formed. Therefore, the fibers treated with excess silane concentration demonstrate the silane characteristics in nature, resulting from increasing the intermolecular equilibrium distance between fibers and silane or not exhibiting the specific component of surface free energy in a silane characteristic (Park, 1999).

Iglesias, González-Benito, Aznar, Bravo, & Baselga (2002) observed the influence of different aminosilanes fiber coatings on the resistance of epoxy-based composite materials. They concluded that the mechanical properties of glass fiber/epoxy composites are strongly dependent on the molecular structure of the coupling region. It has been suggested that an interpenetrating network mechanism seems to be the most important contribution to the adhesion and therefore to interfacial strength.

Zhou, Wagner, & Nutt (2001) investigated the interfacial properties for E glass/epoxy composites. Fibers treated with γ-APS showed higher bond strength (~1.7 times higher) and interfacial toughness ((~1.9 times higher) than those of unsized E glass based composites.

An investigation has been made on effects of fiber surface treatments on transverse mechanical behaviour of unidirectional glass/epoxy composites by Benzarti, Cangemi & Dal Maso (2001). Ultimate properties of composites in transverse tension depend on fiber surface treatment. The most reactive sizings lead to a significant improvement of the transverse performance of laminates. It has been shown that interfacial shear strength depends on the reactivity/functionality of the fiber sizing.

Nguyen., Byrd, Alshed, Aouadi, & Chin (1998) reported the role of the polymer/substrate interfacial water layer on the shear strength of glass fiber reinforced polymer matrix composites. Little water was observed at the interface of the silane treated specimens, but 10 monolayers of water accumulated at the epoxy/substrate interface of the untreated samples after exposure to water. Shear strength loss of the untreated composite was twice that of the silane treated materials after a 3 month immersion in 60 ^{o}C water. Further, the treated specimens remained transparent but the untreated specimens became opaque after water exposure. Evidence from mechanical and spectroscopic analyses and visual observation indicated that water at the polymer/fiber interface was responsible for the difference in the loss of the shear strength of the untreated and surface treated composites. They emphasized that untreated glass fiber/epoxy bonds are weak and cannot resist the displacement by water when the composites are exposed to aqueous environment. To prevent water from entering the polymer/fiber interface, surface treatment must be used.

Noobut & Koenig (1999) indicated the interfacial behavior of glass fiber/epoxy microcomposites under cycles of wet and dry environment change by FT-IR. The adsorbed water content in the fiber/epoxy interphase under moist conditions was reduced by treating the glass fibers with a silane coupling agent, γ-APS. Also, there was indication of slow debonding in the silane treated fiber/epoxy interphases relative to that of the heat cleaned fiber/epoxy interphase. Chemical bonds established through the silane coating prevent moisture penetration at the interface, that is, finishes are effective against molecular water penetration by diffusion along

the glass–resin interface. Water absorption does not seriously affect the ILSS. Once water reaches the interface, the siloxane bonds between the silane coupling agent and the glass surface are easily hydrolyzed. In contrast, weaker adhesion provides more pathways to the water and allows more water to be absorbed by the composite (Pavlidou, Krassa, & Papaspyrides, 2005).

González-Benito, Baselga, & Aznar (1999) studied the influence of different activation pretreatments of glass fibers on the structure of an aminosilane coupling agent (γ-APS) layer. On the basis of experimental results, it was reported that the acid activation of glass fibers greatly changes the surface composition and the hydration state of the glass. They found that the degree of silanization is the greatest for the acid activated samples and the lowest for the water activated one. In the other work performed by González-Benito et al. (1996), glass fibers have been treated with γ-aminopropyltriethoxysilane (APES) through different silanizating procedures, which include APES aqueous solutions and APES vapor adsorption. They found that silanization by APES vapor adsorption gives a place to polymer coats with a crosslinking degree that may be a function of treatment time.

1.2.2 Plasma Polymerization Treatments

Many researchers studied different monomer to understand effects of plasma polymer films on the interface formation and mechanical properties of composites.

Cech, Prikryl, Balkova, Vanek, & Grycova (2003) investigated the interphase properties of the glass/polyester system after plasma or wet chemical process. Plasma-polymerized thin films of organosilicon monomers (hexamethyldisiloxane and γ-vinyltriethoxysilane (γ-VTES)) were deposited in an RF helical coupling plasma system on the glass surface. Also, γ-VTES was coated onto an unmodifed glass surface from an aqueous solution. The results revealed that the adhesion bonding could be controlled by plasma process parameters. Their study indicated that the performance of the glass fiber/polyester composite with the fibers modified by pp-VTES was the best within plasma modifications, and the short-beam strength was

110% higher than that for untreated fibers as well as for glass fibers modified by VTES aqueous solution. Cech et al. (2006) characterized plasma-polymerized and polycondensed thin films of γ-VTES on planar glass substrates and glass fibers. They reported that the physicochemical properties of the polycondensed films were invariable, while those of the plasma-polymerized films could be varied in relatively wide ranges by altering the deposition conditions. In contrast to polycondensed films, the pp-VTES films were homogeneous and thus more suitable. In the other work performed by Cech (2007), plasma polymer films of hexamethyldisiloxane, vinyltriethoxysilane (γ-VTES), and tetravinylsilane (γ-TVS) in a mixture with oxygen gas were engineered as compatible interlayers for the glass fiber/polyester composite. The optimized interlayer enabled a 6.5-fold increase of the short-beam strength compared to the untreated fibers. The short-beam strength of glass fiber/polyester composite with the pp-TVS/O_2 interlayer was 32% higher than that with industrial sizing developed for fiber-reinforced composites with a polyester matrix. Cech, Studynka, Conte, & Perina (2007) deposited plasma polymer films of tetravinylsilane on silicon wafers using an RF glow discharge operated in pulsed mode. They reported that an organic/inorganic character (C/Si ratio) of films and a content of vinyl groups could be controlled by the effective power. Also, their results indicate that the elastic modulus and hardness could be varied from 11 GPa (0.05 W) to 30 GPa (10 W) and from 1.4 to 5.9 GPa for an increased power, respectively.

Cokeliler, Erkut, Zemek, Biederman, & Mutlu, (2007) used three different types of monomer, 2-hydroxyethyl methacrylate (HEMA), triethyleneglycoldimethylether (TEGDME) and ethylenediamine (EDA) in the plasma polymerization modification of glass fibers to improve the mechanical properties of the denture material, polymethylmethacrlyate (PMMA). Mechanical tests showed that flexural strength of PMMA can be improved by the coating of glass fibers in a glow-discharge system. The study also showed that the treatment of glass fibers with an amino group containing monomer such as EDA is an alternative method to maintain a higher strength of the dental material.

Liu, Zhao, & Jones (2008) coated E-glass fibers with a functional plasma polymer of 5-15 nm thickness, to provide the composites with a controlled interphase. Untreated and unsized E-glass fiber bundles were continuously coated with acrylic acid/1,7-octadiene and allylamine /1,7-octadiene plasma copolymers of various compositions to optimize the bond with matrix resin. The values of ILSS have been found to be a function of the coating chemistry and thickness. It was found that ILSS was high for the highest functional coating. However, with a coating of lower functionality, ILSS increased as the thickness of the coating decreased. ILSS data demonstrated that an interphase with high shear strength and of the thickness 2–5 nm is a crucial parameter.

1.3 Objectives of the Present Study

The first objective of this study is to analyze the structure of γ-glycidoxypropyltrimethoxysilane (γ-GPS) on glass substrates or glass fiber surfaces after wet chemical and plasma polymerization processes.

The second objective of this study is to investigate the effects of silane and plasma polymerization treatments of glass fibers on mechanical properties of glass fiber/epoxy composites.

CHAPTER TWO
COMPOSITE MATERIALS

2. 1 Definition and Characteristics of Composite Materials

A structural composite is a material system consisting of two or more phases on a macroscopic scale, whose mechanical performance and properties are designed to be superior to those of the constituent materials acting independently. One of the phases is usually discontinuous, stiffer, and stronger and is called reinforcement, whereas the less stiff and weaker phase is continuous and is called matrix (Figure 2.1). Sometimes, because of chemical interactions or other processing effects, an additional phase, called interphase, exists between the reinforcement and the matrix (Daniel & Ishai, 1994).

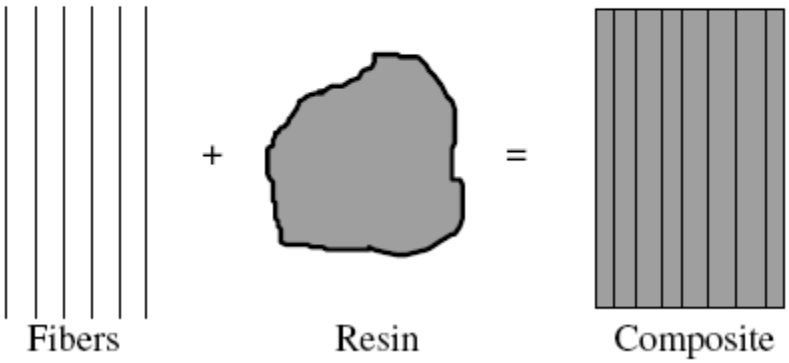

Figure 2.1 Formation of a composite material using fibers and resin (Mazumdar, 2002)

The properties of a composite material depend on the properties of the constituents, geometry, and distribution of the phases. One of the most important parameters is the volume (or weight) fraction of reinforcement, or fiber volume ratio. The distribution of the reinforcement determines the homogeneity or uniformity of the material system (Daniel & Ishai, 1994). In low-performance composites, the reinforcements, usually the form of short or chopped fiber (or particles), provide some stiffening but very little strengthening; the load is mainly carried by the matrix. In high-performance composites, continuous fibers provide the desirable stiffness

and strength, whereas the matrix provides protection and support for the fibers, and, importantly, helps redistribute the load from broken to adjacent intact fibers (Kollár, & Springer, 2003).

The interphase, although small in size, can also play an important role in controlling the failure mechanism, fracture toughness, and overall stress-strain behaviour of the material (Daniel & Ishai, 1994).

2.2 Classification of Composite Materials

Composites can be classified by the form of the components or by their nature.

2.2.1 Classification by the Form of Constituents

As a function of the form of the constituents, composites are classified into two large classes: composite materials with fibers and composites with particles (Figure 2.2) (Berthelot, 1999)

2.2.1.1 Fiber Composites

A composite material is a fiber composite if the reinforcement is in the form of fibers. The fibers used are either continuous or discontinuous in form, chopped fibers, short fibers, etc. the arrangement of the fibers and their orientation allow us to tailor the mechanical properties of composites to obtain materials ranging from strongly anisotropic to isotropic in one plane (Berthelot, 1999).

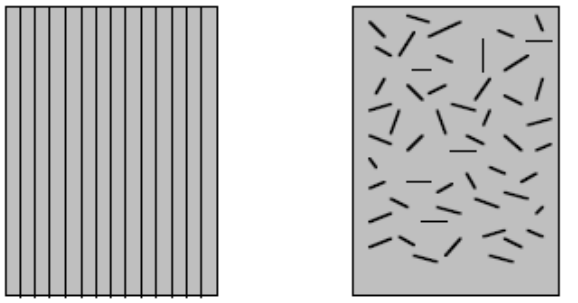

Figure 2.2 Continuous fiber and short fiber composites (Mazumdar, 2002)

2.2.1.2 Particle Composites

A composite material is a particle composite when the reinforcement is made of particles. A particle, in contrast to fibers, does not have privileged directions. Particles are generally used to improve certain properties of materials or matrices, such as stiffness, behaviour with temperature, resistance to abrasion, decrease of shrinkage, etc. In numerous cases particles are simply used as filler to reduce the cost of the material without degrading the characteristics.

The choice of the particle-matrix association depends upon the properties wanted. For example, lead inclusions in copper alloys make them easier to machine. Particles of brittle metals such as tungsten, chromium and molybdenum incorporated in ductile metals improve their properties at higher temperatures while preserving their ductility at room temperatures (Berthelot, 1999).

2.2.2 Classification by the Nature of the Constituents

According to the nature of the matrix, composite materials are classified as organic, metallic, or mineral matrix composite. Composite materials with an organic matrix can be used only in a temperature range not exceeding 200 to 300 ^{o}C, although composite materials with a metallic or mineral matrix are used beyond that up to 600 ^{o}C for a metallic matrix and up to 1000 ^{o}C for a ceramic matrix (Berthelot, 1999).

In consequence, this study will be concerned by polymer matrix composite and interface.

2.3 Polymer Matrix Composites and Interface

Polymer matrix composites are reinforced polymers in which either a thermoset or a thermoplastic polymer is used as the matrix. Thermoplastics consist of long hydrocarbon molecules that are held together by secondary (van der Walls) bonds and mechanical entanglements. The secondary bonds are much weaker than the primary covalent bonds and hence a thermoplastic can be easily melted by increasing its temperature. Large temperature increases would also free the mechanical entanglement of the polymers, thus increasing its mobility. Thermoplastics can be formed repeatedly by heating to an elevated temperature at which softening occurs. Thermoset polymers also consist of long hydrocarbon molecules with primary bonds holding the atoms in the molecule together. However, the polymer molecules are also crosslinked together with covalent bonds as well, instead of the secondary bonds that exist in thermoplastics. This results in gigantic three-dimensional solid structures that are less mobile, stiffer, stronger, and less ductile than thermoplastics. (Sheikh-Ahmad, 2009). Glass fibers, aramid fibers and carbon fibers as reinforcement are usually used for thermoset and thermoplastic composites (Campbell, 2003; 2006).

The fibers ensure the strength of the material, while the matrix helps to keep the shape of the part; the interface, as a key element of the composite, transfers the load from the matrix to the fibers and, thus, it is responsible for the effect of ‘‘reinforcement’’ (Zhandarov & Mäder, 2005).

Interfaces in composites form in the vicinity of fiber surfaces and may exhibit significantly different material characteristics than the bulk resin properties. The chemical composition, as well as the microstructure, of the material at the interphase region mainly controls the properties of the interphase. The thickness of the interphase ranges from 1 to 1000 nanometers depending on materials, sizing and

process conditions. The properties of the interphase and degree of adhesion between the fiber and matrix govern load transfer between the composite constituents (Tanoglu, McKnight, Palmese, & Gillespie, 2001). The interphase is an intermediate region between the fiber and the matrix and it comprises the interlayer and a part of the matrix affected by the presence of the coated fiber (Figure 2.3) (Prikryl, R., Cech, V., Balkova, R., & Vanek, J. (2003)).The properties of the interphase are critical to global composite performance such as strength, toughness, durability and impact/ballistic resistance (Tanoglu, McKnight, Palmese, & Gillespie, 2001).

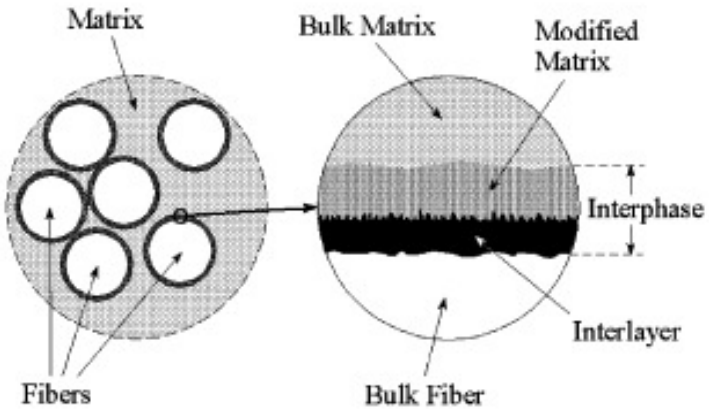

Figure 2.3 Schematic illustration of the composite interphase (Prikryl, R., Cech, V., Balkova, R., & Vanek, J. (2003)).

Fiber surface treatments are often used to create a fiber/matrix interface possessing different characteristics so that the fiber strength is utilized effectively under an optimum bonding. There are many methods or treating agents for surface treatment of glass fibers based on protecting fibers from damage and improving the adhesion between fiber and matrix. In general, the silane coupling agents are applied to fibers as a chemical surface treatment and provides a good adhesion between glass fibers and resin matrix (Zhao, & Takeda, 2000). Surfaces of glass fibers can be also modified by plasma treatment and plasma polymerization techniques.

2.4 Glass Fiber Surface Treatments

2.4.1 Silane Treatment

A silane coupling agent to glass fibers is applied to improve the mechanical bond between the glass fiber and the polymer matrix and form a barrier which is impervious to water, between the glass fiber and the polymer matrix and hence improve moisture sensitivity (Ishida & Miler, 1984).

2.4.1.1. The Structure of A Silane Coupling Agent and Its Properties

Organofunctional silanes are the most widely used coupling agents for improvement of the interfacial adhesion in glass reinforced materials. Organosilanes have the general structure, X_3Si-R. These multi-functional molecules that react at one end with the glass fiber surface and the other end with the polymer phase. R is a group which can react with the resin, and X is a group which can hydrolyze to form a silanol group in aqueous solution and thus react with a hydroxyl group of the glass surface. The R-group may be vinyl, γ-aminopropyl, γ-methacryloxypropyl,etc.; the X-group may be chloro, methoxy, ethoxy, etc. (Kim & Mai, 1998).

Several organofunctional silanes are used commercially since each functional group is somewhat specific for a resin type (Table 2.1). The total amount of silane coupling agent applied is generally 0.1-0.5 % of the weight of glass (Plueddemann, 1974). In particular, the concentration of silane coupling agent is a critical factor in determining the mechanical performance and fracture behaviour of the composite (Hirai, Hamada, & Kim, 1998).

The structure of the silane layer depends on a number of factors including the layer thickness and amount of adsorbed material, the deposition procedure (i.e., solvent polarity, water content, pH, and substrate isoelectric point), the hydrolysis and condensation kinetics of the coupling agent, and the substrate/coupling agent interaction (Lenhart, Dunkers, Zanten,& Parnas, 2003; Nishiyama, Schick, & Ishida,

1991; Daniels, Sefcik, Francis, & McCormik, 1999; Vandenberg et al., 1991; Culler, Ishida, & Koenig, 1985; Ishida & Miller, 1984). Furthermore, the structure of the silane layer depends on the silane structure in the treating solution and its organofunctionality, drying conditions, the morphology of the fiber and the chemical composition of the surface (Hirai, Hamada, & Kim, 1998).

Table 2.1 Typical Commercial Silane Coupling Agents (Plueddemann,1974)

Silane Name	Resin type
Vinylbenzylcationicsilane	All Resins
Vinyl-tris(β-methoxyethoxy)silane	Unsaturated polymers
Vinyltriacetoxysilane	Unsaturated polymers
γ-Methacryloxypropyltrimethoxysilane	Unsaturated polymers
γ-Aminopropyltriethoxysilane	Epoxies, Phenolics, Nylon
γ-(β-aminoethyl) aminopropyltrimethoxysilane	Epoxies, Phenolics, Nylon
γ-Glycidoxypropyltrimethoxysilane	Almost all resins
γ-Mercaptopropyltrimethoxysilane	Almost all resins
β-(3,4-epoxycyclohexyl)-ethyltrimethoxysilane	Epoxies
γ-Chloropropylttrimethoxysilane	Epoxies

Silane coupling agents are generally applied onto the glass fiber surfaces from dilute aqueous solutions, where three time-dependent processes, silane hydrolysis, silane condensation and silane adsorption occur simultaneously, (Norström, Mikkola, Matisons, & Rosenholm, 1998). Arkles, Steinmetz, Zazyczny, & Mehta (1992) showed that the reactions of alkoxysilanes in aqueous solutions and bond formation onto the glass fibers in Figure 2.4.

The trihydroxy silanols, $Si(OH)_3$, are able to compete with water at the glass surface by hydrogen bonding with the hydroxyl groups at the surface (Figure 2.5 (b)), where M stands for Si, Fe, and/or Al. When the treated fibers are dried, a reversible condensation takes place between the silanol and M-OH groups on the glass fiber surface, forming a polysiloxane layer which is bonded to the glass surface (Figure 2.5 (c)). Therefore, once the silane coated glass fibers are in contact with uncured resins, the R-groups on the fiber surface react with the functional groups present in the polymer resin, such as methacrylate, amine, epoxy and styrene groups,

forming a stable covalent bond with the polymer (Figure 2.5 (d)). It is essential that the R-group and the functional group be chosen so that they can react with the functional groups in the resin under given curing conditions. Furthermore, the X-groups must be chosen, that can hydrolyze to allow reactions between the silane and the M-OH group to take place on the glass surface. Once all these occur, the silane coupling agents may function as a bridge to bond the glass fibers to the resin with a chain of primary strong bond (Kim & Mai, 1998).

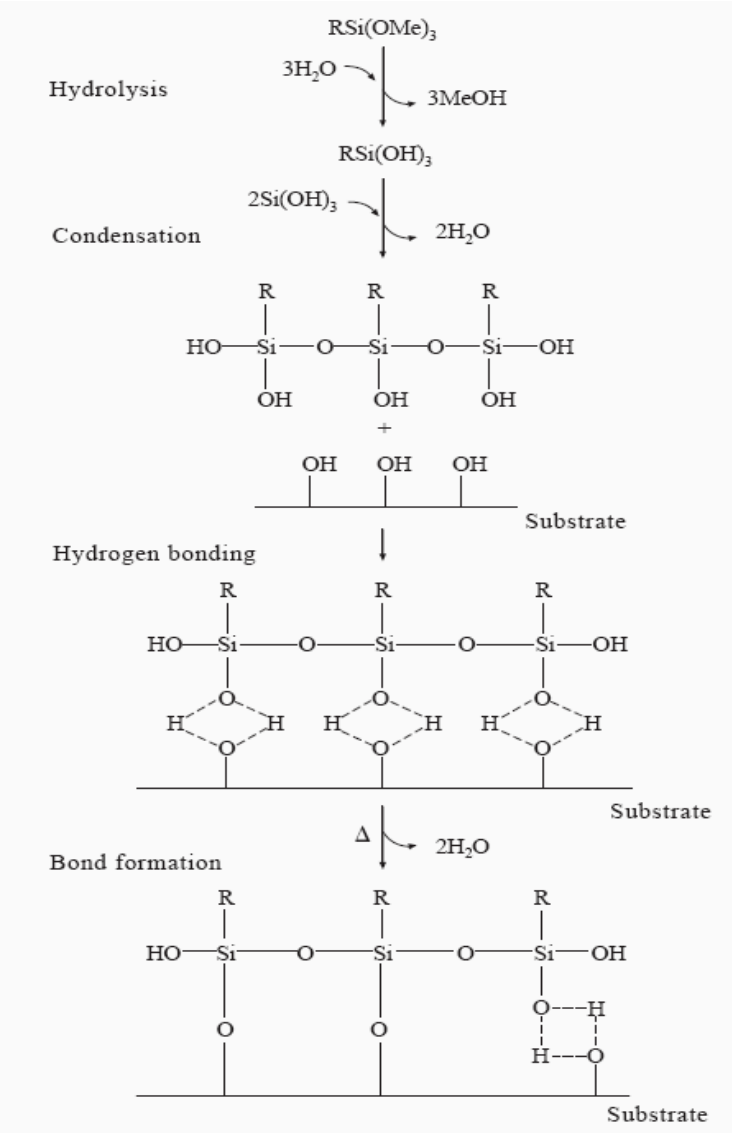

Figure 2.4 Reactions and Bonding of alkoxysilanes (Arkles et al.), 1992)

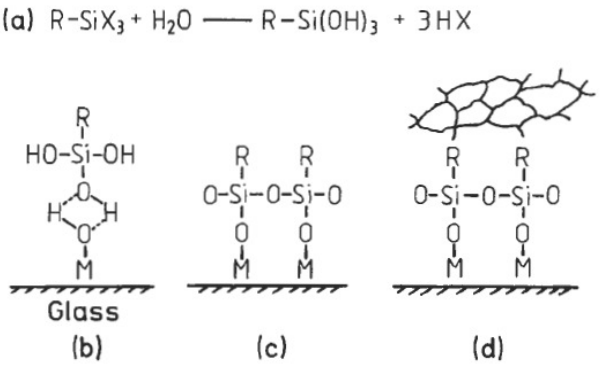

Figure 2.5 Functions of a coupling agent: (a) hydrolysis of organosilane to corresponding silanol; (b) hydrogen bonding between hydroxyl groups of silanol and glass surface; (c) polysiloxane bonded to glass surface; (d) organofunctional R-group reacted with polymer (Kim & Mai, 1998).

Their effectiveness depends on the nature and pretreatment of the substrate, the type of silane used, the thickness of the silane layer and the process by which it is applied. In a relatively dry state, the proper choice of a silane coupling agent is an effective means of promoting interfacial adhesion and enhancing mechanical properties (DiBenedetto, 2001).

2.4.1.2 Bonding Theories Between Glass Fiber and Polymer Matrix.

There are two bonding theories. These are chemical bonding theory and interpenetrating polymer network (IPN).

2.4.1.2.1 Chemical Bonding Theory. In the chemical bonding theory, the bifunctional silane molecules act as a link between the resin and the glass by forming a chemical bond with the surface of the glass through a siloxane bridge, while its organofunctional group bonds to the polymer resin. This co-reactivity with both the glass and the polymer via covalent primary bonds gives molecular continuity across the interface region of the composite (Kim & Mai, 1998).

2.4.1.2.2 Interpenetrating Polymer Network. The chemical bonding theory explains successfully many phenomena observed for composites made with silane treated glass fibers. However, a layer of silane agent usually does not produce an optimum mechanical strength and there must be other important mechanisms taking place at the interface region. An established view is that bonding through silane by other than simple chemical reactivity are best explained by interdiffusion and interpenetrating network (IPN) formation at the interphase region.

The coupling agent-resin matrix interface is a diffusion boundary where intermixing takes place, due to penetration of the resin into the chemisorbed silane layers and the migration of the physisorbed silane molecules into the matrix phase (Kim & Mai, 1998). Figure 2.6 is a representation of the bonding of the siloxane to the polymer through a combination of interpenetration and chemical reaction (DiBenedetto, 2001).

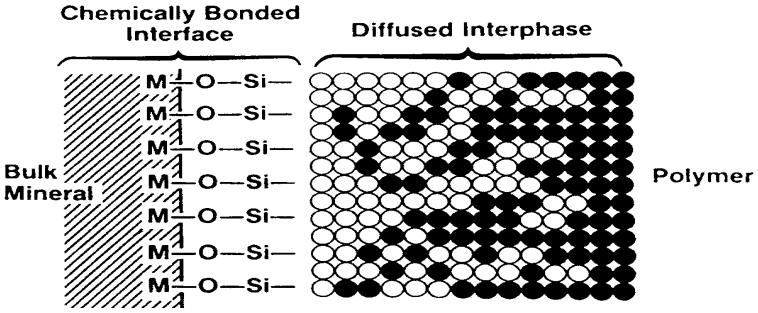

Figure 2.6 Bonding siloxane to polymer through diffusion

2.4.1.3 Silane Layers on Glass Fiber Surface

When glass fibers are treated with a silane solution in an organic solvent, two layers are formed on the glass surface (Figure 2.7). Coupling agents deposited on glass surfaces are usually heterogeneous layers of physisorbed and chemisorbed fractions.

2.4.1.3.1 A Physisorbed Silane Layer. As the silane concentration increases, a physisorbed layer is formed on the chemisorbed layer formed previously. This layer cause a lubrication effect (Park & Jang; 2004; Park & Jin, 2003). Therefore, the mechanical interfacial properties of the composites decrease at a higher silane coupling agent concentration (Park & Jin, 2003). Also, the physisorbed silane prevents the reaction between the chemisorbed silane and the matrix resin (Hamada, Fujihara, & Harada, 2000). The outer physisorbed layers of silane are capable of mixing with and plasticizing the matrix network (Jensen, 1999).

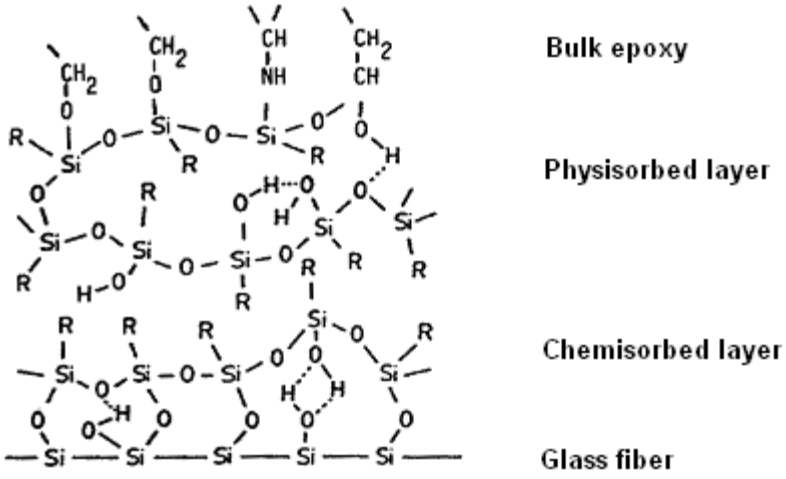

Figure 2.7 Schematic model of the glass-silane coupling agent interphase (Hamada, Fujihara, & Harada, 2000)

2.4.1.3.2 A Chemisorbed Silane Layer. Strongly chemisorbed portion of the layers closest to the glass surface (Lenhart, Dunkers, van Zanten, & Parnas, 2003). The layer was covalently bonded and thus not easily removed (Jokinen, Mikkola, Matisons, & Rosenholm, 1997).

2.4.2 Plasma Treatment and Plasma Polymerization

Plasma is a mixture of electrons, negatively and positively charged particles, and neutral atoms and molecules. Plasma is considered as being a state of materials, and the state is more highly activated than in the solid, liquid or gas state. From this sense, the plasma state is frequently called the fourth state of materials (Inagaki, 1996).

2.4.2.1 Plasma Treatment

Textile materials subjected to plasma treatments undergo major chemical and physical transformations including (i) chemical changes in surface layers, (ii) changes in surface layer structure, and (iii) changes in physical properties of surface layers. Plasmas create a high density of free radicals by disassociating molecules through electron collisions and photochemical processes. This causes disruption of the chemical bonds in the fiber polymer surface which results in formation of new chemical species. Both the surface chemistry and surface topography are affected and the specific surface area of fibers is significantly increased. Plasma treatment on fiber and polymer surfaces results in the formation of new functional groups such as —OH, —C=O, —COOH which affect fabric wettability as well as facilitate graft polymerization which, in turn, affect liquid repellence of treated textiles and nonwovens (Shishoo, 2007).

Proper selection of starting compounds and external plasma parameters (e.g. power, pressure and treatment time) allow creation of desired characteristics on substrate surfaces. In a plasma treatment system, depending on the type and nature of the gas used, surface cross-linking can be introduced, surface energy can be increased or decreased, and reactive free radicals and groups can be produced (Yuan, Jayaraman, & Bhattacharyva, 2004; Denes, Nielsen, & Young, 1997). The enhancement of the adhesion between a polymer matrix and a plasma-treated fiber is caused by both physical and chemical modifications (Cokeliler, Erkut, Zemek, Biederman, & Mutlu, 2007).

2.4.2.2 Plasma Polymerization

Plasma polymerization takes place in a low pressure and low temperature plasma that is produced by a glow discharge through an organic gas or vapor (Gaur & Vergason, 2000). Plasma polymerization is a unique process for the formation of ultrathin films. Any organic compound that can be vaporized is a monomer that can be plasma polymerized. A variety of new polymer thin films can be treated through

plasma polymerization (Zuri, Silverstein, & Narkis, 1996). Plasma polymerization can also be used to produce polymer films of organic compounds that do not polymerize under normal chemical polymerization conditions because such processes involve electron impact dissociation and ionization for chemical reactions (Gaur &. Vergason, 2000).

The chemical structure of plasma polymers strongly depends on the fragmentation of the monomer (Zuri, Silverstein, & Narkis, 1996; Sakata, Yamamoto, & Hirai (1986); Matsuyama, Kariya, & Teramoto, 1994; Cai, Fang, & Yu, 1992), but also on the polymer deposition process conditions in the glow discharge, such as pressure, power, flow rate, current densities, temperature, etc. By varying these process parameters, materials with different chemical compositions and structures can be obtained from the same monomer (Zuri, Silverstein, & Narkis, 1996; Radeva, Tsankov, Bobev, & Spassov, 1993; Morra, Occhiello, & Garbassi, 1993; Park & Kim, 1990). In the case of the plasma polymer, their chains are short and in addition they are randomly branched and terminated with a high degree of crosslinking (Biederman, 2004). Thin polymer films prepared by the plasma-polymerization technique may be formed as homogeneous with respect to thickness, uniformity, composition and structure (Cech, Prikryl, Balkova, Grycova, & Vanek, 2002).

Plasma polymer films deposited from organosilicon monomers are potentially applicable as effective functional interlayers for glass fiber/polymer composites. (Prikryl, Cech, Balkova, & Vanek, 2003). Plasma polymerization deposits a conformal, pinhole free film to the surface of the fibers, leading to interfacial control through the chemical functionality resulting from the composition of the monomer gases employed, and not influenced by the underlying fiber surface chemistry or topography (Marks & Jones, 2002; Kettle, Beck, O'Toole, Jones, & Short, 1997). By modifying the deposition conditions, thicker coatings of either low or high modulus can be deposited (Marks & Jones, 2002; Kettle et al., 1998).

2.4.2.3 Plasma Treatment System

A typical plasma treatment system includes a vacuum chamber, electromagnetic grounding and shielding, a vacuum pump system, discharge and bias power supplies and matching network, gas supply and control system as well as sample holder system (Li, Ye, & Mai, 1997).

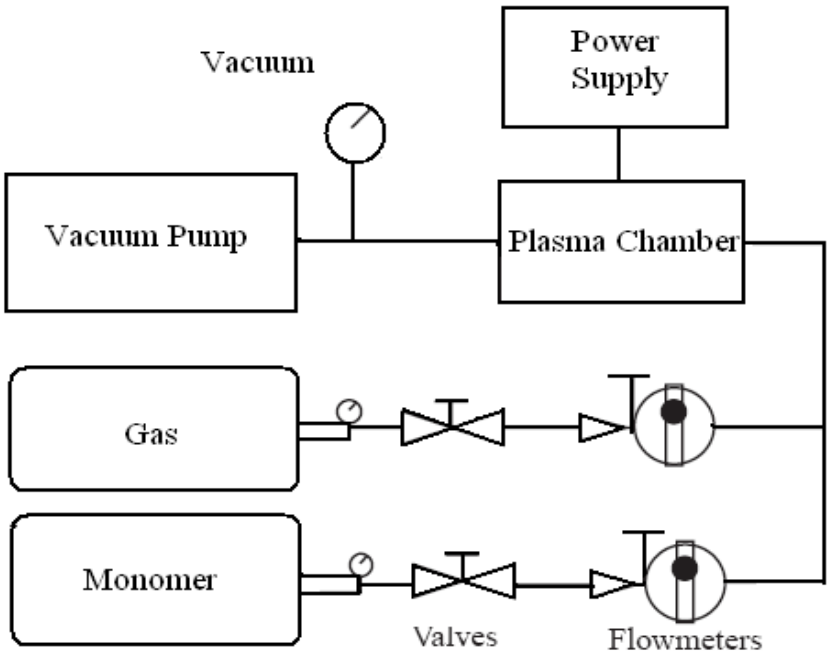

Figure 2.8 Schematic diagram of the plasma

CHAPTER THREE
EXPERIMENTAL DETAILS

3.1 Materials

3.1.1 Glass Fiber and Epoxy Resin

The fiber reinforced polymer composite materials used in the thesis study are manufactured from E-glass fabric and epoxy resin. Areal density of woven roving glass fabric, supplied by Metyx Telateks A.S. of Turkey, was 300 g/m^2. Also, glass fiber rovings was obtained from Cam Elyaf A.S. of Turkey. The roving contained 2400 filaments (each filament having a round cross-section and a diameter of 12 μm).The epoxy system Resoltech R1040 (unmodified liquid epoxy) and hardener Resoltech R1048 (hardener), both manufactured by Resoltech, France, were chosen as the matrix. The composition for the epoxy resin system is specified in the product data sheet from the manufacturer to be (by weight): R1040 (78%) and R1048 (22%).

3.1.2 Glass Substrate

Glass substrates were microscope slides without flaws (IsoLAB, Germany). Prior to use, the glass slides were ultrasonically cleaned with ethanol, acetone and deionized water for 5 min, respectively. Then, the slides were dried at room temperature for 6 h.

3.1.3 Silane Coupling Agent

γ-glycidoxypropyltrimethoxysilane (γ-GPS) was used for fiber surface treatments and was obtained from Dow Corning Corporation under the commercial name of Z-6040. Z-6040 Silane is a bifunctional silane containing a glycidoxy reactive organic group and a trimethoxysilyl inorganic group. The silane was 99.8% and was used as-received.

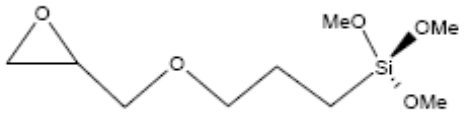

Figure 3.1 The structural formula of Z-6040.

3.1.4 Other Materials

Hydrochloric acid (HCl, 37%) and acetic acid (CH3COOH, 100%) were of analytical grade purchased from Riedel-de Haën and also used without further purification. Ethanol and acetone were purchased from Merck Corp. Commercially available, high purity argon gas (99.995% purity) was used to remove impurities in a vacuum chamber of plasma system before plasma polymerization treatment or to deactivate free radicals in a vacuum chamber of plasma system after plasma polymerization treatment.

3.2 Surface Analysis Techniques

3.2.1 FT-IR Spectroscopic Measurements

A Fourier transform infrared spectrophotometer (Perkin Elmer BX-II) was employed. One milligram of the samples, heat cleaned, activated, and silane treated glass fabric were ground into powder with high purity infraredgrade KBr powder (100 mg) and pressed into a pellet for measurement. Each spectrum was recorded in the range of 400–4,000 cm^2 with a resolution of 2 cm^2. The background spectrum of KBr pellet was subtracted from the sample spectra.

3.2.2 X-ray Photoelectron Spectroscopy (XPS) Analysis

XPS was used to determine the surface elemental compositions of the glass samples and to investigate the changes in the chemical functionality of the glass sample surfaces at different plasma powers and exposure times. The XPS spectra were obtained with a Specs ESCA instrument (Germany), equipped with a non-

monochromatic monochromatic Mg Ka radiation source at a power of 200W (10 kV, 10 mA) and EA 200 hemispherical electrostatic energy analyzer. The base pressure in the XPS analysis chamber was about 10^{-9}–10^{-10} torr. The analyzer was operated in constant analyzer energy (CAE) mode with pass energy of 96 eV for elemental quantification purposes and 48 eV for C1s peak shape comparison purposes. The concentrations of different chemical states of carbon and silicon in the C1s and Si2p peaks were determined by fitting the curves with Gauss–Lorentz functions.

3.2.3 Contact Angle Measurements

3.2.3.1 Sessile Drop Method

Contact angle measurements of a drop of glycerin on glass fabric were carried out using the sessile drop method with a CAM 100 KSV (KSV, Finland). Recording the drop profile with a CCD video camera allowed monitoring changes in wetting. All reported data were the average of at least five measurements at different locations of the fabric surface. The experiments were conducted at 25^{o}C and at about 65% relative humidity. The volume of the drops was always about 2 µl. The piston is moved by a micrometer to obtain good control in applying liquid to the surface.

3.2.3.2 Captive Bubble Method

Captive bubble method was used for contact angle measurements of glass slides. This method also provides reliable contact angle values for quantification of surface free energy (SFE) of a material. In this method, a special microscope (QX3 computer microscope, 60X, Intel) and a computer system were used to measure contact angles in a three-phase system consisting of water, solid surface, and bubbles of air or liquid n-octane. The glass cell was filled with ultra pure water and the glass samples (1 cm^2) were placed in it. A special L shaped syringe needle containing n-octane (purity, 99%, Acros Organics, Belgium) or gas (air) releases bubbles beneath the sample. The volume of these bubbles did not exceed 5 µl. A computer screen provided an image of the captive bubble. The supporting computer software

(Wettability Pro Classic, version 2.0.0 from Czech Republic) used these data to calculate the contact angles between n-octane and the solid surface, θ_o, and between air and solid surface, θ_a. Contact angle experiments were repeated for five times for each sample surfaces. The SFE of the each sample was determined by contact angle measurements. Contact angle results of air and n-octane from captive bubble experiments were used to find the polar and dispersive interaction components of surface energy.

3.2.4 Scanning Electron Microscopy (SEM) Observation

The morphologies of glass fiber and silane coupling agent deposited on glass fiber were observed using the SEM at an accelerating voltage of 4- 5 kV in the secondary electron mode. The fracture surfaces of tensile-tested specimens were also examined using the scanning electron microscope (JEOL JSM 6060) at accelerating voltage equal to 5 kV in the secondary electron mode. To reduce the extent of sample arcing, the samples were coated with a thin layer of metallic gold in an automatic sputter coater (Polaran SC7620) prior to examination by SEM.

3.2.5 Atomic Force Microscopy (AFM) Examination

The atomic force microscope (AFM) was used to examine the morphology of glass surfaces and to determine surface topography and roughness of the plasma polymerized glass samples. AFM measurements were performed in contact and tapping modes at room temperature and in the air using MultiMode SPM (AFM/STM) Nanoscope IV from Digital Instrument. Roughness parameters (Ra and Rms) calculation and image processing were performed using Nanoscope IV software. Silicon nitride probe in contact mode and silicon probe in tapping mode were employed. Sample surfaces were scanned without any surface modification. Measurements were made twice or thrice on different zones of each sample. Surface roughness values were determined in three random areas per sample, scanning across areas of 2 *2 mm^2.

3.3 Mechanical Tests

3.3.1 Tensile Test

According to ASTM standard D-3039, tensile tests on composite sheets were performed in a Shimadzu Autograph AG-G Series universal testing machine with a video extensometer system (Shimadzu Noncontact Video Extensometer DVE-101/201), with trapezium (advanced software for materials testing) for machine control and data acquisition. The specimens with length of 197 mm and width of 25 mm were prepared using a water jet cutter. Tensile tests were conducted at a constant crosshead speed of 2 mm/min at room temperature in air. At least six specimens were tested for each type of composite sheet to check for repeatability.

3.3.2 Flexure Test

Flexure tests were determined according to ASTM D 790 standard. The flexural strength and modulus of the composites were evaluated using a three point bending test. The three-point bending fixture was manufactured by Shimadzu for use in a universal test machine running in three point bending mode. For the flexure tests, test specimens with length of 80 mm and width of 25 mm were prepared using a water jet cutter and a span-to-depth ratio of 16:1 at a crosshead speed of 1.3 mm/min was used. At least four samples were measured and the results were averaged.

3.3.3 Short Beam Shear Test

Short beam shear tests were carried out according to ASTM standard D-2344. A sliding roller three-point bending fixture, which included a loading pin (diameter 6.4 mm) and two support pins (diameter 3.2 mm), was mounted in a 5-kN capacity, screw-driven load frame. Shimadzu Autograph AG-G Series universal testing machine was used, with a crosshead speed of 1.3 mm/min. The tests were carried out at four times for each type of composite sheet. Test specimens were cut from the laminates using water jet technique. The length and width of the test specimens were

26.3 and 6.4 mm, respectively. The apparent interlaminar shear strength of composites was determined from specimens that were tested with a support span/ sample thickness ratio of 5:1. The simply supported specimens allow lateral motion and a line load is applied at the mid span of the specimens.

3.4 Surface Treatments

3.4.1 Heat Treatment

As-received glass fibers were heat cleaned at 450^{o}C for 1.5 h to remove presizing and organic impurities from the glass fiber surface.

3.4.2 Acid Activation Treatment

Heat cleaned fibers were subjected to an activation pretreatment with a hydrochloric acid aqueous solution (HCl 10% (v/v)) for 1 and 3 h at room temperature (for first study) and (HCl 1% (v/v) and HCl 3% (v/v), separately) for 1 h (for second study) at room temperature to regenerate the hydroxyl groups. After acid activation, all of the samples were washed with distilled water several times until chloride-free, determined by an $AgNO_3$ test. Then, all the samples were dried at 110^{o}C for 1 h.

3.4.3 Silane Treatment

Aqueous solutions were prepared by adjusting the pH of the distilled water to about 4.5 with acetic acid. The silane coupling agent was added to acidified water. The mixture was stirred for about 15 min before the silanes were hydrolyzed by dilute acetic acid solution. In the first and second studies, the concentration of silane aqueous solutions was 0.3% (v/v) for the heat cleaned and activated fibers. After 15 min of the hydrolysis reaction of γ-GPS agent, the glass fabric was immersed into the silane aqueous solution.

While various immersion durations was selected for first study (Table 1), immersion duration into silane aqueous solution was only 1 h for second study. In third study, in order to treat the heat cleaned glass surface under different silane concentrations, the silane solution at various concentrations was prepared under a constant condition. The silane coupling agent concentration was varied from 0.1 to 0.5 % (v/v). Then, the glass fabrics were immersed in the γ-GPS solution for 1 h. It can be noted here that the used concentrations in this study covers the range usually employed in the practical application of glass fiber reinforced plastics technology.

Then γ-GPS treated glass fabric was dried for 30 min at 105^{o}C to drive the condensation of silanol groups at the surface and to remove traces of methanol from hydrolysis of the methoxysilane.

3.4.4 Plasma Polymerization

Plasma polymerization was carried out in low frequency (LF) plasma generator (operating at 40 kHz with a maximum power 200 W), Model Pico, from Diener Electronic GmbH + Co. (Germany). Glass samples were subjected to plasma polymerization treatment. In a typical plasma treatment, at first, the chamber containing the samples was evacuated to a pressure of 0.12 mbar. Then, argon gas was introduced into the chamber for 10 min at a pressure of 0.3 mbar before generation of the plasma to remove impurities and to ensure a uniform gas environment. After that, the chamber was re-evacuated to approximately 0.12 mbar again. Thereafter, monomer gas inlet was opened and the monomer gas was allowed to flow through the chamber for 5 min at a pressure of 0.16–0.17 mbar. Then, the generator was turned on and the samples were exposed to LF-generated γ-GPS plasma at different plasma powers (30, 60 and 90 W) and exposure times (5, 15 and 30 min). At the end of the process, the generator was turned off automatically and monomer inlet was closed manually. The plasma system was fed with argon gas for 10 minutes at a pressure of 0.3 mbar. Finally, the plasma system was placed in 0.1 mbar vacuum pressure for 15 minutes. Argon feeding and vacuum applications were

applied to deactivate free radicals in the plasma atmosphere after plasma polymerization treatment.

3.5 Composites Preparation

a) For wet chemical studies;

The epoxy resin and hardener mixture were applied onto the as-received and the surface treated glass fabrics by a hand lay-up technique. Twelve layers were added successively in order to get about 3.5-mm-thick composite. The laminate was compressed thereafter, in a mold (250 mm * 350 mm) at a pressure of 100 bar, and the pressure was applied to the composite at room temperature for 150 min. After fabrication, the glass composites were cured at room temperature for two weeks before being tested.

b) For plasma polymerization studies;

Unidirectional (UD) composites were prepared by a hand lay-up technique in a teflon mold. Glass fibers were pre-impregnated with matrix material consisting of epoxy and hardener in the aforementioned ratio. The impregnated glass fibers were placed in the mold cavity. Then, matrix material was poured into the mold. The composites were cured for 1 hour at 85^{o}C.

CHAPTER FOUR
RESULTS AND DISCUSSION

4.1 Wet Chemical Studies

4.1.1 The Structure of γ-Glycidoxypropyltrimethoxysilane (γ-GPS) on Glass Fiber Surfaces

In order to change the composition of the glass and regenerate to the hydroxyl groups, activation pretreatment of heat cleaned woven glass fabric was performed using a 10% (v/v) HCl aqueous solution for different durations before silane treatment. The treatment of silanization of heat cleaned and acid activated glass fibers with γ-GPS were conducted at various time intervals. Samples codes and conditions for their preparation are presented in Table 4.1. The effect of acid activation on glass surface and the interaction between glass fibers and silane coupling agent were examined using Fourier transform infrared spectroscopy (FT-IR). The morphologies of glass fiber and silane coupling agent deposited on glass fiber were observed using the SEM. Contact angle measurements on glass fibers were also performed to evaluate surface structure.

Table 4.1 Samples codes and conditions for the glass surface treatments

Sample Code	Activation Treatment	Activation Time (h)	Silanization Treatment	Silanization Time (min)
F	None	None	None	None
HF	None	None	None	None
AHF1	HCl 10%	1	None	None
AHF3	HCl 10%	3	None	None
HF-Si15	None	None	γ-GPS	15
AHF1-Si15	HCl 10%	1	γ-GPS	15
AHF3-Si15	HCl 10%	3	γ-GPS	15
AHF3-Si30	HCl 10%	3	γ-GPS	30
AHF3-Si60	HCl 10%	3	γ-GPS	60

4.1.1.1 Fourier Transform Infrared (FT-IR) Spectroscopic Measurements

Figure 4.1 exhibits FTIR spectra of glass fiber (as received (F), heat cleaned (HF), %10 HCl (v/v) 1h activated (AHF1), %10 HCl (v/v) 3h activated (AHF3)).

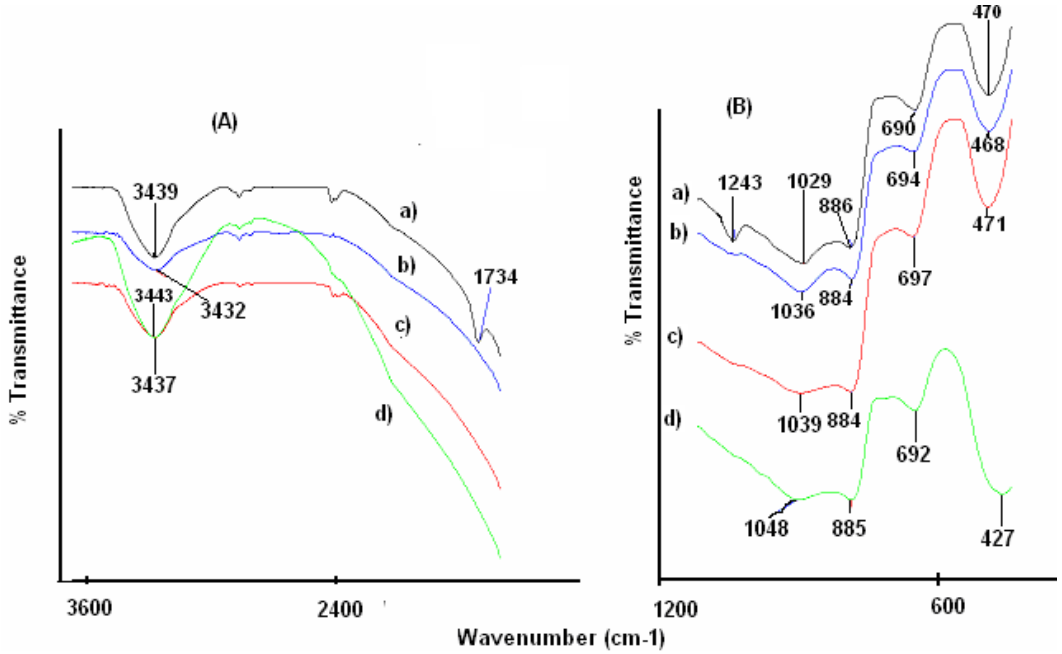

Figure 4.1 FTIR spectra of the samples a) F b) HF c) AHF1 d) AHF3, A: high energy portions B: low energy portions

The effect of the heat cleaning and acid activation can be seen in Figure 4.1. The band centered at 1734 cm^{-1} (probably due to C=O group of sized glass fiber) and 1243 cm^{-1} in the spectrum of as received fiber (F) can not be seen in the spectra of HF, AHF1 and AHF3. The band at 1029 cm^{-1} corresponds to the stretching vibration of Si-O-Si bonds. This band shifted to 1039 cm^{-1} and 1048 cm^{-1} after acid treatment for 1h and 3h, respectively. The band centered at 3400-3500 cm^{-1} is due to OH stretching vibration. After 3h acid activation, this band broadens when compared to OH band of heat cleaned fibers. Presumably acid activation increases the Si-OH surface content of the heat cleaned fiber. The band at 470 cm^{-1} for F and 468 cm^{-1} for HF is due to Si-O deformation band. After acid activation for 1h, this band seemed at 471 cm^{-1}. However, acid activation for 3h, this band shifted to 427 cm^{-1}. This band is also more broaden than the others. It can be inferred that acid activation time affects

the interaction level between glass fiber and hydrogen ions. It is probable that when acid activation time increases more Al will be leached out from glass fiber. Therefore the surface content of Si-OH increases as reflected by the increasing of the intensity of the Si-O band.

The FTIR spectra of silanized glass fibers were given in Figure 4.2. FTIR spectra of HF, AHF3-Si15, AHF1-Si15, HF-Si15 can be seen in Figure 4.2 a, b, c and d, respectively.

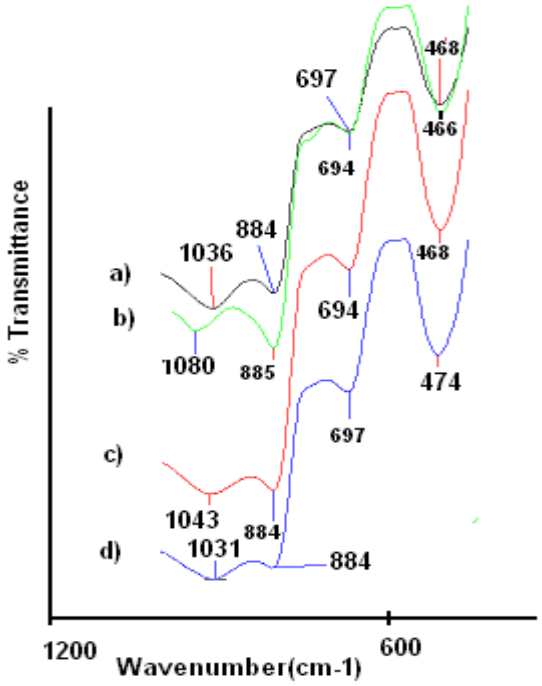

Figure 4.2 FTIR spectra of the samples a) HF b) AHF3-Si15 c) AHF1-Si15 d) HF-Si15

As can be seen from Figure 4.2 a, the band centered at 1036 cm^{-1} in the spectrum of heat cleaned fiber is assigned to stretching vibration of Si-O-Si. This band shifted to 1031 cm^{-1} after silanization of heat cleaned fiber. However, after silanization of acid activated heat cleaned fiber, this band increases to 1043 cm^{-1} and 1080 cm^{-1} for 1h and 3h of acid activation time, respectively (Figure 4.2 c and b). The significant increase was observed for AHF3-Si15 due to greater acid activation duration. Of particular interest is the stretching vibration of Si-O deformation band at 427 cm^{-1} in the spectrum of AHF3 (Figure 4.2 d) increases to 466 cm^{-1} after silanization

procedure. It can be put forward to that an interaction takes place between silane coupling agent and glass fiber.

The effect of silanization time was presented in Figure 4.3. 15, 30 and 60 min for silanization time intervals were chosen as shown in Figure 4.3 a, c and b, respectively.

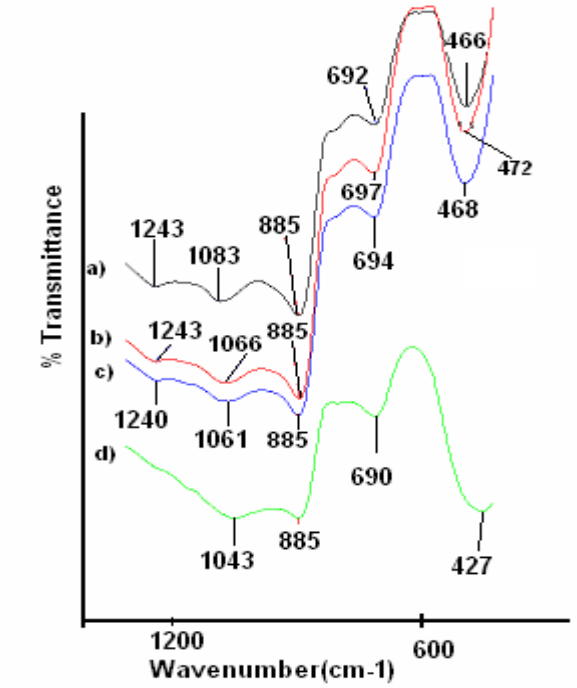

Figure 4.3 FTIR spectra of the samples a) AHF3-Si15 b) AHF3-Si60 c) AHF3-Si30 d) AHF3

Figure 4.3 d shows FTIR spectrum of AHF3. It can be said that two significant changes were observed in the spectra of silanized fibers at different time intervals. The first one is the band where the stretching vibration of Si-O-Si takes place at 1043 cm^{-1} (Figure 4.3 d). This band shifted to 1083, 1061 and 1066 cm^{-1} after 15, 30 and 60 min silanization time intervals, respectively. This result can be rationalized on the basis that silanization time creates significant difference in terms of the interaction between glass fiber and silane coupling agent. The difference between 15 and 30 min is 22 cm^{-1}. The second important difference was observed at the band of 427 cm^{-1}. As pointed out earlier, this band can be assigned to Si-O deformation band of low energy portions of the spectra. This band increased to 466, 468 and 472 cm^{-1} for 15,

30 and 60 min of silanization times, respectively. It is noticeable that this confirms an interaction between silane coupling agent and glass fiber. One point can be added that after silanization a small band at 1243 cm^{-1} for 15 min silanization time (1240 and 1243 cm^{-1} for 30 and 60 min, respectively) takes place. These bands are attributed to symmetric stretching vibration of C-O-C band of the silane coupling agent. This striking change supports grafting of silane to the surface of the glass fiber.

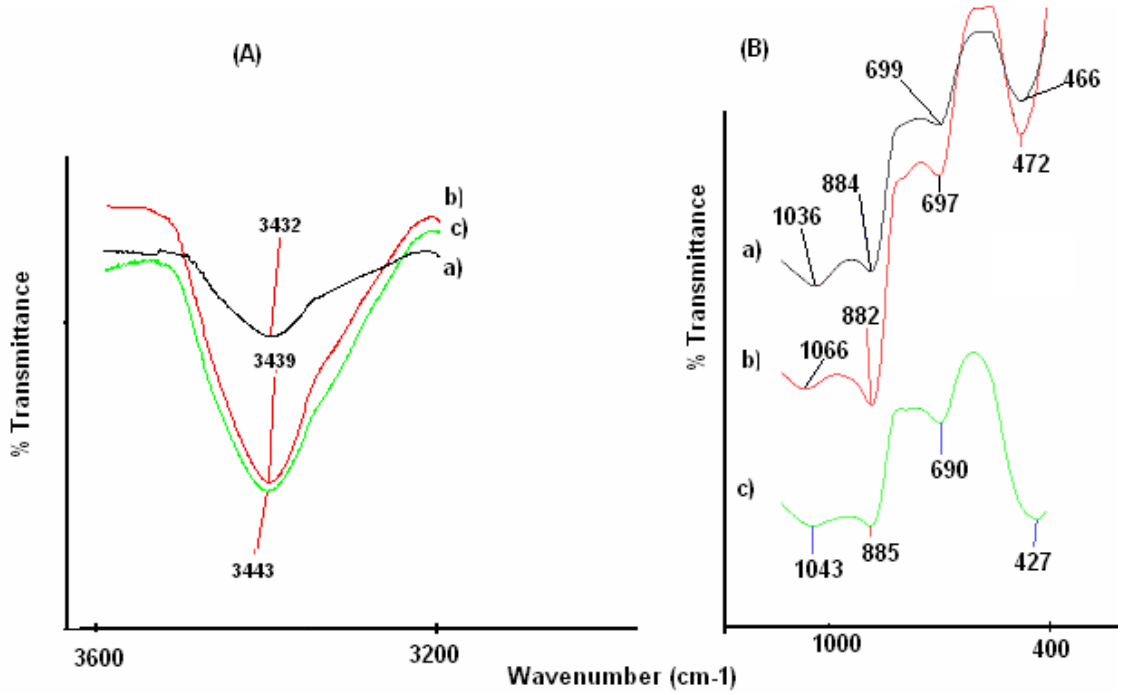

Figure 4.4 FTIR spectra of the samples a) HF b) AHF3-Si60 c) AHF3 A: high energy portions B: low energy portions

FTIR spectra of HF, AHF3 and AHF3-Si60 were provided in Figure 4.4. OH stretching vibration of HF was observed at 3432 cm^{-1}. As can be rendered in Figure 4.4 c, OH stretching band increased to 3443 cm^{-1} when heat cleaned fiber acid activated. After silanization procedure, this band shifted to 3439 cm^{-1} (Figure 4.4 b). Here we pay a great deal of attention to intensity of the bands. The intensity of the OH stretching vibration of HF increased after acid activation procedure. As mentioned earlier, along with leaching out Al from glass fiber, it seems as if surface content Si-OH increases. Beyond a reasonable doubt it is an important result, although small shifts were observed. The second significant change is the stretching

vibration of Si-O-Si at 1036 cm^{-1} for heat cleaned glass fiber. Considering acid activation, this band took place at 1043 cm^{-1}. But, silanization of AHF3 for 60 min brings about a significant increase approximately 23 cm^{-1}. Such being the case, we deduced that silane coupling agent and glass fiber interacted and Si-O-Si bonding resulted in. There is also significant change at the band of 427 cm^{-1} which is ascribed to Si-O deformation band. The explanations for shifts in this band were included in above part. Since the explanation are the essentially the same, it is not available here. On the face of it, this modification of glass fiber with silane coupling agent takes place successfully. This case may make the hydrophobic environment possible on the surface of glass fiber.

4.1.1.2 SEM Observation

We applied the electron microscope to an investigation of the amount and state of aggregation of γ-GPS layers applied to glass fibers. Comparing the SEM micrographs of HF-Si15 and AHF3-Si60 samples (Figure 4.6) with 'original' as-received glass fiber (Figure 4.5 a), coating layer was observed on the surface of glass fiber. The silanizated glass fibers (Figure 4.6 a) are noticeably thicker, however, the silanizated fibers after HCl activation treatment (Figure 4.6 b, c) display the characteristic cracks along the fiber surface. The HF and silane agent interaction is not uniform along the fiber surface, implied by the nonuniform of the silane coupling agent on the clean fiber surface. This is possibly owing to the nonuniform interaction between the silane coupling agent and the glass fiber. Plueddemann (1974) also reported that thicker films deposited by hydrolysis and condensation of silane coupling agents are oils, cheesy gels, or friable solids, but not tough, water resistant polymers. They are not effective unless they contact the glass surface in their silanol form. The most striking feature of Sterman & Bradley (1961) findings was that the commercial method of applying coupling agents resulted in deposition of a thick (in terms of molecular dimensions) non-uniform layer of the material, which tended to form agglomerates in the cavities between the fibers. In our study, it was clearly observed that agglomerations of silane agent in the cavities among the heat cleaned

fibers (Figure 4.6 a) are available. The results are agree with the above findings of Sterman & Bradley (1961).

However, by activated the glass fiber with the HCl, the γ-GPS/fiber interaction is more uniform along the glass fiber (Figure 4.6 b). It has been observed that pretreatments of the substrate surface with acid solution may be very important for quantification of the number and distribution of surface silanol groups (Iler, 1979; Van Der Voort, Gillis-D'Hamers, Vrancken, & Vansant, 1991; Yoshinaga, Yoshida, Yamamoto, Takakura, & Komatsu, 1992). According to González-Benito, Baselga, & Aznar (1999), the acid activation of glass fibers greatly changes the surface composition and the hydration state of the glass. Regeneration of surface silanol groups by treating the fibers with HCl aqueous solution may be responsible for the uniform γ-GPS coatings deposited on activated fiber surfaces. The micrographs of AHF3-Si60 (Figure 4.6 c) when compared to those of AHF3-Si15 (Figure 4.6 b) have greater and more visible cracks on coatings. One possible explanation for the reason of cracks on coatings may be that a wide mismatch in coefficients of thermal expansion between silane coupling agent and glass fiber. Additionally, it is known that the difference in the thermal expansion coefficient between glass substrates and most of silane chemicals is significantly large. From a scientific and practical point of view, differences between the coefficient of thermal expansion of the fibers and coating constituents generate internal stresses and stress cracks on heating and cooling due to constraints of the surrounding coating material. During the last part of surface treatment of glass fiber, the adsorbed coupling agent was dried at 110 °C for 30 min. Upon cooldown, temperature changes are believed to be responsible for producing stresses in the coating. It is thought that the stresses in coatings are the reason of the cracking. The potential explanation of this result may be that the silane coupling agent is loaded in tension on cooling since it tries to contract at a much higher rate than do the fibers. This loading may result in cracks occurring between the fiber and the silane chemicals. The remark, based on the SEM observations (Figure 4.6 a and c), is that maximum coating defect sizes decrease with decreasing coating thickness.

Figure 4.5 a shows the micrographs of as-received glass fibers, indicating the smooth surfaces with small islands of sizing spread and impurities over its surfaces. On the other hand, the heat cleaned glass fibers exhibited a clean, smooth surface indicating that the sizing and impurities had been completely removed from the fiber surface (Figure 4.5 b). It is of interest to note here that in spite of HCl activation pretreatment, the heat cleaned glass fibers did not exhibit significant change in surface morphology in terms of view of the micrograph (Figures 4.7 a and b). SEM micrographs of activated glass fibers have revealed a smooth surface morphology. This conclusion is compatible with the results obtained by González-Benito, Baselga, & Aznar (1999) in which silane treatment of HCl activated glass fibers was conducted.

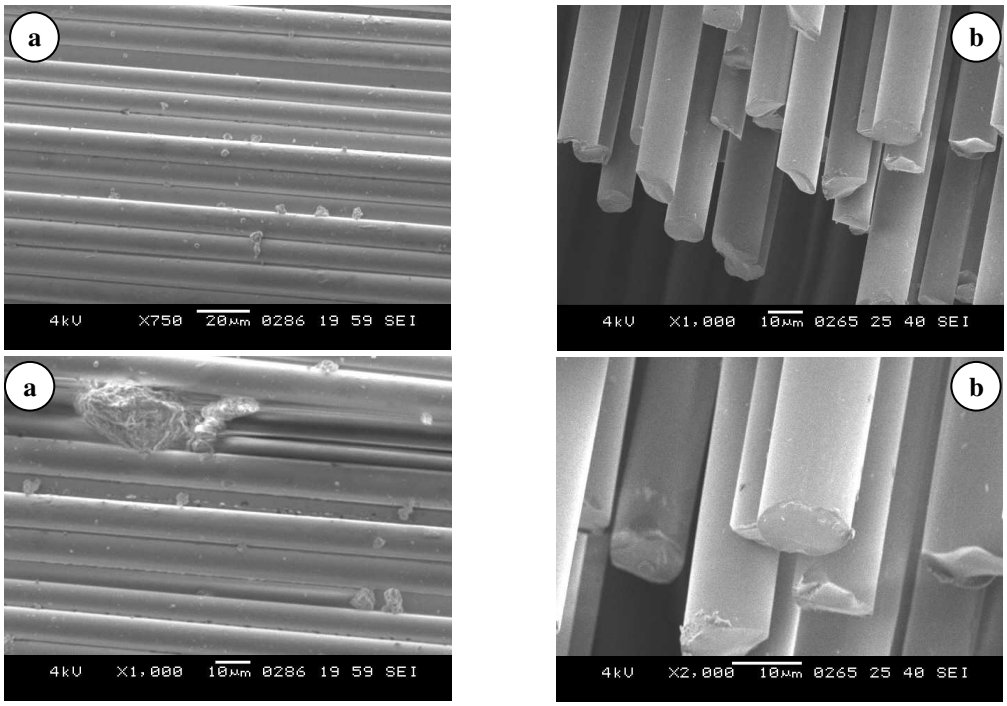

Figure 4.5 SEM micrographs of the surface of a) F and b) HF glass fibers at various magnification levels

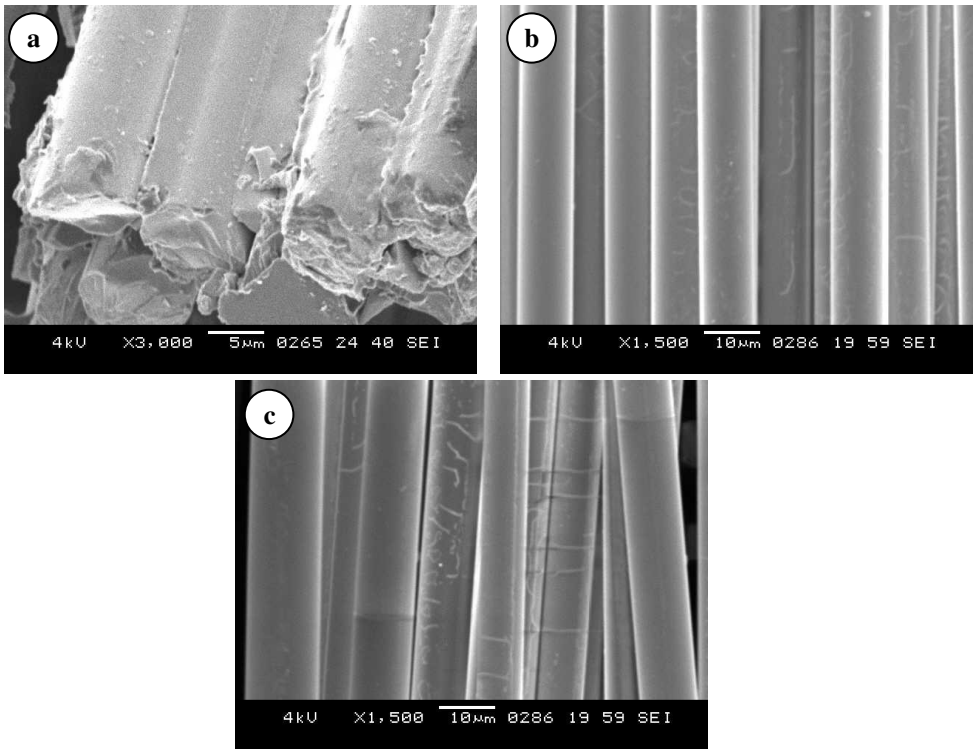

Figure 4.6 SEM micrographs of the surface of a) HF-Si15 b) AHF3-Si15 and c) AHF3-Si60

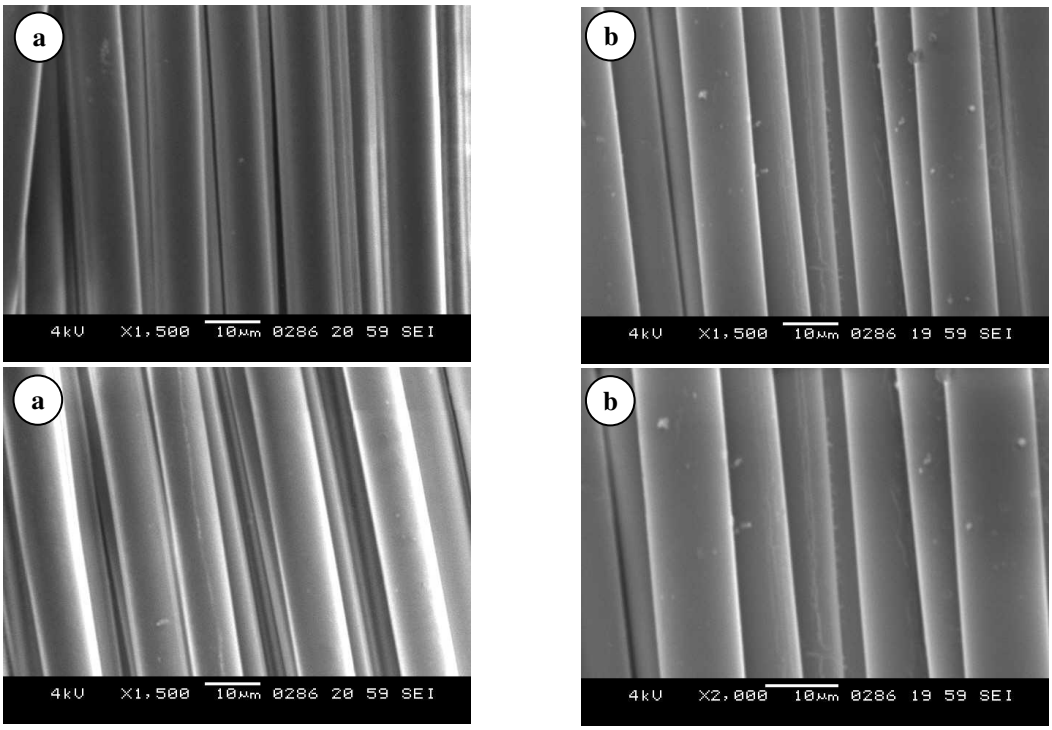

Figure 4.7 SEM micrographs of the surface of a) AHF1 and b) AHF3 glass fibers at various magnification levels

4.1.1.3 Measurement of Contact Angle

Changes of contact angle in glass fabrics treated under activation and silanization conditions are shown in Table 4.2, Figures 4.8 and 4.9. As noted in Table 4.2, contact angle data of heat cleaned fibers in glycerin decreased after acid activation and silanization treatments.

Table 4.2 Contact angle values and hysteresis (Δθ). Advancing (θ_a) and receding (θ_r) contact angles measured in .°

Sample Code	Δθ (θ_a-θ_r) (°)	Contact angle (°)
F	15.4 ± 4.71	70.4 ± 6.23
HF	6.8 ± 3.26	99.3 ± 4.60
AHF1	4.9 ± 3.87	93.0 ± 4.26
AHF3	5.4 ± 4.38	86.1 ± 5.38
HF-Si15	11.4 ± 5.68	86.6 ± 6.10
AHF1-Si15	13.8 ± 6.13	71.3 ± 5.30
AHF3-Si15	11.3 ± 6.57	77.4 ± 3.71
AHF3-Si30	13.4 ± 2.79	71.4 ± 6.14
AHF3-Si60	10.8 ± 5.08	80.1 ± 5.23

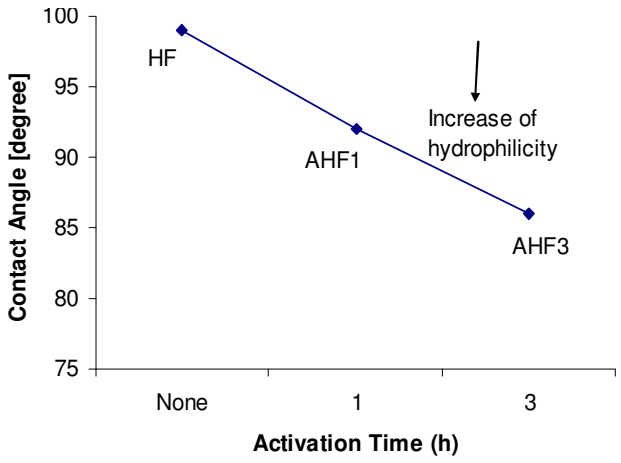

Figure 4.8 The effect of acid activation time on contact angle measurements

The angle of heat cleaned fibers before activation and silanization treatments was 99.3° and shows a relatively hydrophobic surface. Contact angle data of AHF1 and AHF3 were 93.0° and 86.1°, respectively and slightly changed into a hydrophilic surface in direct proportion to the time of activation treatment (Figure 4.8). This is an expected result because of the leaching out (Al) and increasing of OH groups after acid activation which is also confirmed by FTIR analysis. Namely, acid activation treatments lead to more hydrophilic surface.

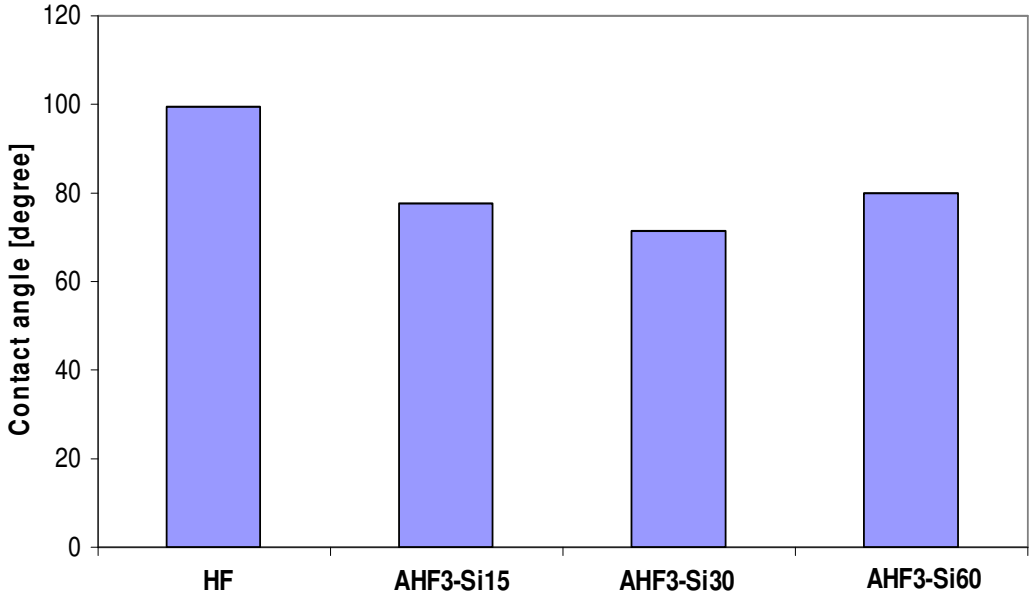

Figure 4.9 Variations of contact angle as a function of silanization time for acid activated glass fiber (3 h)

It can be observed from Table 4.2 and Figure 4.9 that contact angles of HFSi15, AHF1Si15, AHF3Si15, AHF3Si30, AHF3Si60 was obtained to be 86.6°, 71.3°, 77.4°, 71.4° and 80.1°, respectively. These results show that surface treated fibers in silane aqueous solution exhibited lower contact angles than HF and resulted in an increase in wettability.

Figure 4.9 shows the effect of silanization time on contact angle data for acid activated (3h) fibers. While the contact angle data get lower in the range 0-30 min, beyond 30 min, the contact angle value increases up to 60 min. As it is well known, the amount of silane adsorbed should be proportional to the silane treatment time. In

the case of excess silanization time (60 min), the silane treatment may be formed in the thick layer on glass fibers. Therefore, the fibers treated with excess silanization time may demonstrate the silane characteristics in nature. This may cause a hydrophobic environment on the surface of glass fiber. As a result of this event, contact angle value for AHF3Si60 increases (Figure 4.9).

Another important characteristic of a solid-liquid interface is the contact angle hysteresis ($\Delta\theta$), which is the difference between the contact angle at the front of the droplet (advancing contact angle, θ_a) and the contact angle at the back of the droplet (receding contact angle, θ_r) for a droplet moving along the solid surface (Jung & Bhushan, 2006). As can be seen from the hysteresis values (Table 4.2), one can realize that hysteresis increases after silanization procedure. This is an anticipated result owing to fact that silane treatment changes surface structure of glass fiber. This result is also supported by SEM micrographs and FTIR analysis of fibers, as discussed earlier.

4.1.2 Effects of Fiber Surface Treatments on Mechanical Properties of Epoxy Composites Reinforced with Glass Fabric

Effects of different fiber surface treatments (acid activation and silane treatment) on mechanical behavior and fracture mechanism of glass fiber/epoxy composites were investigated experimentally. To regenerate the hydroxyl groups of glass fibers, activation pretreatment of heat cleaned woven glass fabric was performed using (v/v) HCl aqueous solution at different concentrations (1% and 3% (v/v)). The treatment of silanization of heat cleaned and acid activated glass fibers with γ-GPS (γ-glycidoxypropyltrimethoxysilane) were performed. Mechanical properties of the composites have been investigated by tensile tests, short beam shear tests and flexural tests. The short beam method was used to measure the interlaminar shear strength (ILSS) of laminates. The tensile and flexural properties of composites were characterized by tensile and three-point bending test, respectively. The fracture surfaces of the composites were observed with a scanning electron microscope (SEM).

4.1.2.1 Tensile Test

Typical stress–strain curves obtained from the tensile tests are shown in Figure 4.10. It is first noted that the tensile strength and elongation at break vary considerably depending on the acid activation treatments of heat cleaned glass fibers prior to silanization. When the glass fibers are first treated with HCl solution and then with silane coupling agent, the tensile strengths of the composites seem to decrease significantly. It is known that the change in fiber strength has a direct influence on the mechanical properties of glass fiber composites because the fiber strength determines the ultimate load-bearing capacity of the composites. The decreased tensile strengths due to acid pretreatments may be attributed to the reduction of fiber strength. Table 4.3 demonstrates the mechanical properties of the composite laminates.

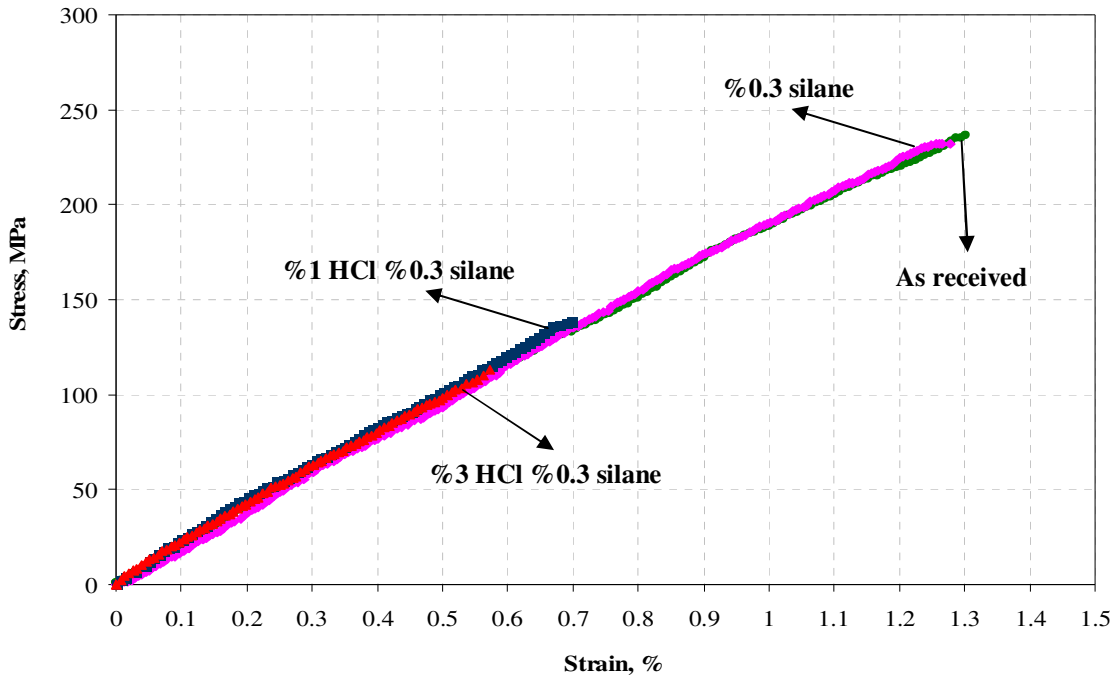

Figure 4.10 Tensile stress–strain curves of laminates

Table 4.3 Mechanical properties of glass fiber/epoxy composites

Composite	**Fiber volume fraction V_f (%)**	**Tensile modulus (GPa)**	**Tensile strength (MPa)**	**Elongation at break (%)**	**Flexure modulus (GPa)**	**Flexure strength (MPa)**	**ILSS (MPa)**
As received	39.3±1.6	17.12±0.85	236.26± 9.04	1.30± 0.12	19.76 ± 0.72	402.72 ± 12.80	27.98 ± 0.73
%0.3 silane	38.9±1.5	18.66 ± 0.91	232.15 ± 10.10	1.28 ± 0.11	19.56 ± 0.91	467.83 ± 13.40	50.87 ± 1.10
%1 hcl+%0.3 silane	39.1±1.5	17.93 ± 0.86	138.29 ± 6.01	0.70 ± 0.06	20.35 ± 0.92	251.36 ± 10.30	26.72 ± 0.68
%3 hcl+%0.3 silane	39.2±1.6	18.34 ± 0.91	113.27 ± 5.05	0.57± 0.05	19.26 ± 0.87	184.45 ± 9.52	21.20 ± 0.57

* The values after the (±) in all the tables refer the standard uncertainty of the measurement

As can be seen from Table 4.3, when the HCl concentration for acid pretreatment is increased to 3%, a further decrease of the tensile strength of the composite is noticed. The tensile strengths of the composites are decreased by approximately 41.5% for 1% HCl pretreatment + 0.3% γ-GPS treatment and 52% for 3% HCl pretreatment + 0.3% γ-GPS treatment in comparison with that of the as-received sample.

The decrease in fiber strength is possibly owing to chemical corrosion of glass fibers exposed to hydrochloric acid. E-glass is comparatively sensitive to acid attack and the soluble components are leached and resulted in siliceous hydrated material (Tanaka, Kuraoka, Yamanaka, & Yazawa, 1997). Strength loss of the glass fibers is caused by an ion exchange reaction (Jones & Betz, 2004; Qiu & Kumosa, 1997). The glass fibers will be chemically deteriorated as a consequence of non-siliceous ion leaching by ion-exchange reactions, i.e., the non-siliceous ions in the glass are replaced by the hydrogen ions in the acid (Qiu & Kumosa, 1997). Mechanism of the corrosion process is accepted, an ion exchange reaction, in which metal ions associated with the glass surface such as Ca2+ and Al3+ are replaced by H+ from the acid medium (Jones & Betz, 2004). It is believed that the acid treatments of the glass fibers prior to silanization may be responsible for the reduction in the tensile strength of the composites. It is thought that 3% HCl were strong and the fibers could be further damaged by occurring the interaction between the glass surface and HCl solution, thus resulting in lower tensile strength. On the other hand, González-Benito, Baselga, & Aznar (1999) investigated the influence of different activation pretreatments of glass fibers on the structure of an aminosilane (γ-aminopropyltriethoxysilane) coupling agent layer. According to their study, under acidic conditions, a great number of silanol groups are generated and greater coating degrees can be achieved. They found that the degree of silanization is the greatest for the acid activated samples. However, it is important to point out that the reduction in the tensile strength of the composites due to the chemical corrosion of glass fibers exposed to hydrochloric acid plays a vital role in the performance of composite materials. However, in the absence of acid activation, there is a little difference (1.7%) in the tensile strength of the composite containing only silane treated glass

fibers as compared to as-received glass fiber reinforced epoxy composite. It is interesting to note that although composite samples manufactured by acid activated fibers show small elongation at break values, all the test samples have almost similar tensile modulus. This indicates that all composites exhibit the same behaviors under tensile load.

4.1.2.2 Flexure Test

Flexural strength–middle span deflection curves of laminates were given in Figure 4.11. The flexural strengths of glass fiber/epoxy composites are presented in Table 4.3.

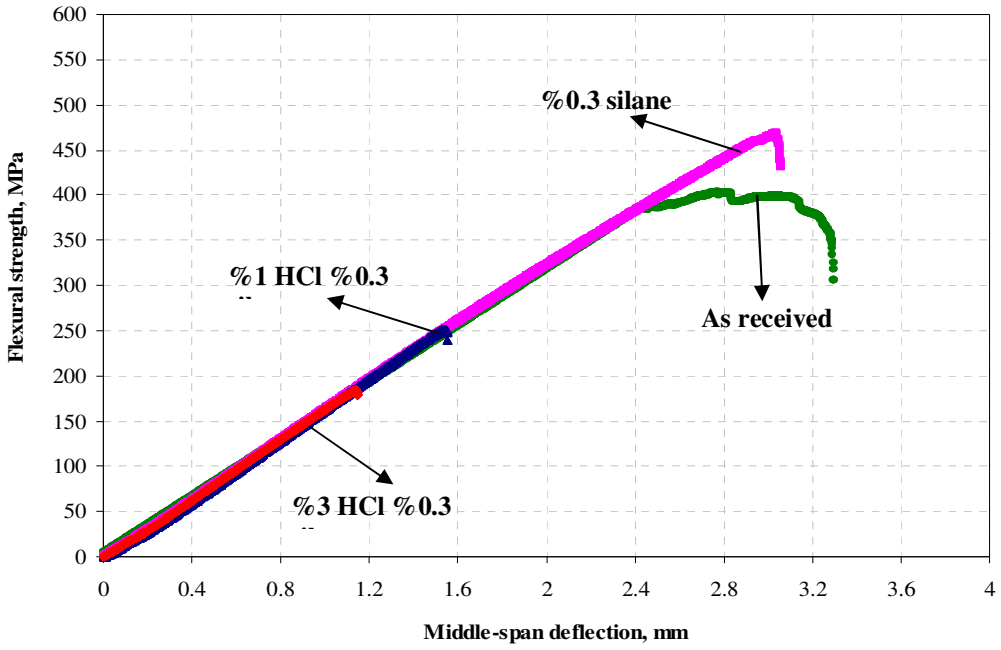

Figure 4.11 Flexural strength–Middle span deflection curves of laminates

It can be seen in Table 4.3 that the flexural strength of the composite is increased only with the silane treatment on the heat cleaned glass fiber. The flexural strength is enhanced by approximately 16% in comparison with that of the asreceived sample. This may indicate the contribution of the silane treatment in terms of enhancement of fiber/matrix adhesion. The flexural strength of fiber reinforced composites depends on the adhesion between the fiber and the matrix, as well as on the strength of both constituents (Li, Ye, & Mai, 1997). . Wang, Blum, & Dharani (1999) investigated

effect of interfacial mobility on flexural strength and fracture toughness of glass/epoxy laminates. Their results showed that the presence of silane coupling agent increased the flexural strength in both dry and wet samples. In their study, it was reported that the flexural strength increased probably due to the chemical bonding which occurs between the dissimilar phases. Shih & Ebert (1986) also point out that stronger interfacial strength leads to an increase in flexural strength. On the other hand, the flexural strengths of the composites are decreased with the acid activation treatments on the glass fibers. The flexural strengths of the composites are decreased by approximately 38% for 1% HCl pretreatment + 0.3% γ-GPS treatment and 54% for 3% HCl pretreatment + 0.3% γ-GPS treatment in comparison with that of the as-received sample. The remarkable reduction in the mechanical properties found in the composites may be mainly the result of glass fiber damage as mentioned above.

4.1.2.3 Short Beam Shear Test

The results from the short beam shear tests of the composites show the relationship between surface treatments of the glass fibers and mechanical interlaminar properties of the composites (Table 4.3). When the glass fibers are first treated with HCl solution particularly activated with 3% HCl solution and then with silane coupling agent, it can be seen that the ILSS values of the glass fiber/epoxy composites reduced as compared to that of composites containing as-received fibers. The interlaminar strengths of the composites are decreased by approximately 5% for 1% HCl pretreatment + 0.3% γ-GPS treatment of the glass fibers and 25% for 3% HCl pretreatment + 0.3% γ-GPS treatment of the glass fibers in comparison with that of the as-received sample (Table 4.3). It is clear from Table 4.3 that the composite prepared from γ-GPS treated glass fiber shows superior properties as compared to other composites. Kim & Mai (1998) point out that a decrease in bond strength and other deteriorating effects are expected to occur if the surface treatment is excessive, leading to severe damage of the fiber. Jones & Betz (2004) and Qiu & Kumosa (1997) reported that glass fibers in acid solution will be chemically deteriorated and cause strength loss of the glass fibers. It is believed that the acid treatments of the

glass fibers prior to silanization may be responsible for the reduction in the interlaminar shear strength of the composites. As shown in Table 4.3, use of silane coupling agent, only 0.3% γ-GPS treatment, for surface treatment improves the interlaminar shear strength of glass fiber/epoxy composite in comparison with the as-received one. The improvement indicates that the adhesion at the interfaces between the fiber and the resin is largely increased. The interlaminar strength is enhanced by approximately 82% in comparison with that of the as-received sample. It is probable that the improvement of the interlaminar shear strength of glass fiber/epoxy composite may be due to the chemical interaction at the fiber–matrix interface.

4.1.2.4 SEM Observation

Figure 4.12 a–d shows the SEM micrographs of the composite fracture surface obtained from tensile tests. As can be seen in Fig. 4.12 a, it was found that the surfaces of as-received fibers were smooth and clean and the fibers were pulled out from epoxy matrix. There is no evidence or traces of matrix resin adhering to the fiber. Indeed, the fiber surfaces seem to be clean and free from any adhering polymer. It is clear that the interfacial adhesion between the fibers and the matrix is poor. This observation suggests an adhesive failure in the interface (Iglesias, González-Benito, Aznar, Bravo, & Baselga, 2002). Therefore, the fracture mode of the as-received fiber reinforced composite is at the interface of the fiber/matrix and the interface structure cannot transfer stress effectively. When the fibers had only the silane coupling agent surface treatment, the failure surface seem to be different from the previous case. Improved fiber/matrix adhesion was able to be seen in SEM photographs of fracture surfaces of the glass fiber/epoxy composite (Fig. 4.12 b). A large amount of epoxy resin adhered to the fiber surfaces and formed a thick layer clearly indicate good interfacial interaction between the fiber and the resin and the cohesive failure at the matrix occurs. There are large amount of resin adhered on 1% HCl pretreated + 0.3% γ-GPS treated glass fiber surface (Fig. 4.12 c) which shows to enhance the interfacial adhesion between the glass fiber surface and resin and the cohesive failure at the matrix occurs. For 3% HCl pretreated + 0.3% γ-GPS treated glass fibers (Fig. 4.12 d), all fibers seem in epoxy resin after failure. The failure

surface seems to be uniform. The cohesive failure at the matrix indicates an increase when the HCl concentration is increased up to 3%. This suggests the strongest interfacial interaction between fiber and matrix. On the other hand, as shown in Figure 4.12 c and d, it is emphasized here that the increase in fiber–matrix interfacial interaction did not cause the increase in ILSS values (Table 4.3). This is due to fact that when the surface treatment is excessive, this will lead to severe damage of the fiber and cause a decrease in ILSS of the composites.

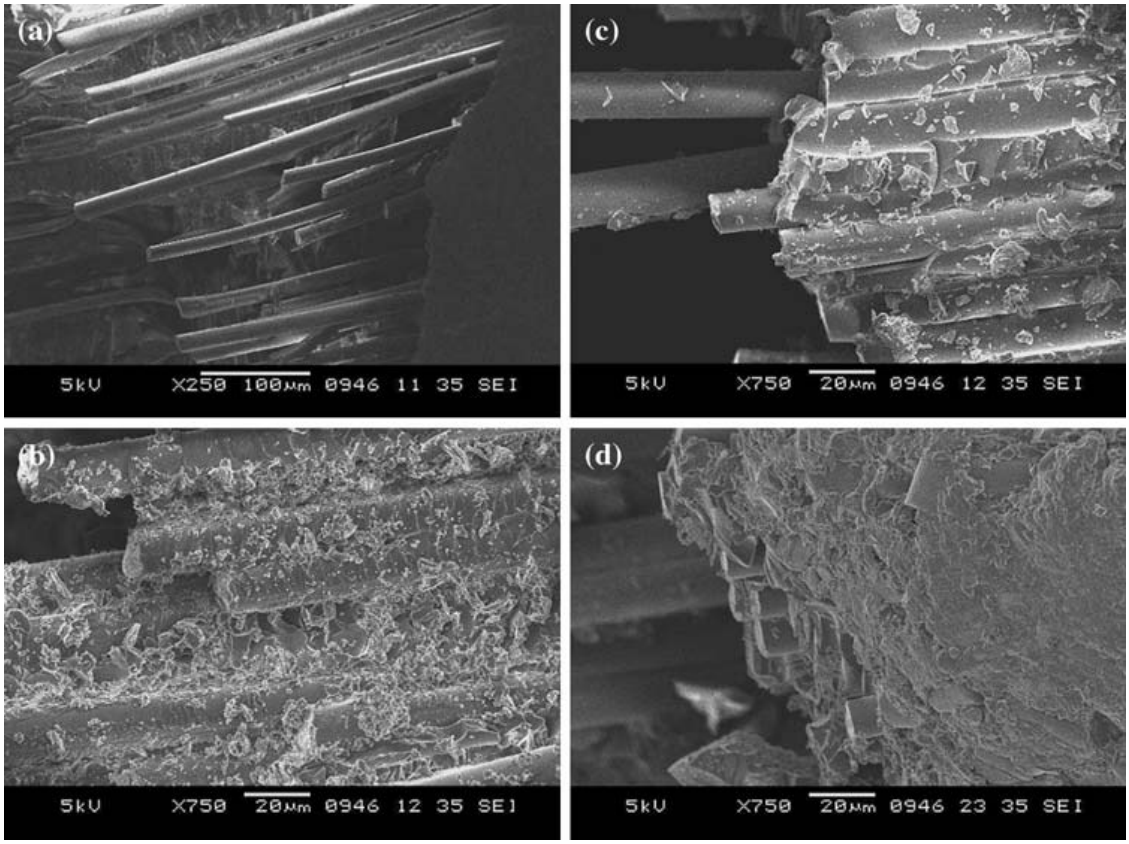

Figure 4.12 Representative SEM images of the breakage region for (a) as-received glass fiber reinforced epoxy composite; (b) 0.3% Silane treated glass fiber reinforced epoxy composite; (c) 1% HCl and 0.3% silane treated glass fiber reinforced epoxy composite; (d) 3% HCl and 0.3% silane treated glass fiber reinforced epoxy composite that were tensile-tested in machine direction

4.1.3 Concentration Effect of γ-Glycidoxypropyltrimethoxysilane on the Mechanical Properties of Glass Fiber–Epoxy Composites

Heat cleaned glass fibers were modified using γ-glycidoxypropyltrimethoxysilane (γ-GPS) of different concentrations to improve the interfacial adhesion at interfaces between fibers and matrix. Effects of γ-GPS on mechanical properties and fracture behavior of glass fiber/epoxy composites were investigated experimentally. Mechanical properties of the composites have been investigated by tensile tests, short beam shear tests, and flexure tests. The short-beam method was used to measure the interlaminar shear strength (ILSS) of laminates. The tensile and flexural properties of composites were characterized by tensile and three-point bending tests, respectively. The fracture surfaces of the composites were observed with SEM.

4.1.3.1 Tensile Test

The variations of tensile properties of the heat-cleaned and γ-GPS silane-treated fiber composites were shown in Table 4.4 and Figure 4.13.

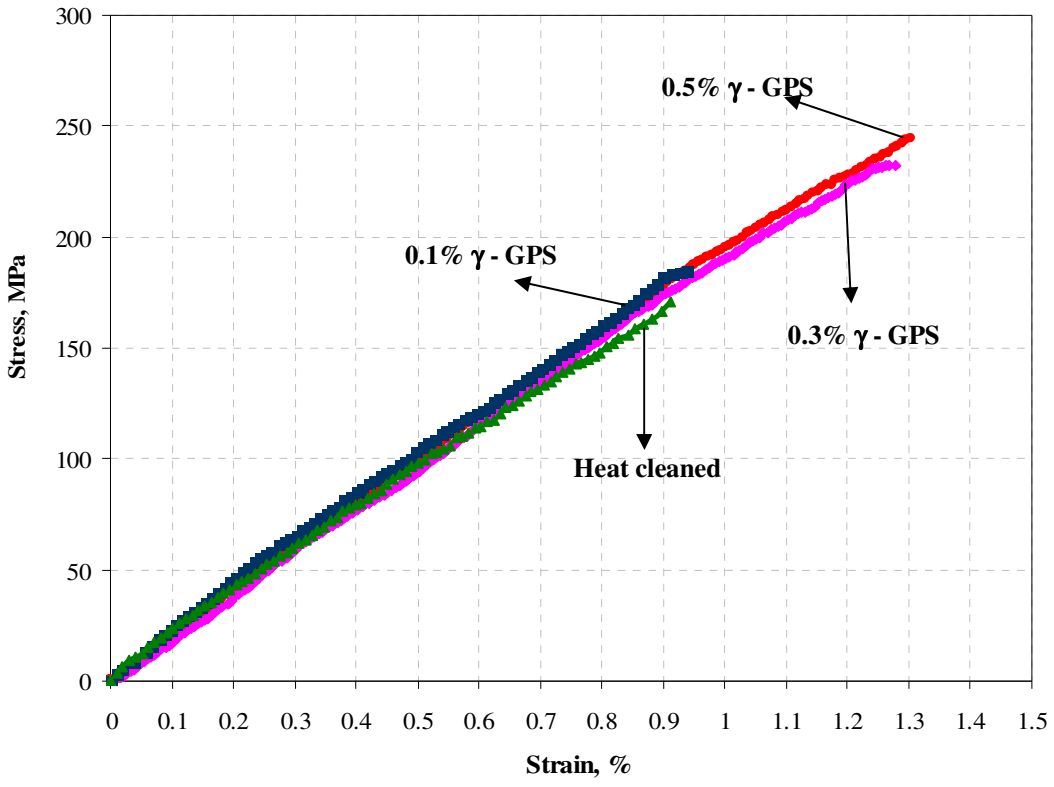

Figure 4.13 Tensile stress–strain curves of composite laminates

Table 4.4 Mechanical properties of glass fiber/epoxy composites

Composite	**Fiber volume fraction V_f (%)**	**Tensile modulus (GPa)**	**Tensile strength (MPa)**	**Elongation at break (%)**	**Flexure modulus (GPa)**	**Flexure strength (MPa)**	**ILSS (MPa)**
As received	39.3±1.6	17.12±0.85	236.26± 9.04	1.30± 0.12	19.76 ± 0.72	402.72 ± 12.80	27.98 ± 0.73
Heat cleaned	37.8±1.6	18.69 ±0.87	170.74 ± 6.35	0.92± 0.05	17.15± 0.72	257.05 ± 7.60	31.05 ± 0.81
%0.1 silane	40.3±1.5	20.18 ± 0.94	184.81 ± 7.67	0.94± 0.05	18.75± 0.87	381.23 ± 10.60	42.78 ± 1.52
%0.3 silane	38.9±1.5	19.68 ± 1.07	232.15 ± 10.00	1.28± 0.11	18.49 ± 0.91	467.834 ± 13.40	50.87 ± 1.10
%0.5 silane	39.8±1.5	20.17 ± 1.16	245.95 ± 11.00	1.30± 0.12	19.56 ± 0.93	481.54 ± 14.20	52.72 ± 0.57

* The values after the (±) in all the tables refer the standard uncertainty of the measurement.

The normalized tensile properties of glass fiber/epoxy composites with the volume fraction of 38.9% were presented in Figure 4.14. The comparisons were carried out according to normalized values.

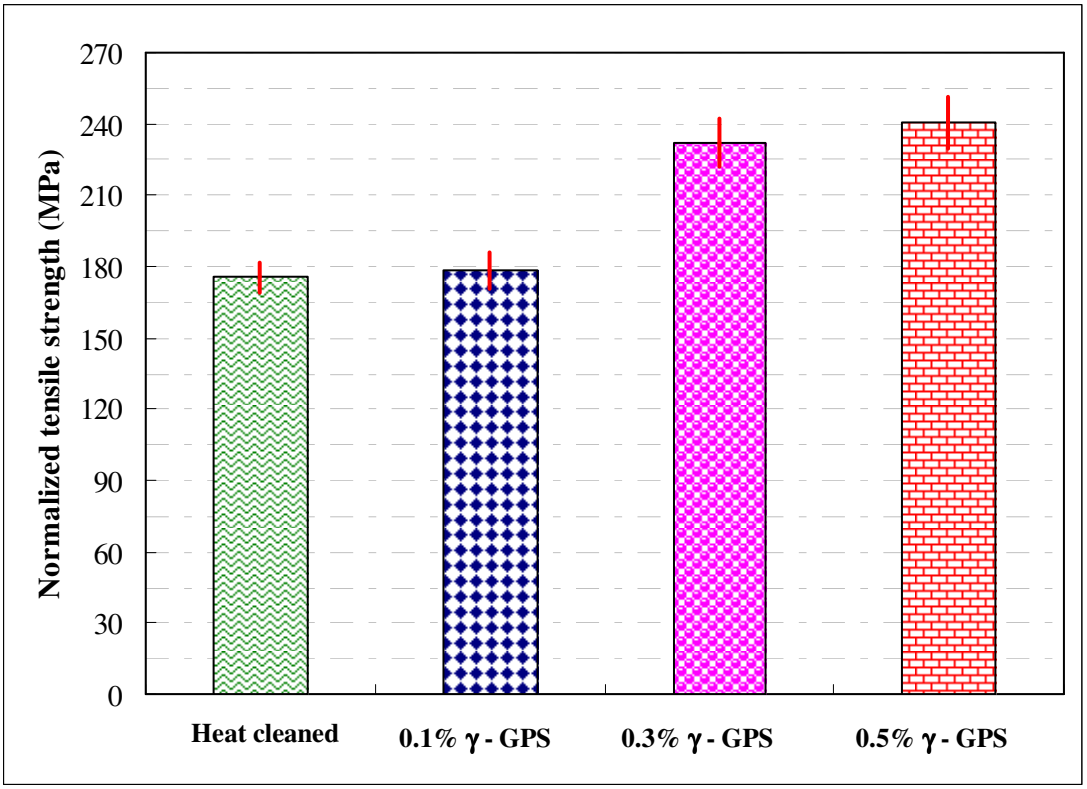

Figure 4.14 Effect of silane concentration on normalized tensile strength

The tensile strengths of epoxy composite containing γ-GPS silane-treated glass fiber reinforcement were higher than that of heat-cleaned glass fiber composite. It is clearly seen that among the surface-treated fiber composites, 0.1% (v/v) γ-GPS treated fiber composite shows the least improvement in terms of tensile strength. Moreover, the tensile strength increases with the increase of γ-GPS concentration in the range of 0.1–0.5%. As the concentration of silane solution increased up to 0.3% (v/v), the tensile strength of composites increased by 32.2% over that of heat-treated fiber composites. A maximum strength value was observed for a silane concentration of 0.5% (v/v). The tensile strength is increased from 175.71 MPa for the heat-cleaned glass fiber–epoxy composite to 240.39 MPa for the 0.5% GPS-treated glass fiber–epoxy composite, that is, a 37% increase. The enhancement in tensile strength of the

silane-treated glass fiber-based epoxy composites may be due to the improved adhesion between the fiber and the matrix. This improved adhesion might have enhanced the interfacial bonding, and thus made it easier for the stress to be effectively transferred from the matrix to the fiber. Mehta, Drzal, Mohanty, & Misra (2006) reported that increase in tensile strength and modulus of the chemically treated fiber-based composites may be a result of the improved adhesion between the fiber and the matrix. Morales, Olayo, Cruz, Herrera-Franco, & Olayo (2006) signified that materials with strong interfaces have a high tensile strength and high rigidity. Also, they reported that the structure and properties of the interface play a very important role on the physical and mechanical properties of the composites because of the stress transfer between the matrix and the fibers. The work by Madhukar & Drzal (1991) has revealed that the improvement in longitudinal tensile strength depends on the improved interfacial adhesion strength. Briefly, it may be reported that improved adhesion between the fiber and the matrix leads to an increase in tensile strength of silane-treated glass fiber–epoxy composites.

4.1.3.2 Flexure Test

It is known that flexure test emphasizes the importance of fiber–matrix adhesion on flexural strength. Figure 4.15 shows the flexural properties of the heat cleaned and γ-GPS silane-treated glass fiber reinforced composites. The normalized flexural properties of glass fiber/epoxy composites with the volume fraction of 38.9% were summarized in Figure 4.16.

Heat-cleaned glass fiber reinforced composites had the lowest flexural strength, which was due to a poor interface between fiber and resin. Also, the flexural strength of heat-cleaned glass fiber reinforced composites was 36.2 % lower as compared with that of asreceived. γ-GPS-treated glass fiber reinforced composites (0.5%) had the highest flexural strength. Besides, all γ-GPS-treated glass fiber–epoxy composites showed the tendency to significantly increase the flexural strength compared to heatcleaned glass fiber–epoxy composites.

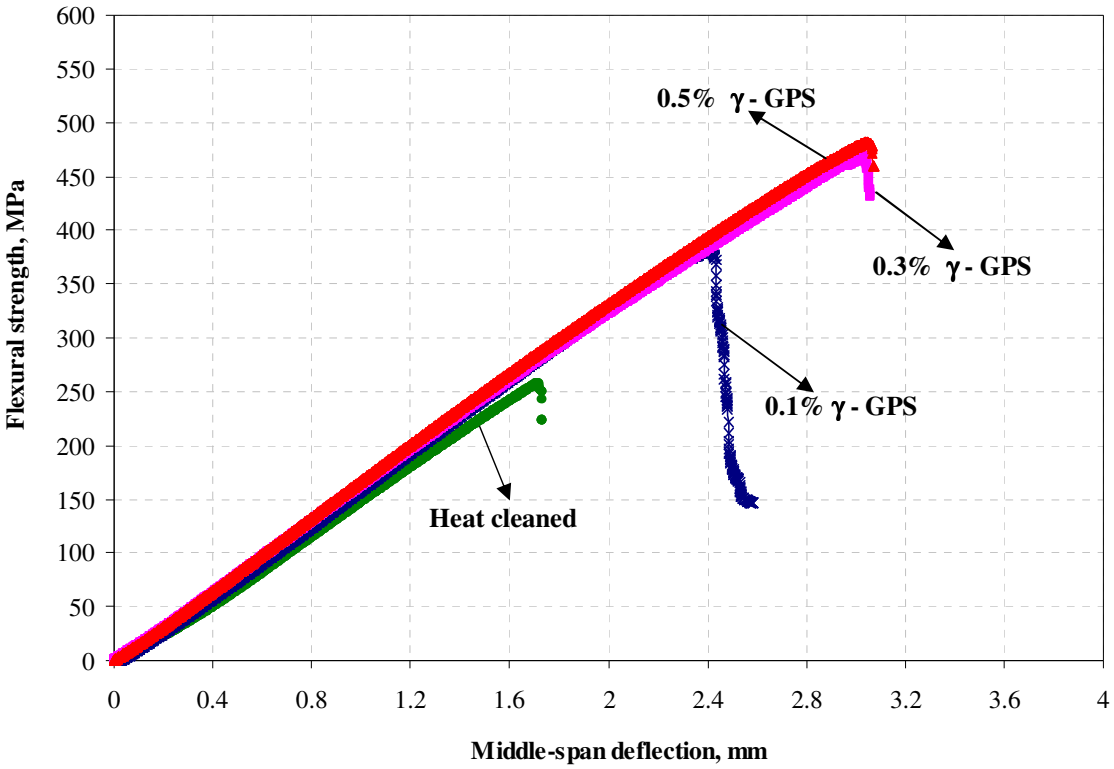

Figure 4.15 Flexural strength–Middle span deflection curves of laminates

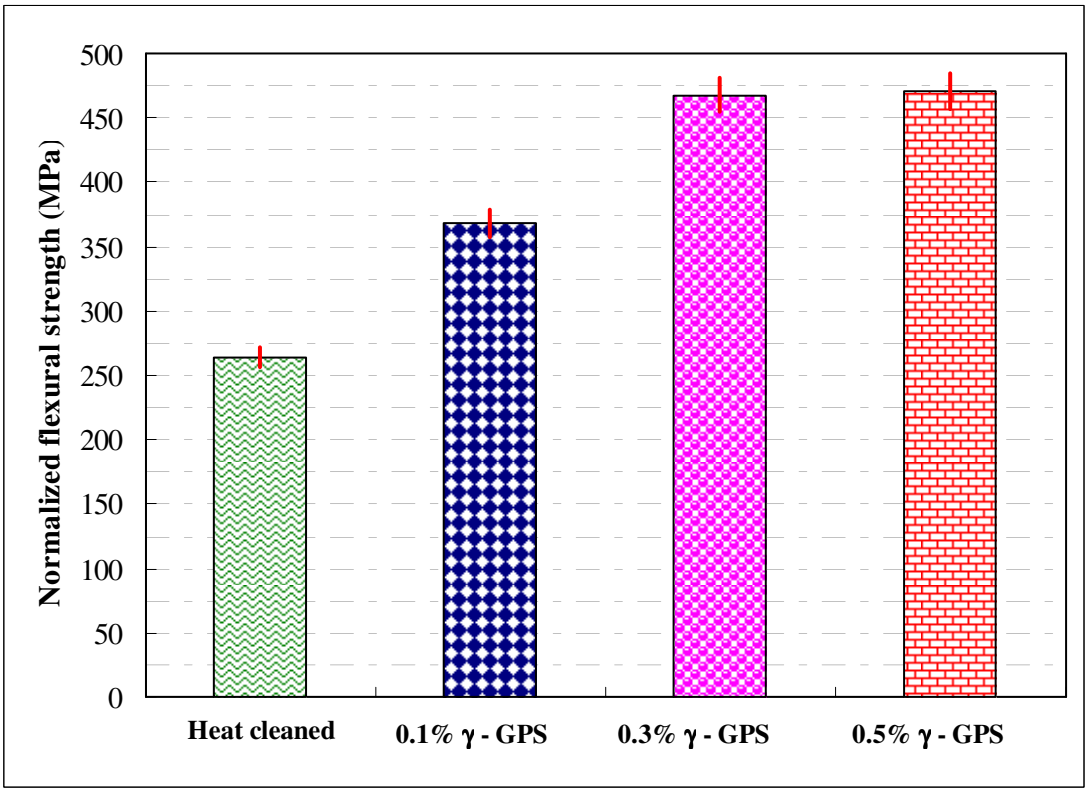

Figure 4.16 Effect of silane concentration on normalized flexural strength

As it was also seen in Figures 4.15 and 4.16 that the flexural strength of the composites increases with increasing γ-GPS silane concentration. The flexural strengths of the composites are increased by 39% for 0.1% γ-GPS treatment, 77% for 0.3% γ-GPS treatment, and 78% for 0.5% γ-GPS treatment in comparison with that having no treatment. It is probable that the increased flexural strength was the result of good adhesion between the glass fibers and epoxy. This may indicate the contribution of the silane treatment in terms of enhancement of fiber/matrix adhesion. According to Wang, Blum, & Dharani (1999), the presence of silane coupling agent increases the flexural strength in both dry and wet samples probably because of the chemical bonding occurring between the dissimilar phases.

4.1.3.3 Short Beam Shear Test

ILSS results of composites reinforced by glass fibers treated at different concentrations were shown in Table 4.4. The normalized ILSS properties of glass fiber/ epoxy composites with the volume fraction of 38.9% were given in Figure 4.17. From this figure, it is seen that the γ-GPS treatment improves the ILSS of glass fiber-epoxy composites. The ILSS values of heat-cleaned glass fiber reinforced composite is enhanced by 27, 57, and 59% as a result of fiber treatment with 0.1, 0.3, and 0.5% γ- GPS respectively. Besides, the ILSS of the γ-GPS treated glass fiber/epoxy composites enhanced as compared with that of as-received one. This increment was obtained to be approximately 88%. It is generally known that the lowest ILSS is the result of inadequate fiber–matrix interaction. From the ILSS results, it is noted that the presence of silane coupling agent leads to an increase of ILSS of the composites. It can be related to increase in the degree of adhesion at interfaces among the three elements, i.e., fiber, matrix, and silane coupling agent (Park & Jin, 2001, 2003; Park, Jin, & Lee, 2000). The chemical bonding between glass fibers and matrix resin may be responsible for these results. γ-GPS possesses both organic and inorganic reactivity that allows it to react with organic polymers and inorganic surface. The methoxysilyl group of γ-GPS is subject to hydrolysis in water, and as a consequence of this reaction silanetriol forms as follows: Silanol groups are capable of condensing with hydroxyl groups at the surface of glass and

siliceous minerals. It can be written this way as after condensing with the glass surface, the remaining silanol groups are capable of hydrogen bonding or condensing with adjacent silanol groups. By this combination of covalent and hydrogen bonding, the coupling agent is bonded to the inorganic surface, and modifies it so that it becomes organoreactive. Thereafter, this organoreactivity improves the adhesion capability of glass fiber with epoxy matrix.

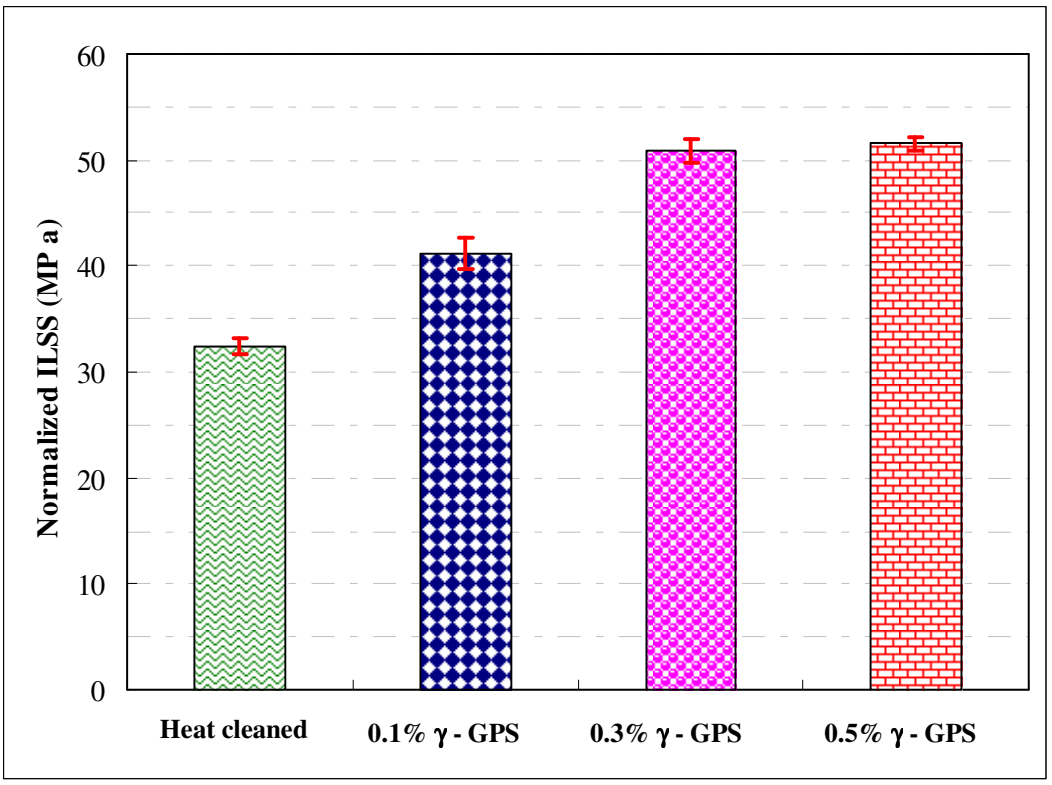

Figure 4.17 Effect of silane concentration on normalized interlaminar shear strength

4.1.3.4 SEM Observation

Tensile fracture surfaces of produced composites were examined by means of SEM, which was used to analyze the level of fiber/matrix adhesion. Figure 4.18 a–d shows the SEM micrographs of the composite fracture surface obtained from tensile tests. As can be seen in Figure 4.18 a, it was observed that the fiber surfaces almost seem to be clean and free from any adhering polymer. The surfaces of heat-cleaned fibers were smooth, and the fibers were pulled out from epoxy matrix. It indicates a weak interface between heat-treated fibers and epoxy matrix. In other words, when

stress is applied on the composite that is produced by using heat-cleaned fiber, fibers will be easily pulled out from the epoxy matrix. Although cavities or gaps cannot be seen from SEM images, it is probable that, after pull-out, it may leave gapping holes in the matrix. When the fibers had the γ-GPS silane treatment, the failure surface seems to be different from the previous case. Improved fiber/matrix adhesion was seen in the SEM photographs of fracture surfaces of the glass fiber/ epoxy composite (Figure 4.18 b–d). It can be noted that fibers do not exhibit pull-out effect due to good adhesion between epoxy resins and γ-GPS-treated glass fibers. The surfaces of the fibers were not smooth and clean. A large amount of epoxy resin adhered to the fiber surfaces and formed a thicker layer, clearly indicating good interfacial interaction between the fiber and the resin. As a result, SEM images support that chemical modification of glass fibers with γ-GPS has altered the fiber surface and improved the adhesion between the fiber and epoxy matrix.

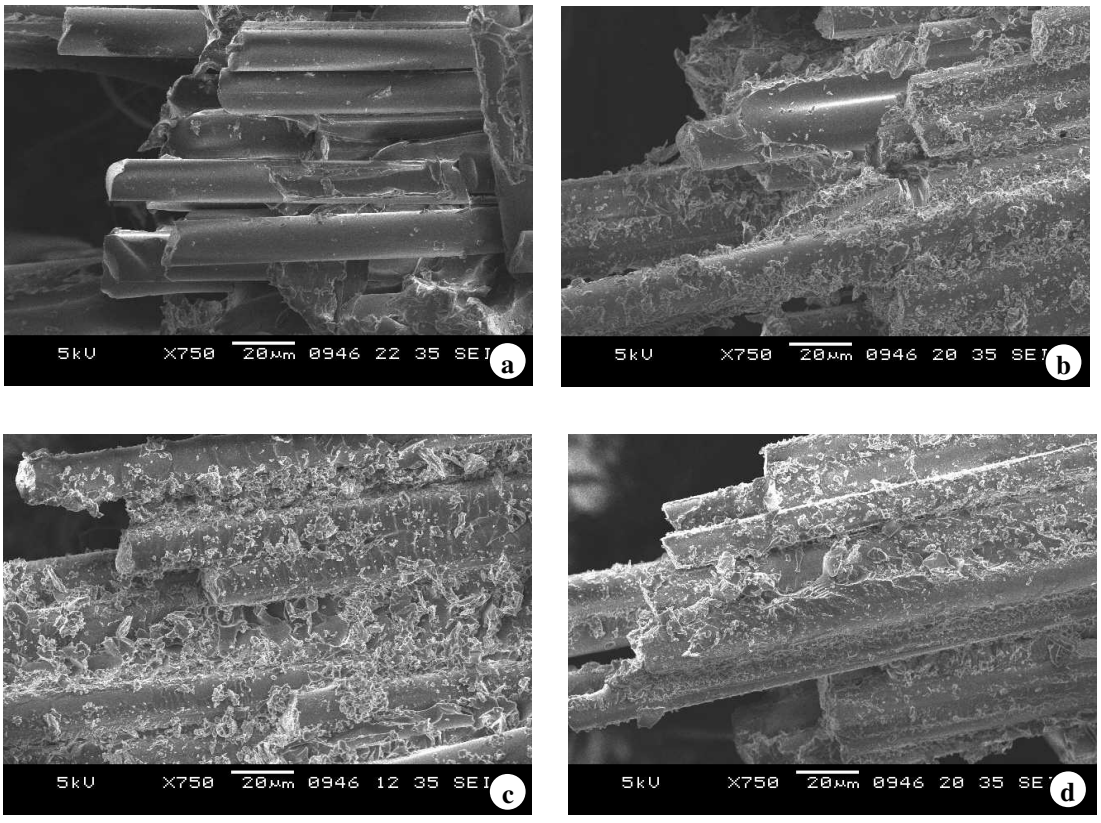

Figure 4.18 Representative SEM images of the breakage region for **(a)** heat cleaned glass fiber reinforced epoxy composite; **(b)** 0.1% γ-GPS treated glass fiber reinforced epoxy composite **(c)** 0.3% γ-GPS treated glass fiber reinforced epoxy composite **(d)** 0.5% γ-GPS treated glass fiber reinforced epoxy composite that were tensile tested in machine direction.

4.2 Plasma Polymerization Studies

4.2.1 Preparation and Characterization of Thin Films by Plasma Polymerization of γ-GPS

The study examines the influence of plasma power and exposure time on the properties of thin films prepared by plasma polymerization of γ-GPS on the glass substrate. Low frequency plasma generator was used to prepare plasma polymer thin films of γ-GPS (PlzP-γ-GPS) on glass substrates at different plasma powers (30, 60 and 90W) and exposure times (5, 15 and 30 min). The obtained films are characterized by different techniques of surface analyses. XPS analyses were utilized to reveal the presence of functional groups in plasma polymer films. Contact angle measurements were performed to evaluate surface characteristics. Morphologies of the plasma polymer thin films of γ-GPS (PlzP-γ-GPS) formed on the glass substrates were investigated by atomic force microscopy (AFM).

4.2.1.1 XPS Analysis

Elemental compositions from XPS spectra were at different plasma powers and plasma exposure times were given in Figures 4.19 and 20, respectively. As can be seen from Figure 4.19, C content of PlzP-γ-GPS films decreases with increasing of power from 30 to 60 W. However with the increasing of plasma power from 60 to 90 W, C content increases. From the viewpoint of oxygen content, it was obtained that firstly increase and later decrease, which is also in opposite to C regime from 30 to 90 W, was observed. Yue & Padmanabhan (1999) indicated that the surface oxygen content is crucial for good wetting and bonding of the resin. Lai et al. (2006) also reported that the ratio of oxygen atom on the surface increases due to fact that the number of oxygen-containing groups rises up. Also, their results showed that varieties of oxygen-containing groups on surface were responsible for the change of hydrophilicity. Si content pursued an increase with increasing of plasma power from 30 to 60 W. But, increasing power to 90 W, Si content did not change so much. When plasma power increases from 30 to 60 W, Si/C ratio increases, it implies a

more inorganic plasma polymer. However a decrease was observed at plasma power of 90 W. This exhibits organic character of plasma polymer with enhanced power to 90 W. Namely, plasma power causes changes in organic/inorganic character of plasma polymer. As can be seen in Figure 4.20, with the increasing of plasma exposure time at 30 W, while Si and O contents are increasing, C content decreases.

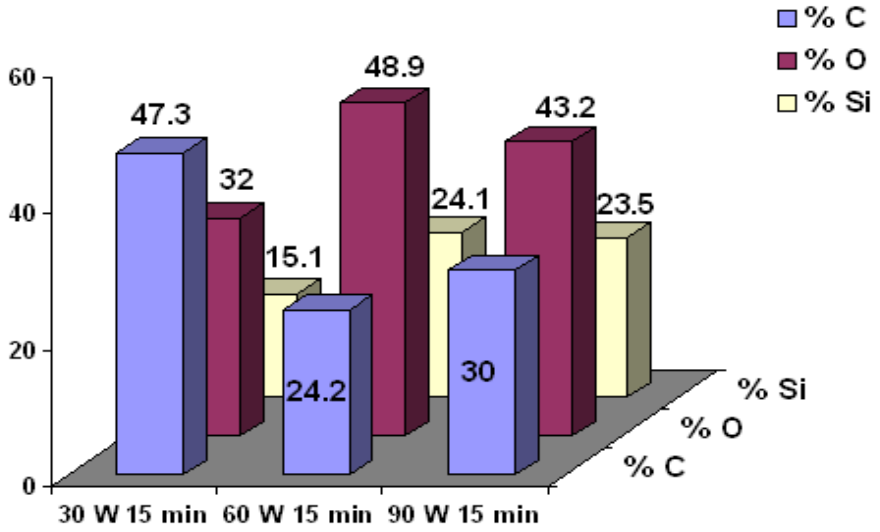

Figure 4.19 Elemental compositions of PlzP-γ-GPS films at different plasma powers (at 15 min)

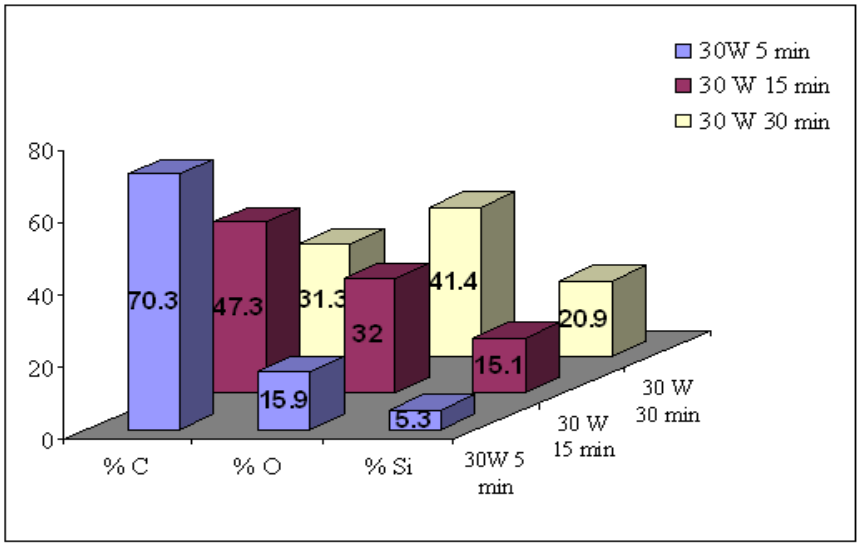

Figure 4.20 Elemental compositions of PlzP-γ-GPS films at different plasma exposure time (at 30 W)

O/C ratios were obtained to be 0.2, 0.7 and 1.3 for 5, 15 and 30 min, respectively. It indicates an increase in the O/C ratio with the increase of plasma exposure time. This shows that the plasma treatment may introduce more oxygen-containing groups. It can be also added that varieties of oxygen-containing groups on surfaces were responsible for the change of hydrophilic character of surface. Si/C ratios appear to be 0.1, 0.3 and 0.7 for 5, 15 and 30 min, respectively. Increasing of plasma exposure time at 30W resulted in increase of inorganic character of PlzP-γ-GPS films on glass substrate. In other words, in the event that plasma exposure time increases, the Si/C ratio increases, implying a more inorganic plasma polymer. In order to accurately determine the contents of functional groups of C and Si atoms, deconvolution was carried out.

Figures 4.21-26 show C1s curve-fitting spectra at different plasma powers (30, 60 and 90 W) and plasma exposure times (5, 15 and 30 min), respectively. C1s core level spectra of PlzP-γ-GPS film were deconvoluted into three distinct components. The first one, C1s(1), located at 284.6 eV corresponds to the carbon atom of C–C or C–H group. The second one C1s(2), located at 286.2 eV is attributed to the carbon atom of C–O or C–O–C group. The third one, C1s(3), located at 284.3 eV is assigned to the carbon atom of C–Si group (Zuri, Silverstein, & Narkis, 1996; Xu et al. 2007). The percent contribution of each curve was calculated from curve fitting of C1s peaks and they were summarized in Tables 4.5 and 4.6 for different plasma powers and exposure times, respectively. As can be seen from Table 4.5, relative content of C–Si bonds decreases with the increasing of plasma power from 30 to 90 W. It is probable that Si–C bonds may be broken with increasing of plasma power during plasma polymerization of γ-GPS onto glass substrate. It is worth mentioning that relative concentration of C–C or C–H bonds also slightly increases with the increasing of plasma power from 30 to 90 W. The relative concentrations of C–O or C–O– C bonds are almost the same. However, C–Si bond which possesses the lowest standard bond energy among these bonds are firstly broken with the application of plasma power. Therefore increasing of plasma power leads to decrease in the relative concentration of C–Si bonds. These changes may be related to chain-scission and

formation of small hydrocarbons and some gases such as carbon dioxide or carbon monoxide. These hydrocarbons contain mostly C–C or C–H and C–Si bonds.

Table 4.5 Relative percentage of **C1s** on PlzP-γ-GPS glass surface at different plasma powers

Power / time / Functional Group	30 W / 15 min (%)	60 W / 15 min (%)	90 W / 15 min (%)
C-C, C-H	64	68	70
C-O or C-O-C	2	3	4
C-Si	34	29	26

Table 4.6 Relative percentage of **C1s** on PlzP-γ-GPS glass surface at different exposure times

Power / time / Functional Group	30 W / 5 min (%)	30 W / 15 min (%)	30 W / 30 min (%)
C-C, C-H	18	65	74
C-O or C-O-C	-	1	8
C-Si	82	34	18

From Table 4.6, the observations exhibit that at low plasma exposure time (5 min) carbon atom is bound to mostly Si atoms and slightly carbon or hydrogen atoms. As can be seen from surface analysis by XPS, C–O or C–O–C functional groups are almost not detected at for 5 and 15 min at 30 W. However with the increasing of plasma exposure time, the percentage of C–O or C–O–C groups increases up to 8% at 30 min. It is probable that due to epoxy ring opening, C–O–C bond formation (cross-linking) may occur and this leads to increase in the concentration of C–O–C group. The relative content of C–C or C–H groups increases from 18% to 74% with increasing of plasma exposure time from 5 to 30 min. In contrast, Si–C group decreases from 82% to 18% with increasing of plasma treatment time from 5 to 30 min at 30 W. This might also be explained by chain fragmentation mechanisms and breaking of the bonds accompanying the decrease of Si–C group. Thus, new

chemical structures generate. It is known that standard bond energy of Si–C is lower than that of Si–O. Such being the case, Si–C bonds are broken firstly and a decrease in Si–C bonds takes place. On the condition that Si–C bonds subjected to plasma power longer time, breaking of Si–C bonds also enhances.

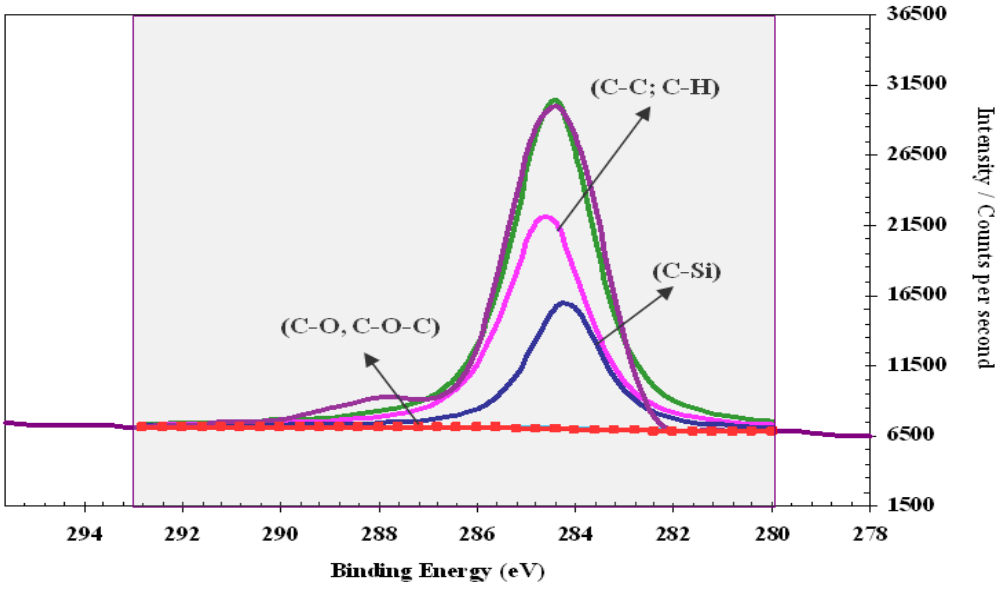

Figure 4.21 High resolution XPS spectra showing the deconvoluted C1s envelope for 30 W–15 min

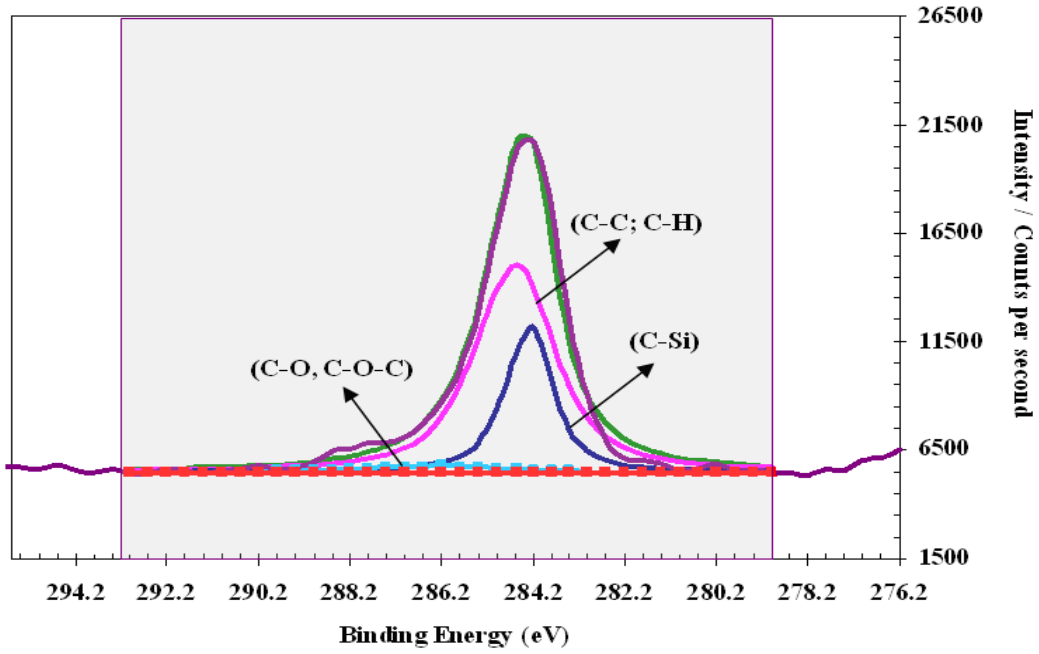

Figure 4.22 High resolution XPS spectra showing the deconvoluted C1s envelope for 60 W–15 min

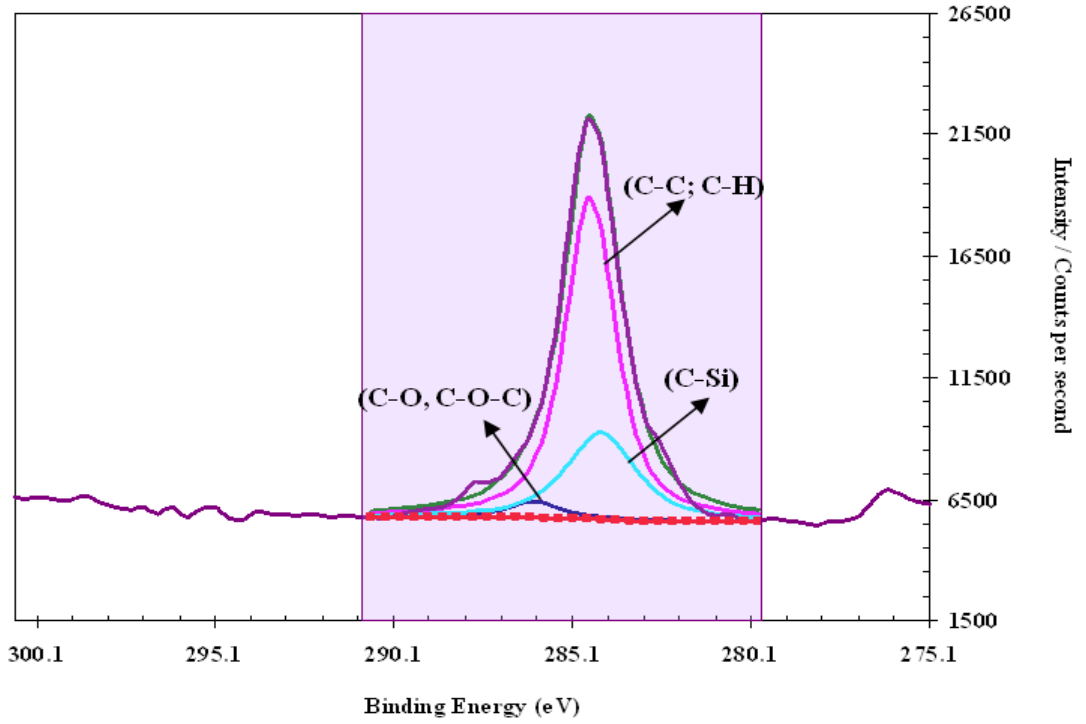

Figure 4.23 High resolution XPS spectra showing the deconvoluted C1s envelope for 90 W–15 min

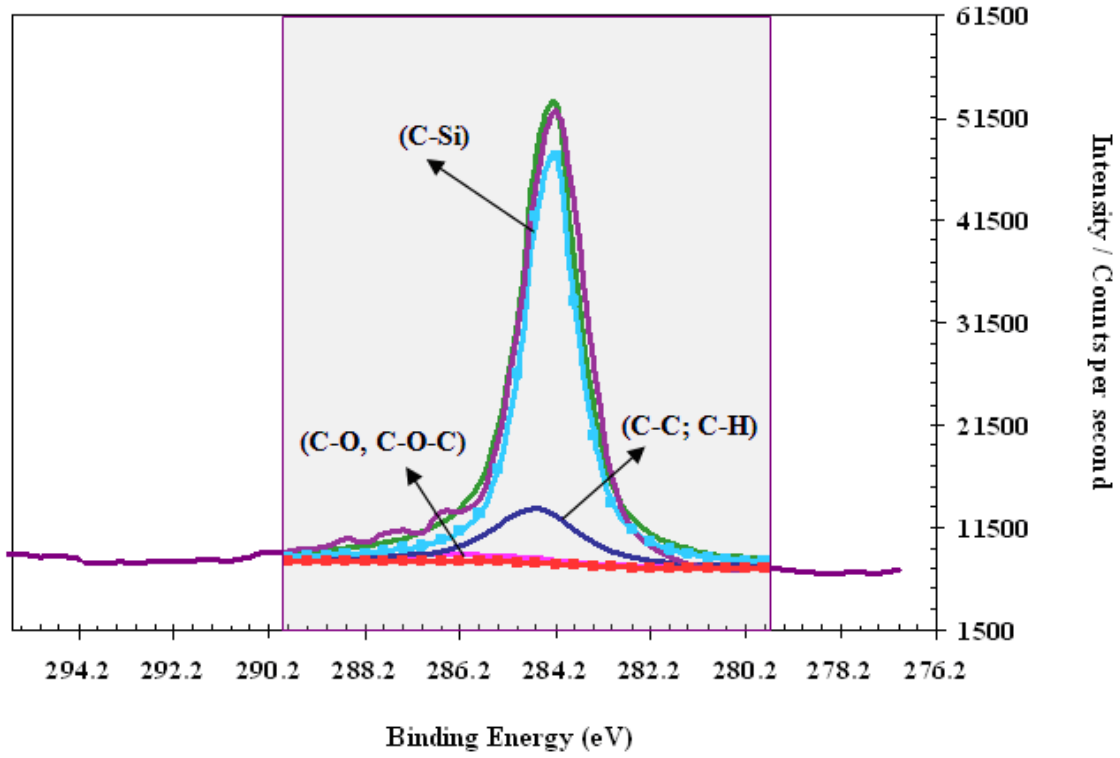

Figure 4.24 High resolution XPS spectra showing the deconvoluted C1s envelope for 30 W–5 min

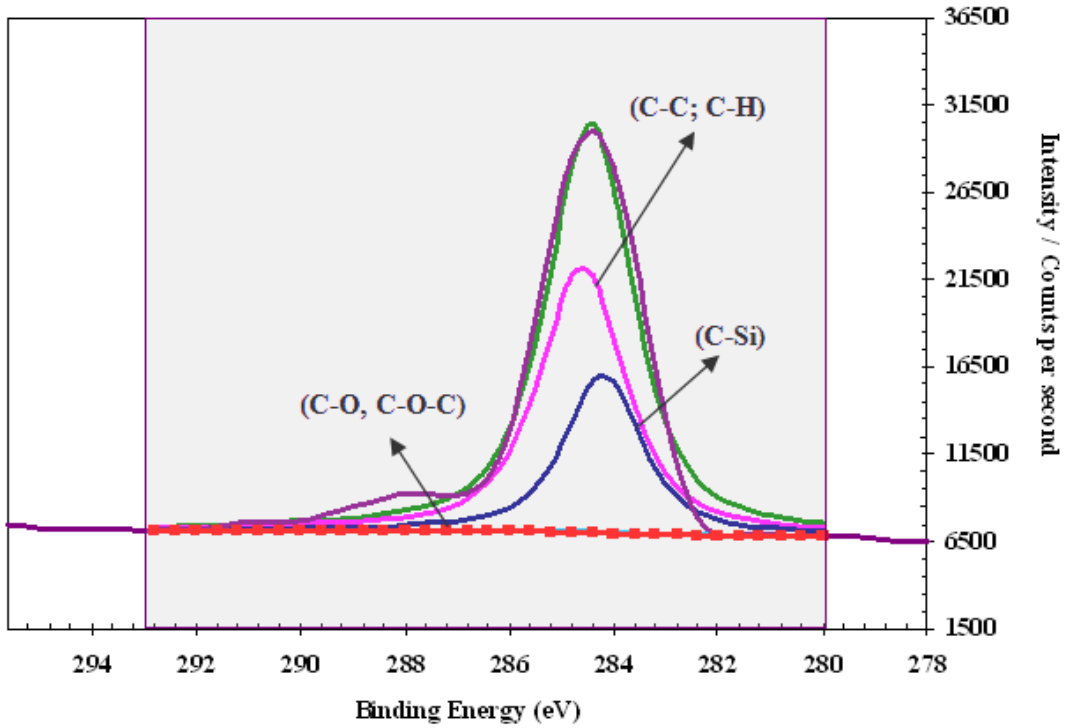

Figure 4.25 High resolution XPS spectra showing the deconvoluted C1s envelope for 30 W–15 min

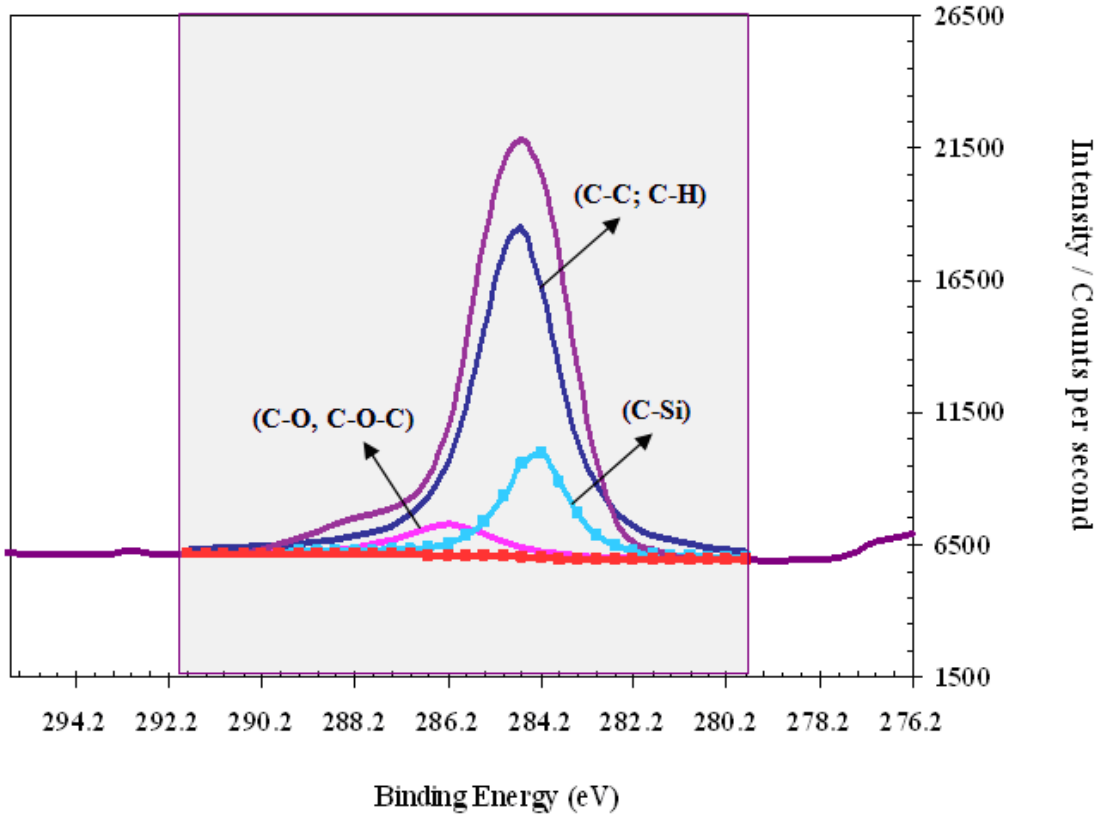

Figure 4.26 High resolution XPS spectra showing the deconvoluted C1s envelope for 30 W–30 min

The narrow scan spectra of the Si2p regions were deconvoluted into the surface functional groups, and contributions were given in Figures 4.27-32 for different plasma powers and exposure times, respectively. Close examination of the Si2p spectrum explains peaks at 103.4, 102.8, 102.1, 101.5, and 100.9 eV corresponding to $Si–(O)_4$, $(R)_1–Si–(O)_3$, $(R)_2–Si–(O)_2$, $(R)_3–Si–(O)_1$ and $Si–(R)_4$, respectively, as presented in Figures 4.27-32 (Lin, Liao, & Hu, 2009).

Relative concentrations of the Si2p at different plasma powers were summarized in Table 4.7. As can be seen from Table 4.7, the relative content of chemical bond $(R)_1–Si–(O)_3$ was obtained to be 24%, 42% and 73% at 30, 60 and 90 W, respectively. In other words, increasing of plasma power increases relative content of $(R)_1–Si–(O)_3$. The proportion of chemical bond $(R)_2–Si–(O)_2$ decreases from 39% to 18% with an increase of plasma power from 30 to 90W. Table 4.7 shows that the proportion of chemical bond $(R)_3–Si–(O)_1$ results in a decrease with the increasing of plasma power from 30 to 90 W. It can be added that the relative content of chemical bond $Si–(R)_4$ also decreases with increasing of plasma power. It is worth noting that there is no any chemical bond $Si–(R)_4$ at 90W. It can be inferred that when higher plasma powers are applied, relative amount of Si–C groups decreases and the amount of Si–O bonds increases.

In other words, the amount of Si–O bonds is greater than that of Si–C bonds at higher plasma powers. It seems that PlzP-γ-GPS on glass substrate is sensitive to plasma power. It can be also said that plasma polymer contains actually hydrocarbon chain containing C–C/C–H, C–O and Si–O. The hydrocarbon chain containing mostly C–C/C–H plays a significant role in the hydrophobic behavior of the surface.

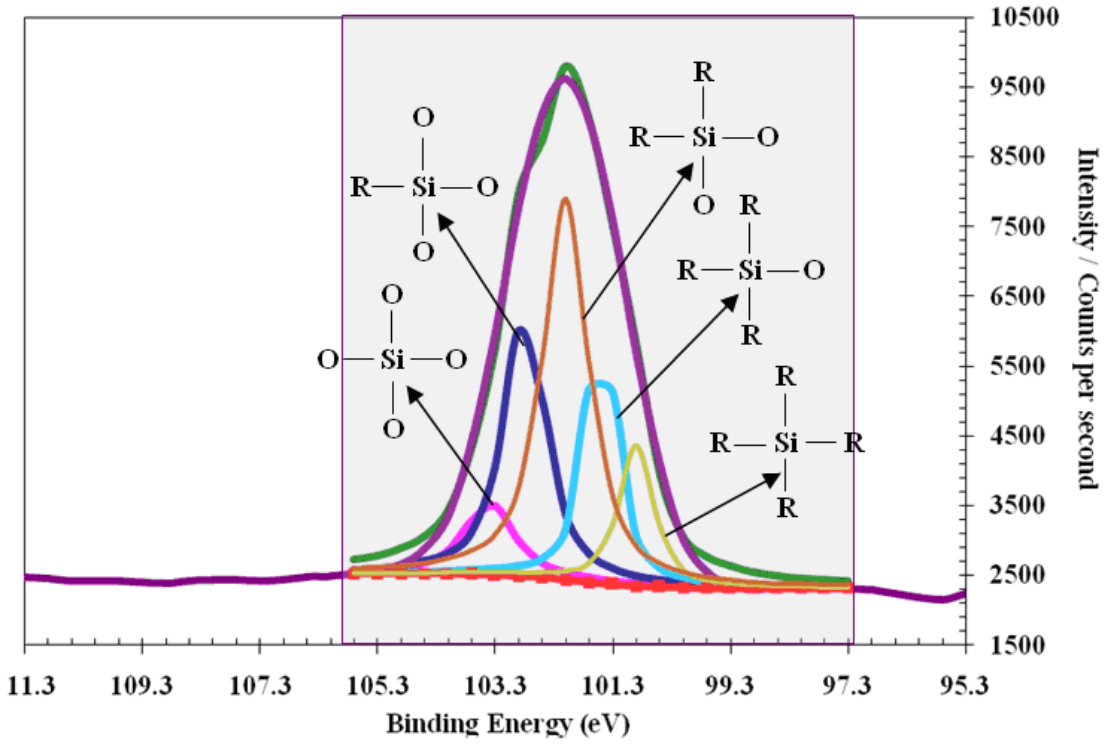

Figure 4.27 High resolution XPS spectra showing the deconvoluted Si2p envelope for 30 W–15 min

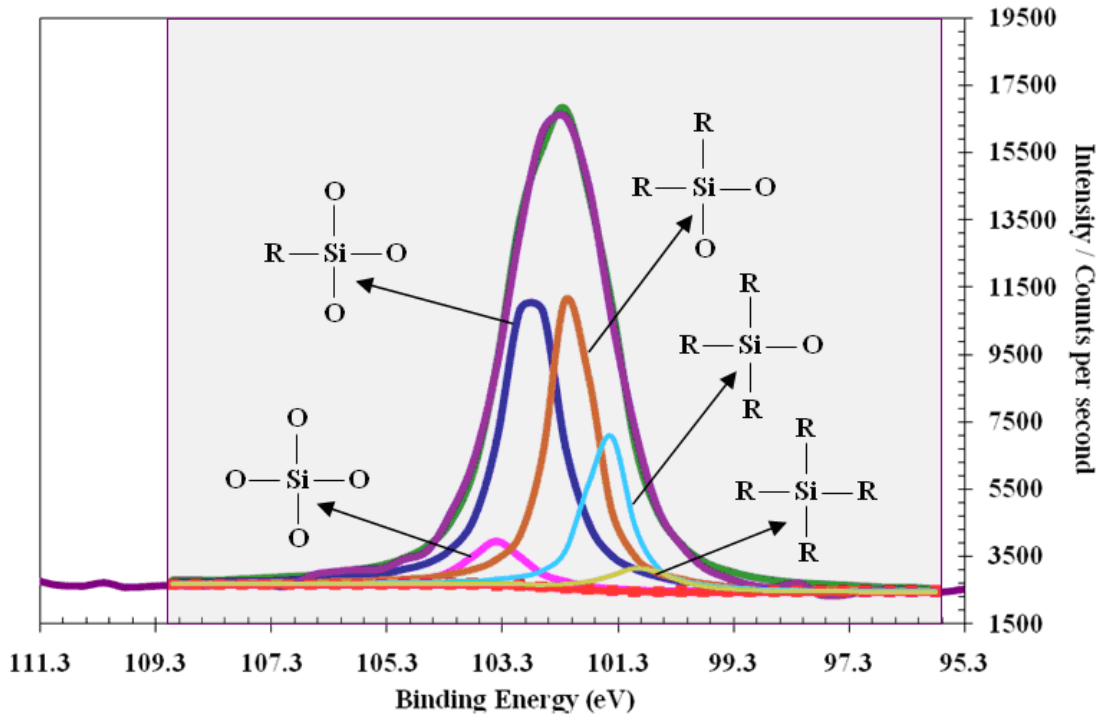

Figure 4.28 High resolution XPS spectra showing the deconvoluted Si2p envelope for 60 W–15 min

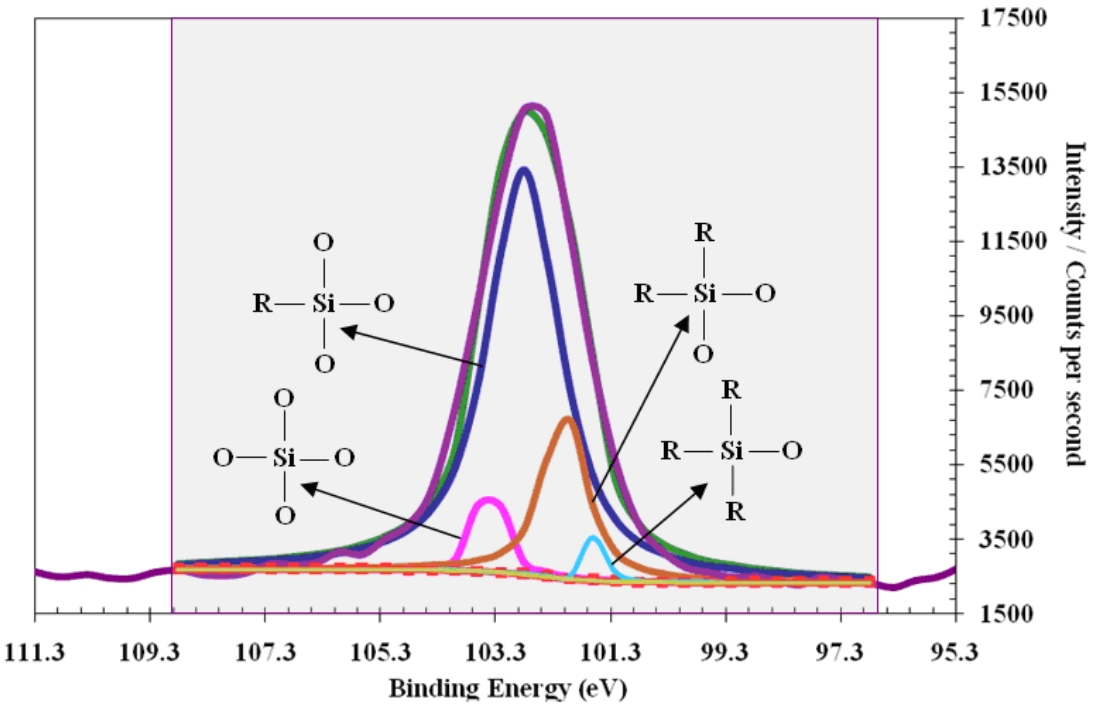

Figure 4.29 High resolution XPS spectra showing the deconvoluted Si2p envelope for 90 W–15 min

Table 4.7 Relative percentage of **Si2p** on glass surface at different plasma powers

Power / time **Functional Group**	**30 W / 15 min (%)**	**60 W / 15 min (%)**	**90 W / 15 min (%)**
Si-$(O)_4$	8	6	6
$(R)_1$-Si-$(O)_3$	24	42	73
$(R)_2$-Si-$(O)_2$	39	32	18
$(R)_3$-Si-$(O)_1$	18	16	2
Si-$(R)_4$	11	4	-

The relative content of chemical bond C–C/C–H slightly increases with increasing of plasma power. As shown in Figures 30-32, silicon atoms are bound to either oxygen or carbon atoms. Relative concentrations of surface functional groups obtained by deconvolution of the Si2p at different exposure times were given in Table 4.8.

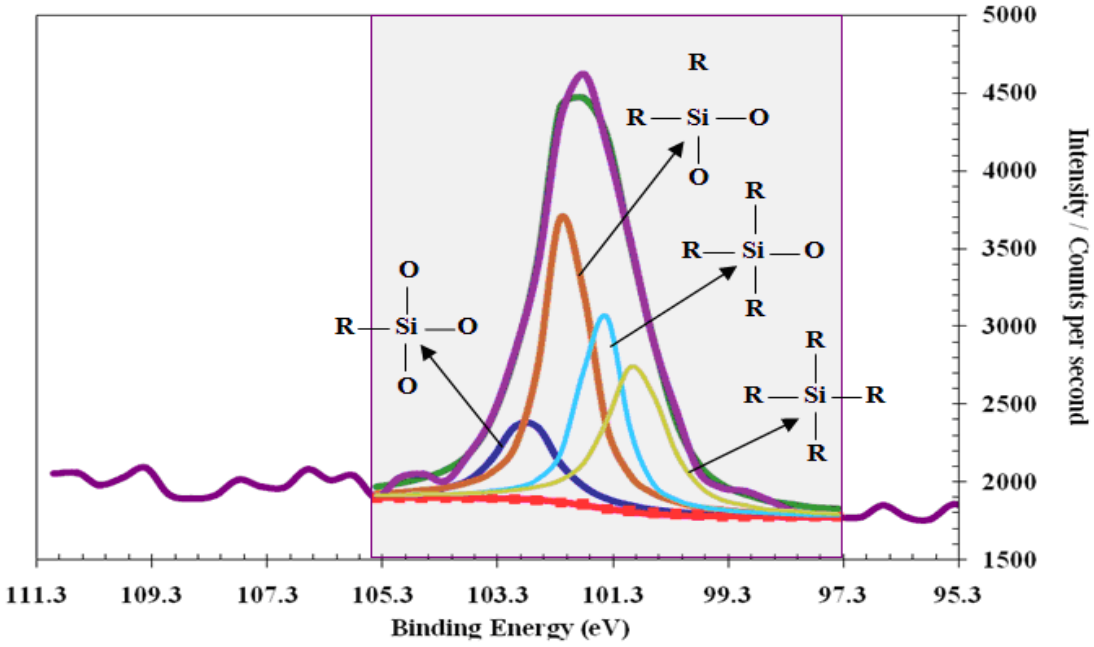

Figure 4.30 High resolution XPS spectra showing the deconvoluted Si2p envelope for 30 W–5 min

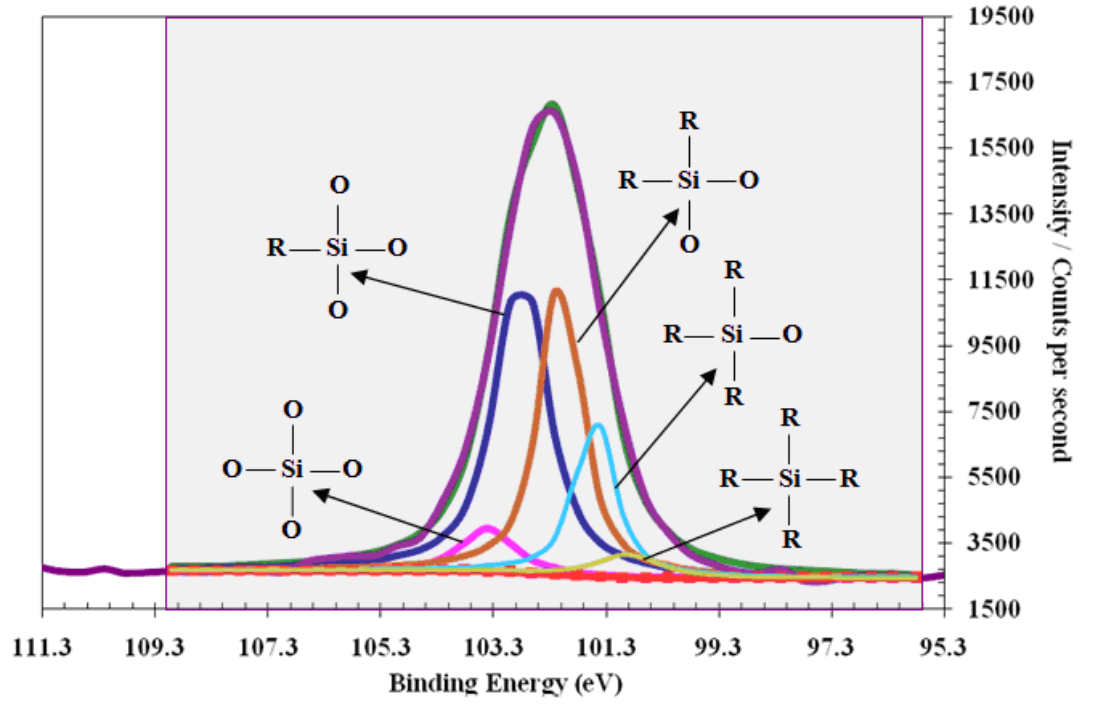

Figure 4.31 High resolution XPS spectra showing the deconvoluted Si2p envelope for 30 W–15 min

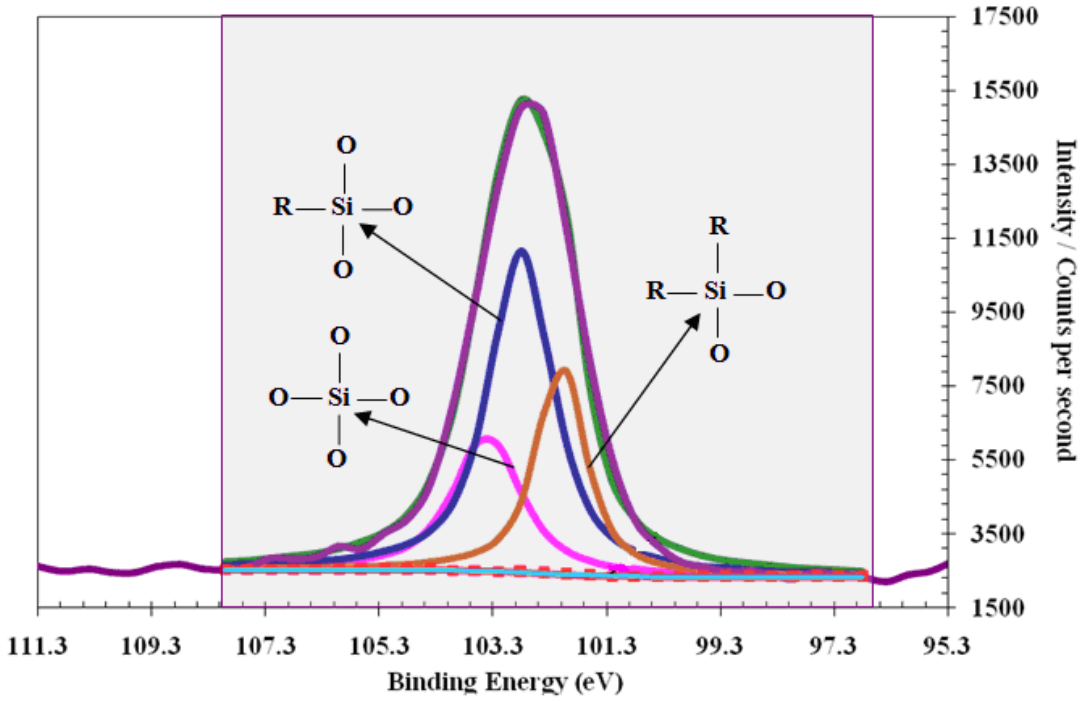

Figure 4.32 High resolution XPS spectra showing the deconvoluted Si2p envelope for 30 W–30 min

Table 4.8 Relative percentage of **Si2p** on PlzP-γ-GPS glass surface at different exposure times

Power / time / Functional Group	30 W / 5 min (%)	30 W / 15 min (%)	30 W / 30 min (%)
Si-$(O)_4$	0	8	23
$(R)_1$-Si-$(O)_3$	13	24	51
$(R)_2$-Si-$(O)_2$	38	39	26
$(R)_3$-Si-$(O)_1$	24	18	0
Si-$(R)_4$	25	11	0

The relative content of Si–$(O)_4$ and $(R)_1$–Si–$(O)_3$ bonds increase with increasing of plasma exposure time from 5 to 30 min at 30W. However, the relative content of $(R)_3$–Si–$(O)_1$ and Si-$(R)_4$ decrease with increasing of plasma exposure time from 5 min to 30 min at 30W. There is no any chemical bonds $(R)_3$-Si-$(O)_1$ and Si–$(R)_4$ for 30 min at 30W. Since the bond energy of C–Si bond is lower than that of Si–O bond,

C–Si bonds are firstly broken with the application of plasma power at a high exposure time. Therefore the relative amount of Si–C bonds decreases at high exposure times. It is interesting to note that the relative content of $Si–(O)_4$ is unavailable for 5 min at 30 W, increasing of exposure time to 30 min increases the relative content of $Si–(O)_4$ up to 23%. Among the silicon chemical bonds, the greatest relative amount belongs to $(R)_1–Si–(O)_3$ (51%) for 30 min at 30W. It is apparent from the results described above that the surfaces of the glass substrates were successfully modified with γ-GPS. It appears that PlzP-γ-GPS on glass substrate is sensitive to plasma powers and plasma exposure times. From XPS results, it seems that the plasma polymerization creates a silicon-oxygen network with hydrocarbon chains containing C–O and C–Si groups.

4.2.1.2 Contact Angle Measurements

An appropriate experimental technique for quantifying the surface properties of solids based on wettability is the measurement of contact angles of liquids on the solid surfaces. The value of the contact angle with water is usually considered as an indicator of the hydrophobicity of the surface of a material. Theoretically, this contact angle may range from 0^o up to 180^o that is to say from complete spreading of the liquid onto the solid surface up to the limit of no wetting. The captive bubble method which was used in this paper provided air and n-octane contact angle values. A high air contact angle value means that a small water contact angle and it implies a hydrophilic surface. The n-octane contact angle can be interpreted by same dialectic. Table 4.9 presents the results of the contact angle measurement obtained for the plain glass surface and for the glasses treated with γ-GPS at different plasma powers and exposure times.

Table 4.9 The air and n-octane contact angle values of plain glass surface and PlzP-γ-GPS films on glass surfaces

Power / time	Air contact angle (^{o})	n-octane contact angle (^{o})
Untreated glass	154±4	137±8
30 W / 15 min	164±4	156±5
30 W / 5 min	157±7	151±7
30 W / 30 min	180±7	115±1
60 W / 15 min	170±7	142±8
90 W / 15 min	154±9	135±4

Plain glass was determined as moderately hydrophilic surface with air contact angle (154 ± 4^o). Hydrophilic surfaces were characterized by water contact angles between 1^o and 40^o and hydrophobic behavior was indicated by angles greater than 40^o. Surface hydrophilicity is due to the presence of a large number of hydroxyl groups on the glass surface. High values of air contact angle were also verified for the plasma polymerized glass surfaces at plasma powers of 30 and 60 W. Elemental analysis results (Figure 4.19) revealed the increased oxygen content of PlzP-γ-GPS films at plasma power of 60W (48.9%). Increasing of plasma power to 90 W, O content decreases (43.2%). High values of air contact angle were observed for the PlzP-γ-GPS glass surfaces from 5 to 30 min exposure time. Elemental analysis results (Figure 4.20) show the increased oxygen content on PlzP-γ-GPS films until the exposure time of 30 min. Lai et al. (2006) indicated that since the number of oxygen-containing groups rises up the ratio of oxygen atom on the surfaces increases. Besides, they showed that varieties of oxygen-containing groups on surfaces were responsible for the change of hydrophilicity. However, the contact angle results were not sufficient to explain the wetting properties of any solid (Gulec, Sarioglu, & Mutlu, 2006). The interaction between water and solid surface must be also evaluated based on surface free energy. The calculation of the polar, dispersive and total surface free energy of a solid material was explained in another paper (Gulec, Sarioglu, & Mutlu, 2006). The polar and dispersive components of surface free energy directly give information related to wettability. A high polar component

of SFE indicates more hydrophilic surface. Figures 4.33 and 4.34 show the changes in dispersive and polar components of surface free energies of the PlzP-γ-GPS films on glass surfaces at different plasma powers and exposure times, respectively. A clear correlation was observed between the polar component in the surface energy and their wettability of water, as can be seen in Figure 4.33. The water contact angle monotonically decreased as the polar component in the surface energy increased. The plasma treatments revealed a higher polar component in surface free energy values of glass, presumably due to Si–O bonds on the surface. At the same time, the dispersive component of the SFE also changed by plasma treatments due to fact that the oxidation reactions result in new additional non-polar groups.

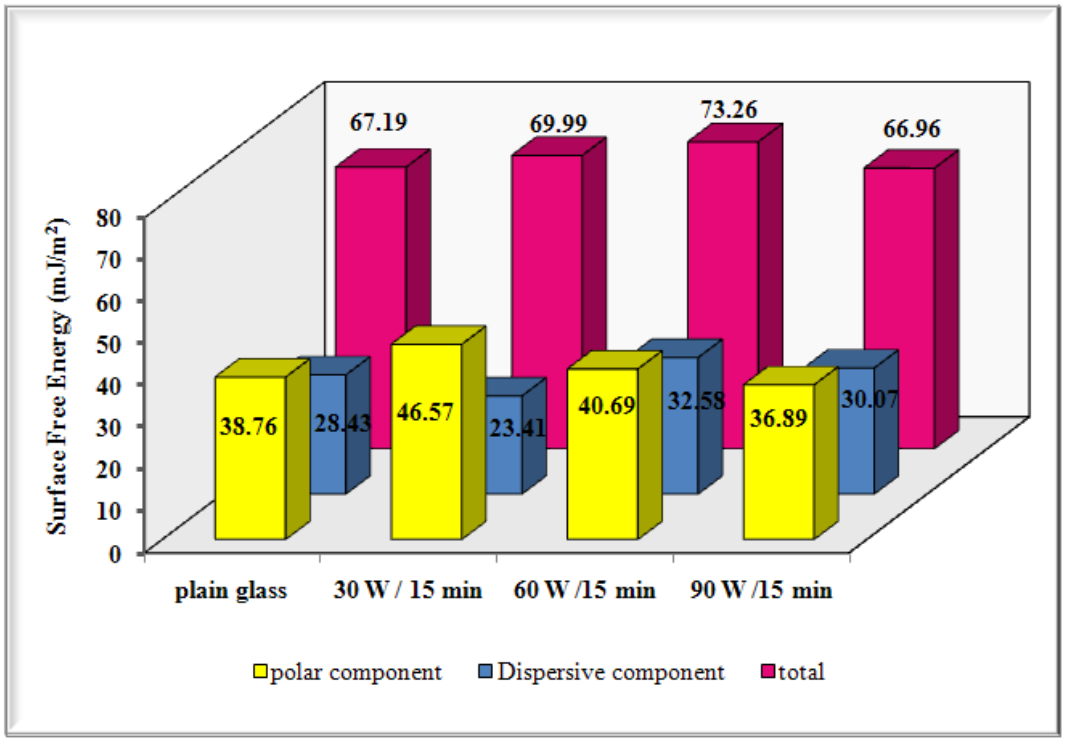

Figure 4.33 The polar, dispersive and total SFE values of plain glass surface and PlzP-γ- GPS films on glass surfaces

As seen in Figure 4.34, the polar component of the SFE of glass substrate monotonically decreased with exposure time of 30 min at 30 W. However, the air contact angle was so high resulting in complete wetting. In particular, attention is paid to this contradictory result. This may be due to instability of polymer thin films on the glass substrates when in contact with water. It is difficult to find the correct

mechanism for the instability of films. However, it can be said that exposing to 30W for a long time (30 min) may be responsible for the thermally instability mechanism. The dispersive component of SFE of glass substrate remarkably increased at the same time due to its low n-octane contact angle. The decrease in the polar SFE value for the treated glass surface with 30 min, when compared to the untreated one, is probably due to the formation of the Si–O–Si network during the plasma procedure and also to the presence of hydrophobic C–H groups. At the same time, the oxidation reactions result in new additional non-polar groups at the surface may be another reason of high dispersive SFE. Plasma polymerization reactions cause complex chemical mixtures which contain different chemically active groups. Therefore, it is expected that different surface characteristics may generate under different plasma conditions.

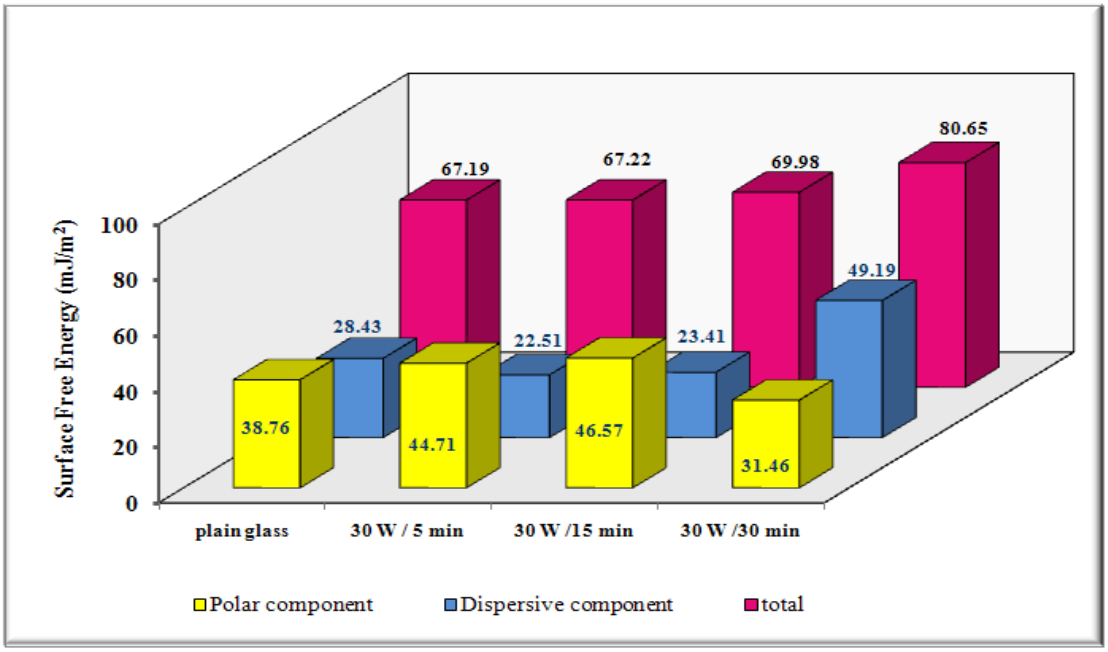

Figure 4.34 SFE components of untreated glass slide and PlzP- γ-GPS films on glass slides

4.2.1.3 AFM Studies

The AFM images of the plasma polymerized glass substrates for different plasma powers and exposure times are shown in Figures 4.35 (a–c) and 4.36 (a–c), respectively. As can be seen from Figure 4.35, the plasma polymerized glass surfaces have almost similar roughness. It was found that the surface roughness slightly increases with the increase of plasma power from 30 to 90 W. RMS (root mean square) values of the roughness were calculated from the AFM images of square 2 * 2 mm^2. The RMS surface roughness of the PlzP-γ-GPS films on the glass surfaces at 30, 60 and 90W (for 15 min) are 0.56, 0.80 and 0.85 nm, respectively. In other words, the surface roughness of PlzP-γ-GPS films was close to 1 nm. AFM measurements reveal that the surface morphology is relatively flat with variation of the roughness from 0.56 nm to 0.85 nm. It can be added that more continuous and homogeneous coating on glass substrate was obtained for 30W-15 min in comparison with other samples (Figure 4.37).

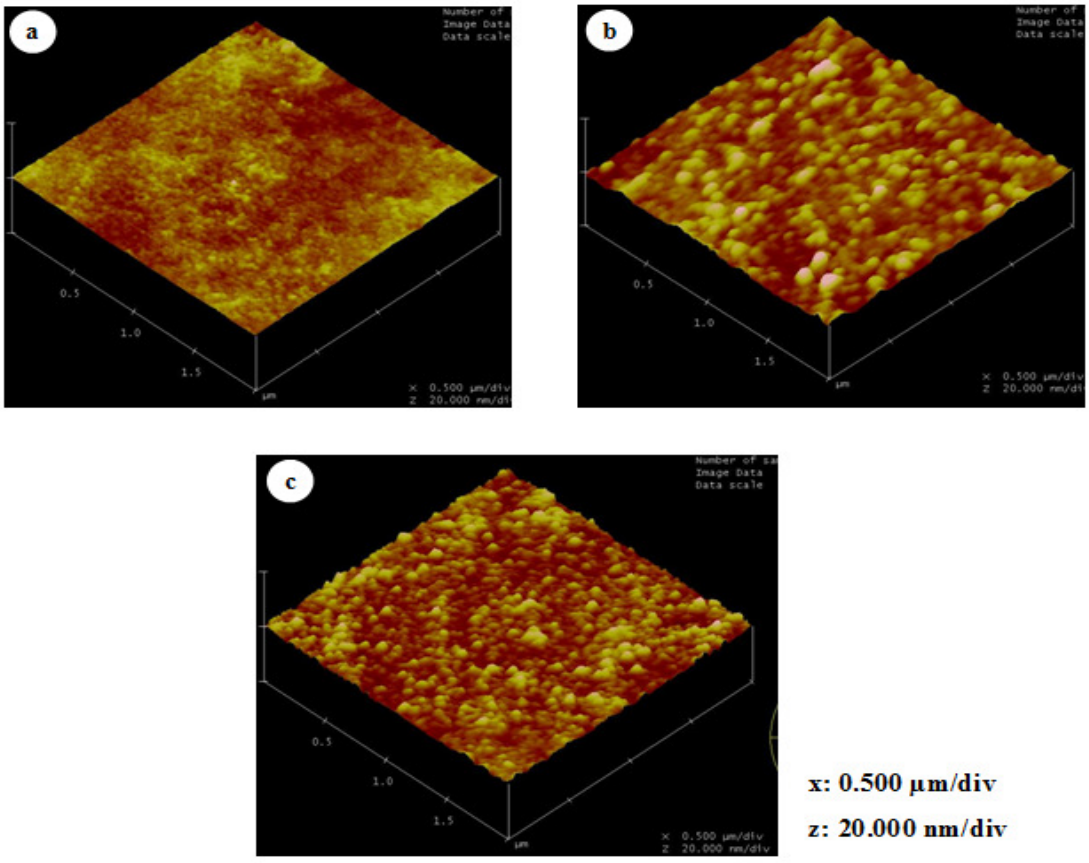

Figure 4.35 AFM images of PlzP-γ-GPS films deposited at (a) 30W (b) 60W (c) 90W for 15

As Figure 4.36 was concerned, the roughness of the surface estimated by RMS deviation of PlzP-γ-GPS film is 2.02 nm for 5 min, 0.98 nm for 15 min and 0.56 nm for 30 min at 30 W. For the glass substrates deposited at 30 W, a slight decrease in roughness with increasing exposure time was observed. It could be said that the PlzP-γ-GPS films on the glass surfaces for 5, 15 and 30 min have a smooth surface, since surface roughness values are approximately a few nanometers. Cech et al. (2006) found that the RMS roughness of the pp-VTES films was only several nanometers, as well. However, a PlzP-γ-GPS film on the glass surface for 5 min has not a continuous surface. More continuous and homogenous coatings on glass substrate were observed for the plasma exposure times of 15 and 30 min (Figure 4.38).

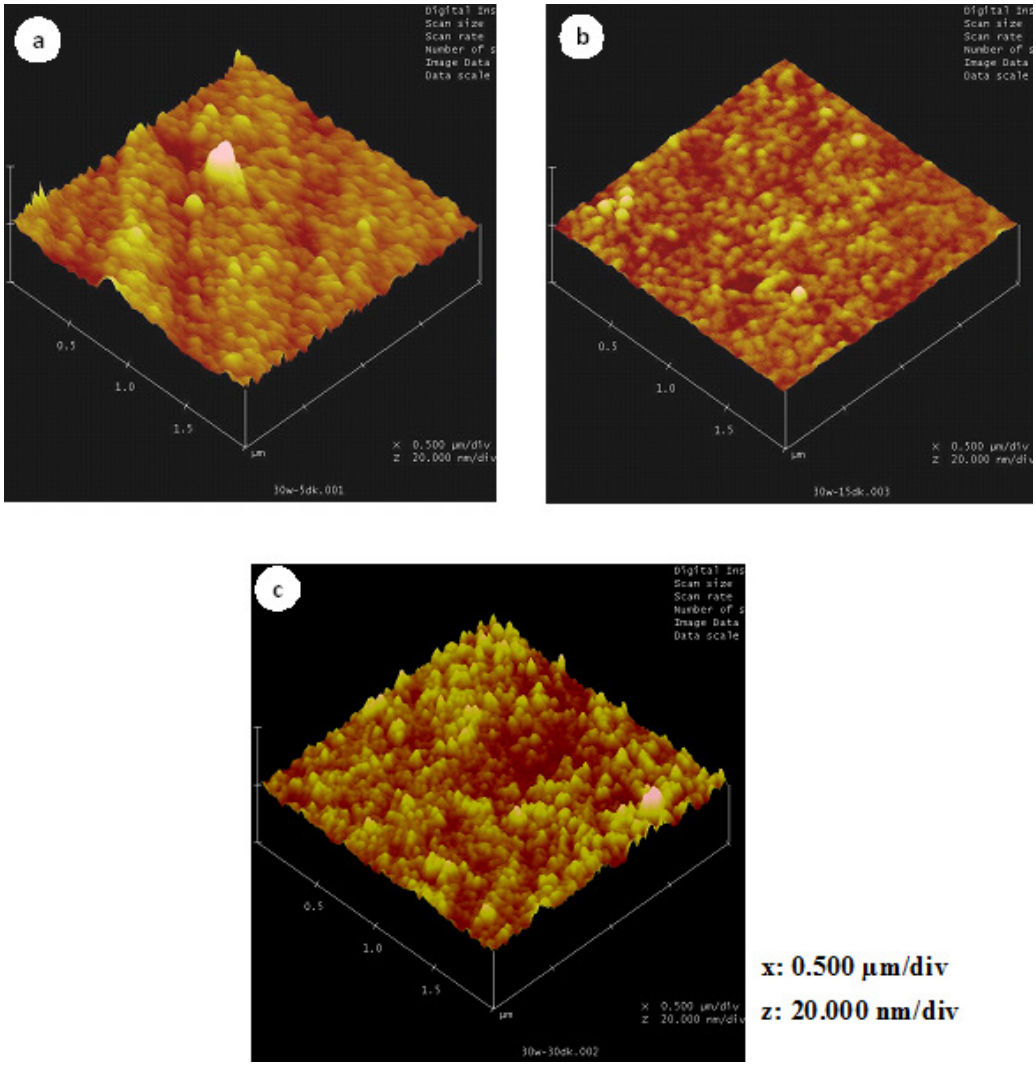

Figure 4.36 AFM images of PlzP-γ -GPS films deposited at (a) 5 min (b) 15 min (c) 30 min for 30 W

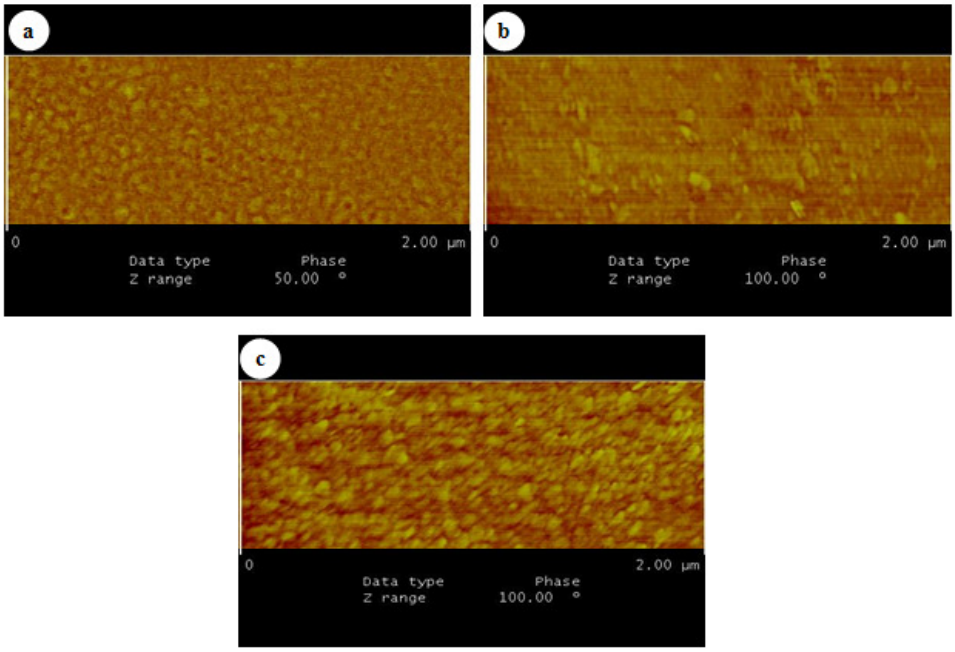

Figure 4.37 AFM characterizations of glass surfaces after plasma polymerization treatment at (a) 30W b) 60W (c) 90W for 15 min.

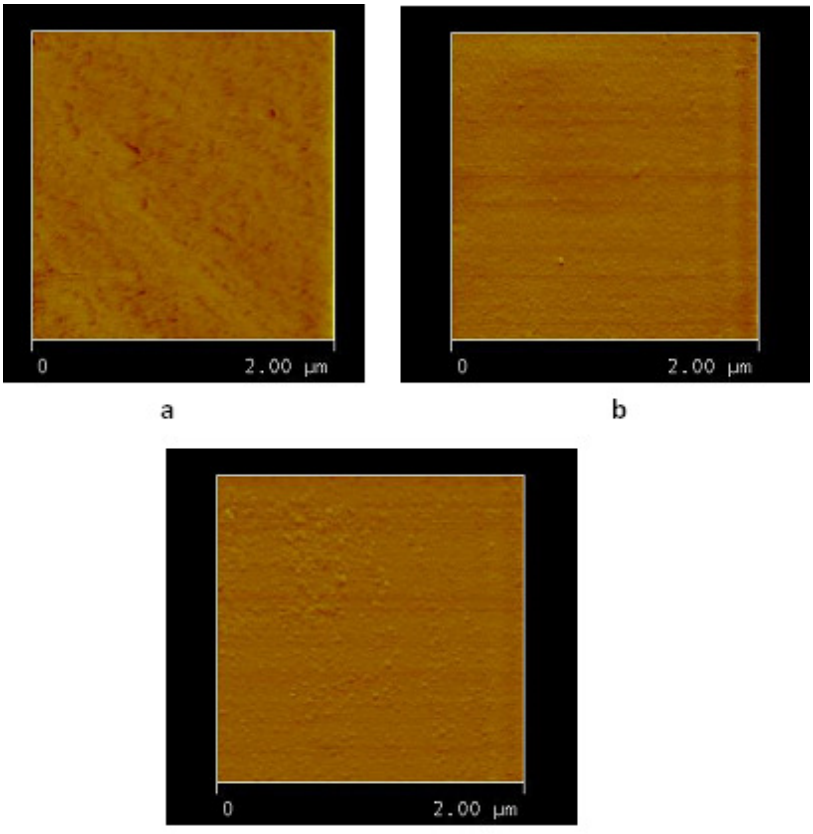

Figure 4.38 AFM characterization of glass surfaces after plasma polymerization treatment at (a) 5 min (b) 15 min c) 30 min for 30 W.

4.2.2 Improvement of Interfacial Adhesion of Glass Fiber/Epoxy Composite by using Plasma Polymerized Silane

This study intends to produce plasma polymer thin films of γ-glycidoxypropyltrimethoxysilane (γ-GPS) on glass fibers in order to improve interfacial adhesion of glass fiber reinforced epoxy composites. Low frequency (LF) plasma generator was used for the plasma polymerization of γ-GPS on the surface of glass fibers at different plasma powers and exposure times. X-ray Photoelectron Spectroscopy (XPS) and SEM analyses of plasma polymerized (pp) glass fibers were conducted to take some information about surface properties of glass fibers. Interlaminar shear strength (ILSS) values of composites reinforced with plasma polymerized glass fiber at different plasma powers and exposure times were evaluated as a measure of interfacial adhesion between glass fibers and epoxy matrix.

4.2.2.1 XPS Analysis

Elemental compositions of the pp-glass fibers at different plasma powers and exposure times were presented in Table 4.10. Si/C ratios are 0.28, 0.38, and 0.24 for 30 W-15 min, 60 W-15 min and 90W-15 min, respectively. A more inorganic character was observed at 60 W for 15 min. However the Si/C ratios for different exposure times 5, 15 and 30 min at 60 W are 0.57, 0.38 and 0.46, respectively. The highest inorganic character of plasma polymerized film on the glass fiber surface was observed with the lowest exposure times (for 5 min) at 60 W. O/C ratios were obtained 1.56, 1.23 and 0.98 at 30, 60 and 90 W, respectively. It indicates that low plasma power leads to more oxygen-containing groups on the surface of glass fiber. On the other hand; O/C ratios are 2.04, 1.56 and 1.83 for 5, 15 and 30 min at 60 W, respectively. More oxygen containing groups were obtained at the lowest exposure time in the studied exposure time in this work.

Table 4.10 Elemental compositions of plasma polymerized glass surfaces

	30 W/ 15 min	60W/ 15 min	90W/ 15 min	60 W / 5 min	60 W/ 15 min	90 W/ 30 min
C%	**40**	**34**	**45**	**28**	**34**	**30**
O %	**49**	**53**	**44**	**57**	**53**	**55**
Si %	**11**	**13**	**11**	**16**	**13**	**14**

The narrow scan spectra of the C1s regions were deconvoluted into the surface functional groups. High resolution XPS spectra showing the deconvoluted C1s envelope for different plasma powers and exposure times were given in Figures 4.39 and 4.40, respectively. The contributions were presented in Figures 4.41 and 4.42 for different plasma powers and exposure times, respectively. C1s core level spectra of pp-γ-GPS film were deconvoluted into three distinct components. The first one, C1s(1), located at 284.6 eV corresponds to the carbon atom of C-C or C-H group. The second one C1s(2), located at 286.2 eV is attributed to the carbon atom of C-O or C-O-C group. The third one, C1s(3), located at 284.3eV is assigned to the carbon atom of C-Si group (Zuri, Silverstein, & Narkis, 1996; Xu et al. 2007). C-O or C-O-C group increases up to 60 W. With the increasing of plasma power to 90 W, C-O or C-O-C group decreases. C-C or C-H group shows the same trend. However, C-Si group decreases to 19.1 % for pp-glass fiber at 60 W. C-Si group increases to 31.9 % with the increasing of plasma power to 90 W. The effect of exposure time at 60 W can be seen in Figure 4.42. As can be seen from Figure 4.42, C-O or C-O-C group increases from 8.8 % for pp-glass fiber at 30 W to 16.2 % for pp-glass fiber at 90 W. The same trend was observed for C-C or C-H group. In contrast to this, C-Si group decreases from 31.9 % for pp-glass fiber at 90 W to 24.5 % for pp-glass fiber at 30 W. C-Si bonds are broken with increasing of plasma power during plasma polymerization of γ-GPS onto glass fibers. C-Si bond which possesses the lowest standard bond energy among these bonds are firstly broken with the application of plasma power. Therefore increasing of plasma power leads to decrease in the relative concentration of C-Si bonds.

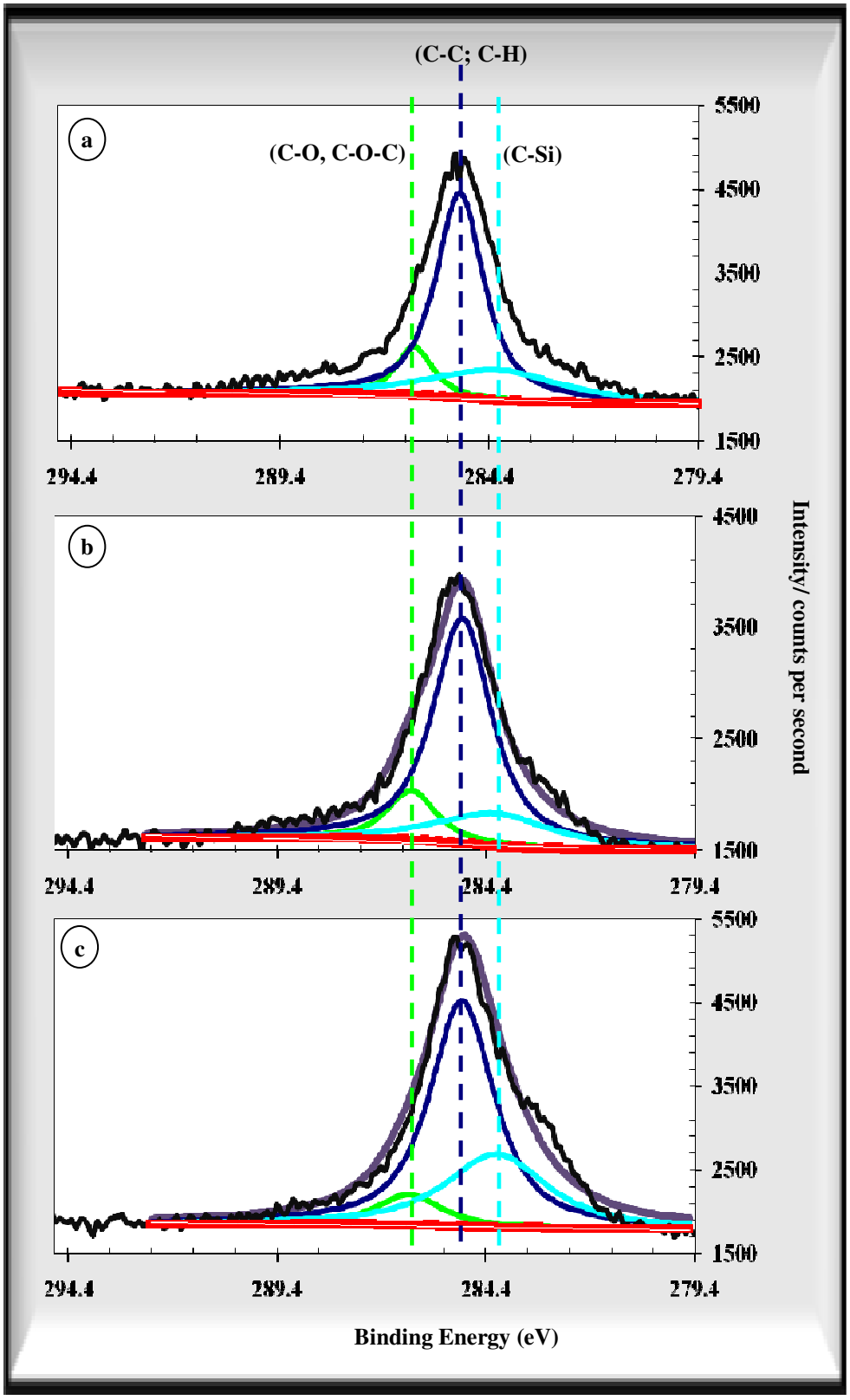

Figure 4.39 High resolution XPS spectra showing the deconvoluted C1s envelope for (a) 30 W–15 min (b) 60 W–15 min (c) 90 W–15 min.

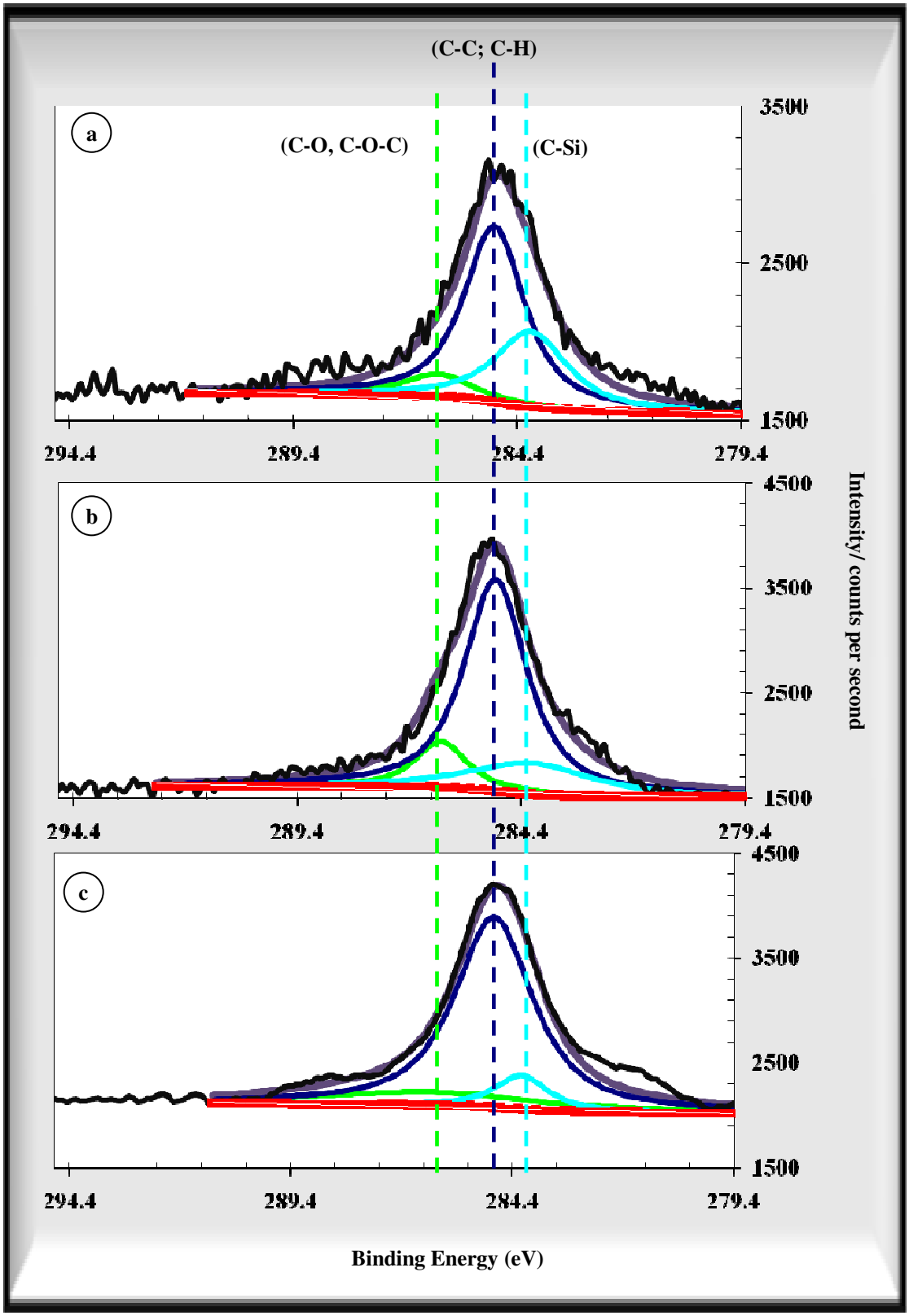

Figure 4.40 High resolution XPS spectra showing the deconvoluted C1s envelope for (a) 60 W–5 min (b) 60 W–15 min (c) 60 W–30 min

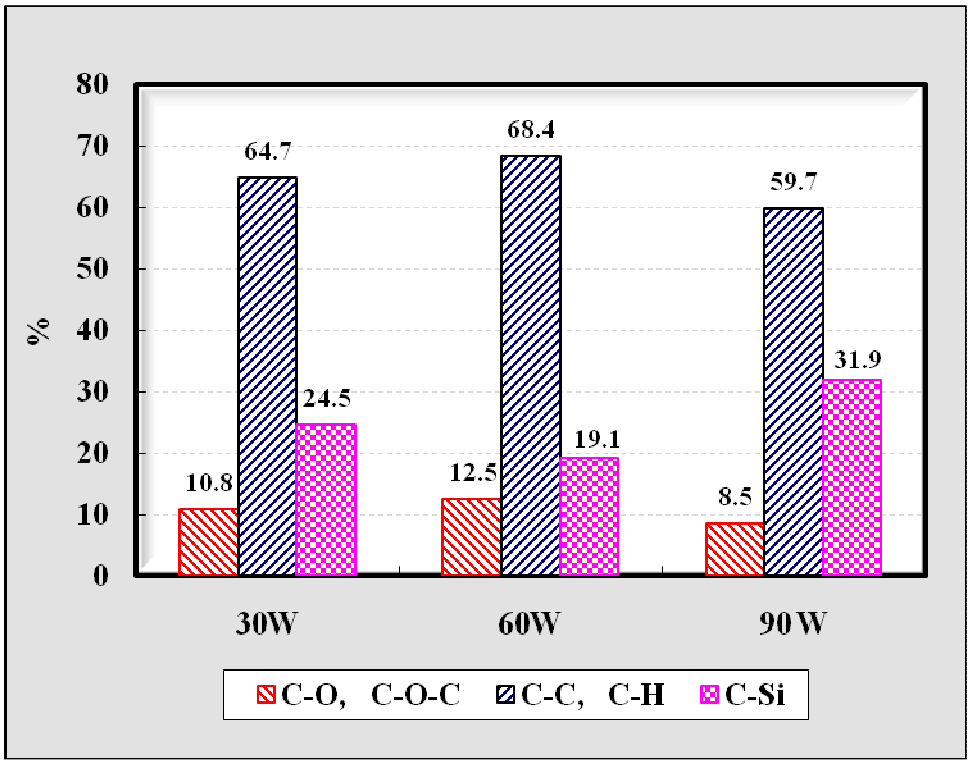

Figure 4.41 Relative percentage of C1s on PlzP-γ-GPS glass fiber surface at different plasma powers

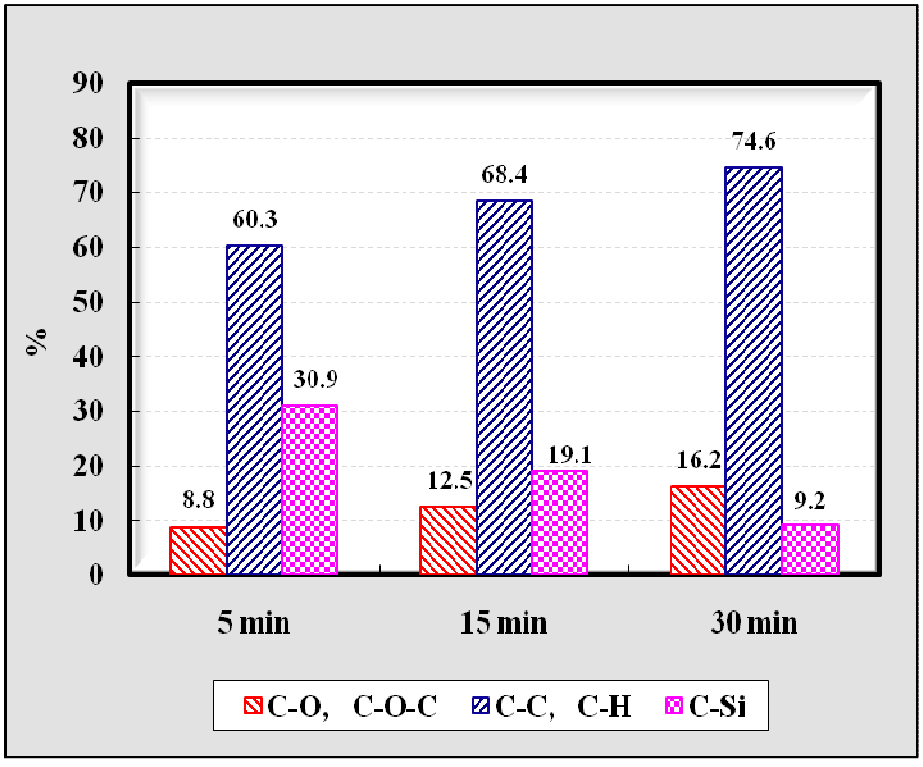

Figure 4.42 Relative percentage of **C1s** on PlzP-γ-GPS glass surface at different exposure times at 60 W

The narrow scan spectra of the Si2p regions were deconvoluted into the surface functional groups. High resolution XPS spectra showing the deconvoluted Si2p envelope for different plasma powers and exposure times were shown in Figures 4.43 and 4.44, respectively. Close examination of the Si2p spectrum explains peaks at 103.4, 102.8, 102.1, 101.5, and 100.9 eV corresponding to Si–$(O)_4$, $(R)_1$ –Si–$(O)_3$, $(R)_2$ –Si–$(O)_2$, $(R)_3$–Si–$(O)_1$ and Si–(R)4, respectively. The contributions at different plasma powers and exposure times were given in Tables 4.11 and 4.12, respectively.

Table 4.11 Relative percentage of **Si2p** on glass fiber surface at different plasma powers for 15 min

	Si-$(O)_4$	**$(R)_1$-Si-$(O)_3$**	**$(R)_2$-Si-$(O)_2$**	**$(R)_3$-Si-$(O)_1$**	**Si-$(R)_4$**
30W	**9.2**	**25.6**	**37.0**	**13.8**	**14.5**
60W	**6.3**	**39.6**	**35.8**	**11.8**	**6.6**
90 W	**2.1**	**62.3**	**27.6**	**6.9**	**1.2**

Table 4.12 Relative percentage of **Si2p** on glass fiber surface for different exposure times at 60 W

	Si-$(O)_4$	**$(R)_1$-Si-$(O)_3$**	**$(R)_2$-Si-$(O)_2$**	**$(R)_3$-Si-$(O)_1$**	**Si-$(R)_4$**
5 min	**9.7**	**21.3**	**39.7**	**14.1**	**15.2**
15 min	**6.3**	**39.6**	**35.8**	**11.8**	**6.6**
30 min	**4.7**	**55.5**	**29.7**	**8.6**	**1.6**

The percent contribution of Si-$(O)_4$ group was 9.2 % for pp-glass fiber at 30W. Increasing of plasma power from 30 W to 90 W, the relative amount of Si-$(O)_4$ group decreases to 2.1 % for pp-glass fiber at 90 W. However relative contribution of $(R)_1$-Si-$(O)_3$ group was obtained to be 25.6 % at 30 W. Increasing of plasma power from 30 W to 90 W increased relative contribution of $(R)_1$-Si-$(O)_3$ to 62.3 %. The contributions of other groups decrease with the increasing of plasma power from 30 to 90 W. As can be seen from Table 4.12, relative contribution of Si-$(O)_4$ was obtained to be 9.7 % after plasma polymerization process for 5 min.

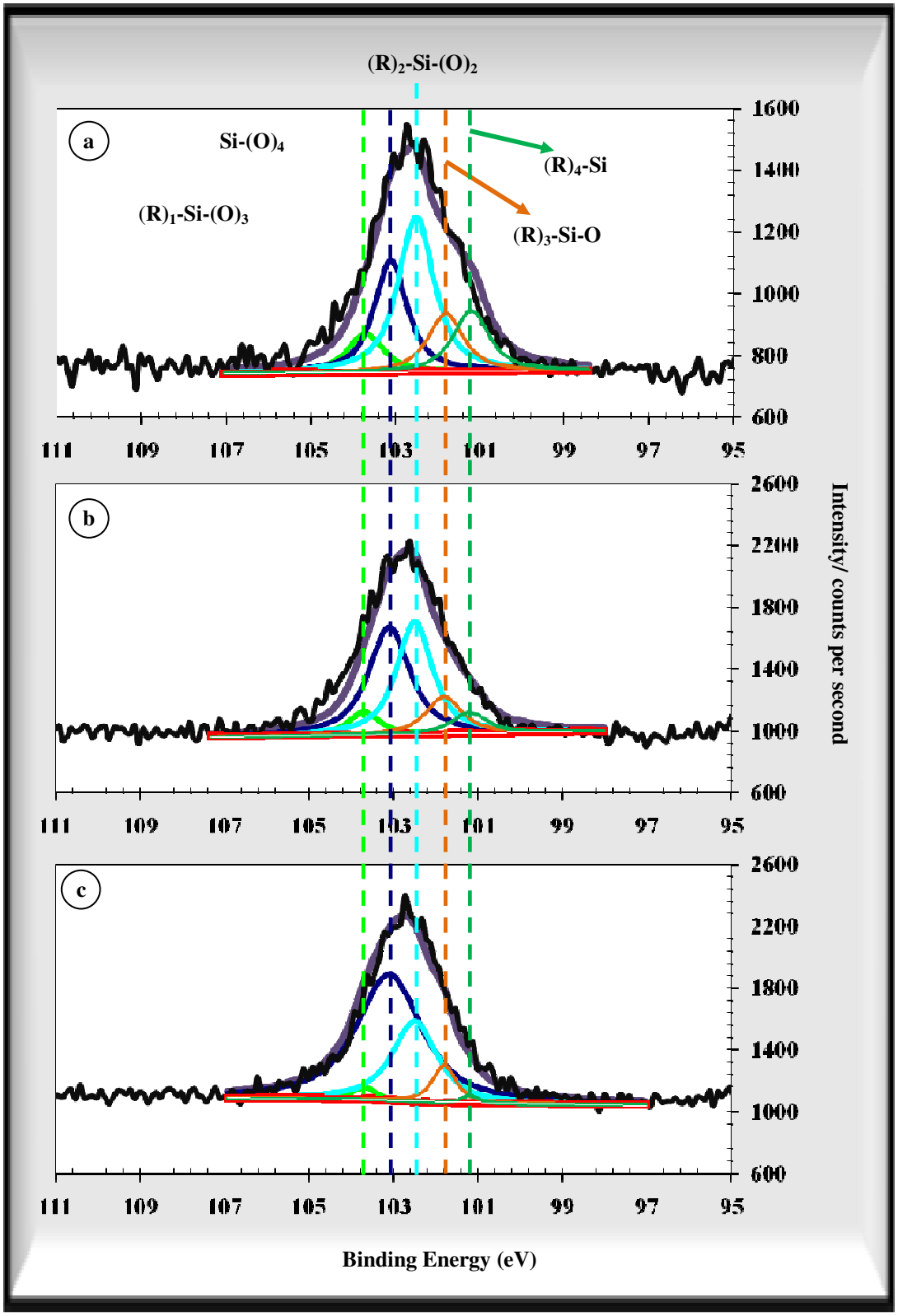

Figure 4.43 High resolution XPS spectra showing the deconvoluted Si2p envelope for (a) 30 W–15 min (b) 60 W–15 min (c) 90 W–15 min.

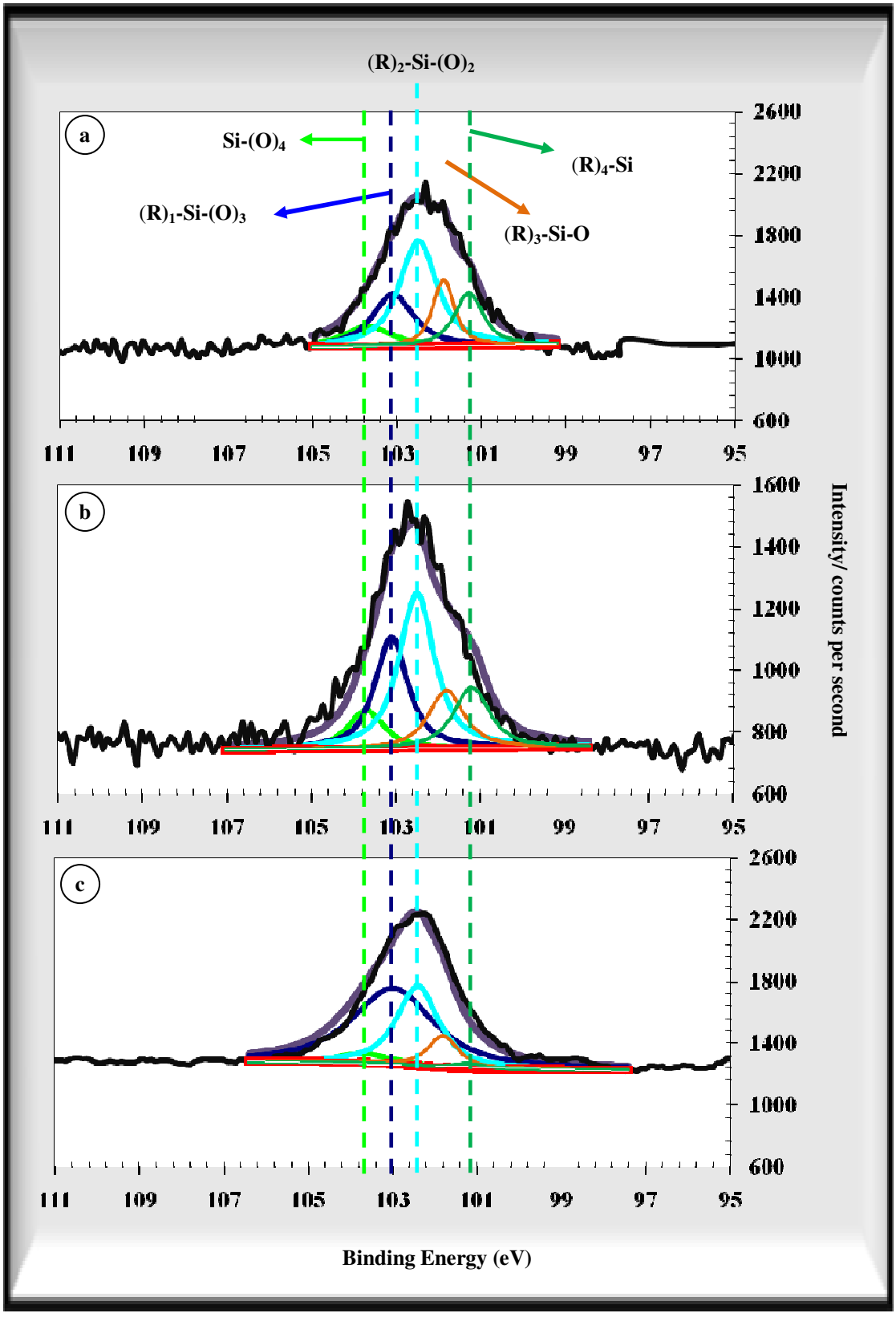

Figure 4.44 High resolution XPS spectra showing the deconvoluted Si2p envelope for (a) 60 W–5 min (b) 60 W–15 min (c) 60 W–30 min

Relative amount of Si-$(O)_4$ group decreases with the increasing of plasma exposure times. The relative contribution of $(R)_1$-Si-$(O)_3$ group increases with the increasing of plasma exposure time from 5 to 30 min. However the relative amounts of $(R)_2$-Si-$(O)_2$, $(R)_3$-Si-$(O)_1$ and Si-$(R)_4$ groups decreases at high plasma exposure times. The relative contribution of Si-$(R)_4$ group after plasma polymerization of glass fiber for 30 min was 1.2 %. It can be said that relative amounts of Si-C bonds decrease with increasing of plasma exposure time. It is an expected result because of the fact that Si-C bonds are broken firstly.

4.2.2.2 SEM Observations of pp-Glass Fibers

We applied the scanning electron microscope (SEM) for investigation of surface morphology of pp-glass fibers. SEM micrographs of the plasma polymerized glass fibers at different plasma powers and exposure times can be seen in Figures 4.45 and 4.46. The SEM micrographs could easily verify the difference between heat cleaned glass fiber and plasma polymerized fibers. Figure 4.45 a shows the micrograph of the heat cleaned glass fiber. The surface of the fiber is smooth and uniform. This type of morphology does not enable mechanical interlocking mechanism. As can be seen from Figures 4.45 (b, c, d) and 4.46 (a, b, c), the surfaces of the plasma polymerized glass fiber at different plasma powers and exposure times are not smooth and uniform. In Figure 4.45 (b, c, d), the SEM photographs show fragments of γ-GPS adhered to the fiber surface in several points. It is probable that the plasma polymerization of glass fibers creates different bonding sites that promote adhesion between glass fibers and epoxy matrix. From the SEM micrographs of glass fibers plasma polymerized at 90 W for 15 min (Figure 4.45 (d)), formation of some cavities during plasma polymerization can be realized. This may create a surface roughness. As can be seen from Figure 4.46, the glass fiber surfaces become rougher as a result of plasma polymerization of glass fibers. Rough surfaces increase the number of anchorage points, thus offering a good fiber - resin mechanical interlocking (Mwaikambo & Ansell, 2002). It is well known that the mechanical interlocking mechanism between fiber and matrix resin plays a key role in improving the interfacial adhesion of fiber reinforced polymer matrix composites.

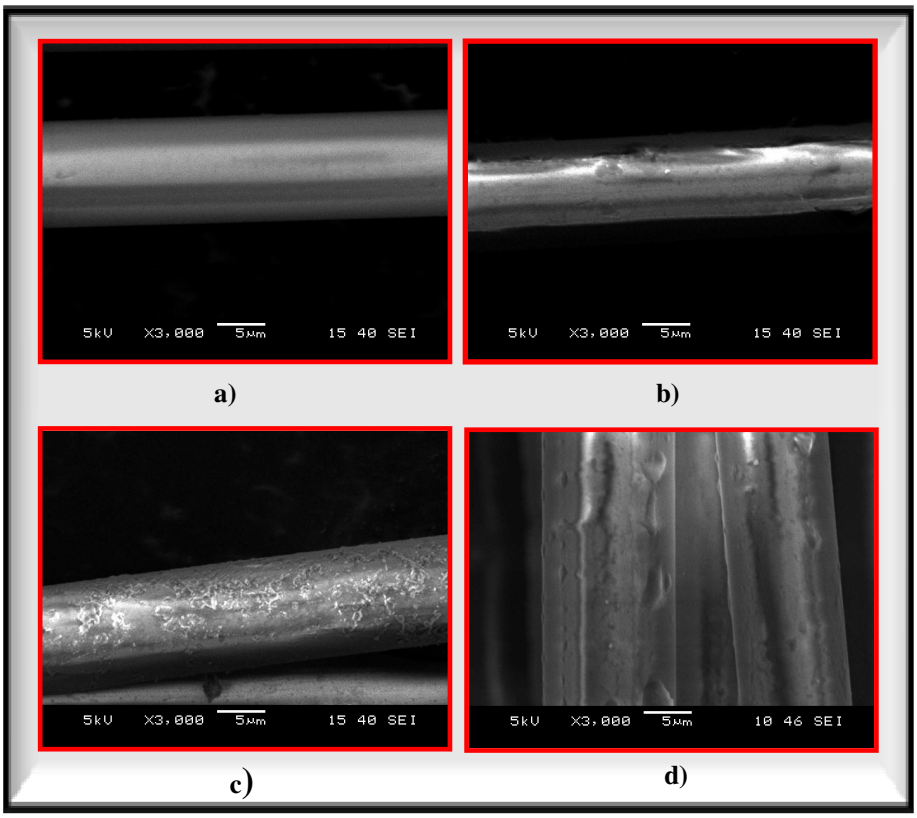

Figure 4.45 SEM micrographs of heat cleaned (a) and plasma polymerized (b) 30 W, (c) 60 W, (d) 90 W for 15 min

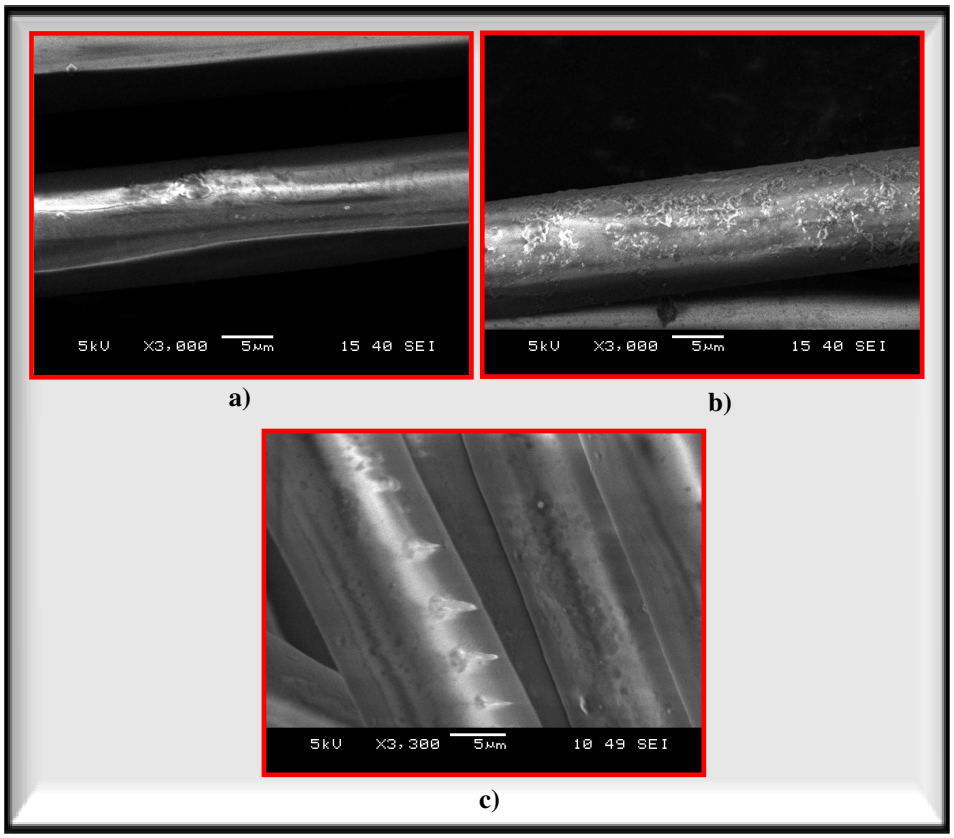

Figure 4.46 SEM micrographs of plasma polymerized glass fibers a) 5 min-60 W b) 15 min-60 W c) 30 min-60 W.

4.2.2.3 Short Beam Shear Test

Interlaminar shear strength values of glass fiber/epoxy resin composites were carried out to evaluate the effect of plasma polymerization on interfacial properties of the composites. The effect of plasma polymerization of γ-GPS on the ILSS of the glass fiber reinforced epoxy composites is shown in Figures 4.47 and 4.48. It is seen in Figure 4.47 that the ILSS values of the composites increased with increasing of exposure time at plasma power of 60 W. The ILSS value of untreated composite is 8.1 MPa, while it increases to 9.8 MPa, 14.9 MPa and 17.0 MPa with the increment of about 21%, 84% and 110% after plasma polymerization by using γ-GPS for 5 min, 15 min and 30 min at plasma power of 60 W, respectively. Namely, the maximum ILSS was obtained for exposure time of 30 min at 60 W. This indicates the greatest interfacial adhesion between glass fiber and epoxy matrix.

As was noted above that relative concentrations of C-O, C-O-C and C-C, C-H groups was obtained to be 16.2 % and 74.6 %, respectively at 60 W for 30 min and these are the greatest values in the studied range. It is interesting to also note that the relative concentration of C-Si group (19.1%) at 60 W for 30 min was the lowest value among the C-Si groups. It is probable that interaction of epoxy matrix with C-O, C-O-C and C-C, C-H groups determines the strength of adhesion between glass fibers and epoxy matrix. A strong bonding may be possible between pp-glass fibers and epoxy matrix.

Figure 4.48 shows the ILSS values of pp-glass fiber/epoxy composites as a function of plasma power under an exposure time of 15 min. The maximum ILSS is observed at plasma power of 60 W and the ILSS of the composite shows 84% improvement compared with that of the untreated one. However, it decreases from 14.9 to 8.7 MPa when the plasma power is 90W. As mentioned above O/C ratios are 2.04, 1.56 and 1.83 for 5, 15 and 30 min at 60 W. Moreover Si/C ratios are 0.28, 0.38, 0.24 for 30 W-15 min, 60 W-15 min and 90W-15 min, respectively. As can be seen here the greatest C/O and Si/C ratios were obtained at 60 W for 15 min. The

ILSS results indicate that plasma polymerization of γ-GPS can improve the interfacial adhesion properties between the glass fiber and the epoxy matrix.

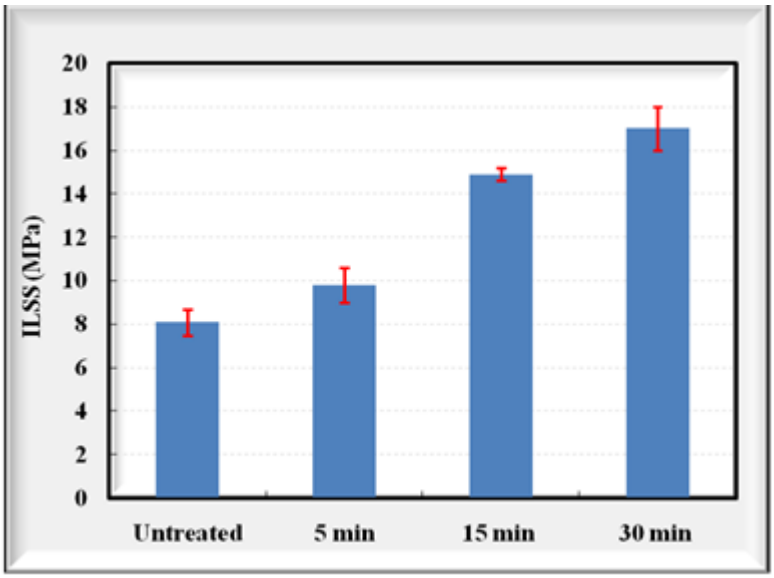

Figure 4.47 ILSS values of the composites as a function of exposure time under a plasma power of 60 W

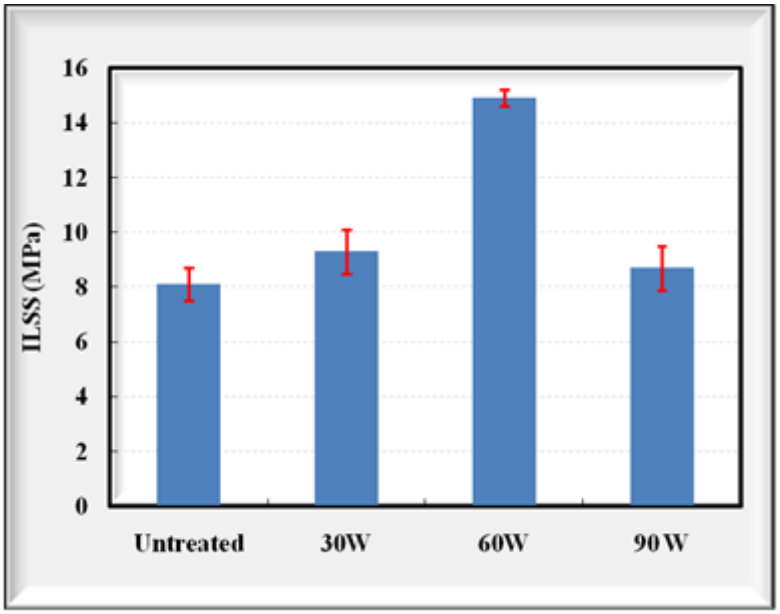

Figure 4.48 ILSS values of the composites as a function of plasma power under an exposure time of 15 min

4.2.2.4 SEM Observations of pp-Glass Fiber/Epoxy Composites

SEM micrographs of the plasma polymerized glass fibers at different plasma powers and exposure times/epoxy composites are shown in Figures 4.49 and 4.50. Figure 4.49 a represents the fracture surface of the heat cleaned glass fiber/epoxy composite. SEM analysis was conducted on the fracture surfaces of the composites to investigate the fracture morphology depending on the plasma surface modification. There was a marked difference in fracture surface topography between heat cleaned glass fiber reinforced epoxy and plasma polymerized glass fiber reinforced epoxy composites. From Figure 4.49, it can be seen that heat cleaned glass fibers were pulled out from the epoxy matrix and the surfaces of the fibers had smooth and clean surfaces with no resin matrix adhered. A large amount of fiber pull-outs and clean fiber surfaces demonstrates that interfacial adhesion between heat cleaned glass fiber and epoxy matrix was very weak. The fracture of heat cleaned glass fiber reinforced epoxy composite occurred at the interface between fiber and matrix and the interface structure cannot transfer stress effectively. In the case of pp-glass fiber reinforced epoxy composites was observed better adhesion between the fiber and matrix as seen in Figures 4.49 (b, c d) and 4.50 (a, b, c). It is obvious that the fiber surfaces were covered with large quantities of resin matrix and a great number of fibers appeared to be embedded in epoxy matrix after failure, indicating a higher fiber/matrix adhesion. Moreover the surface of pp-glass fibers is not as clean as the surface of heat cleaned glass fibers.

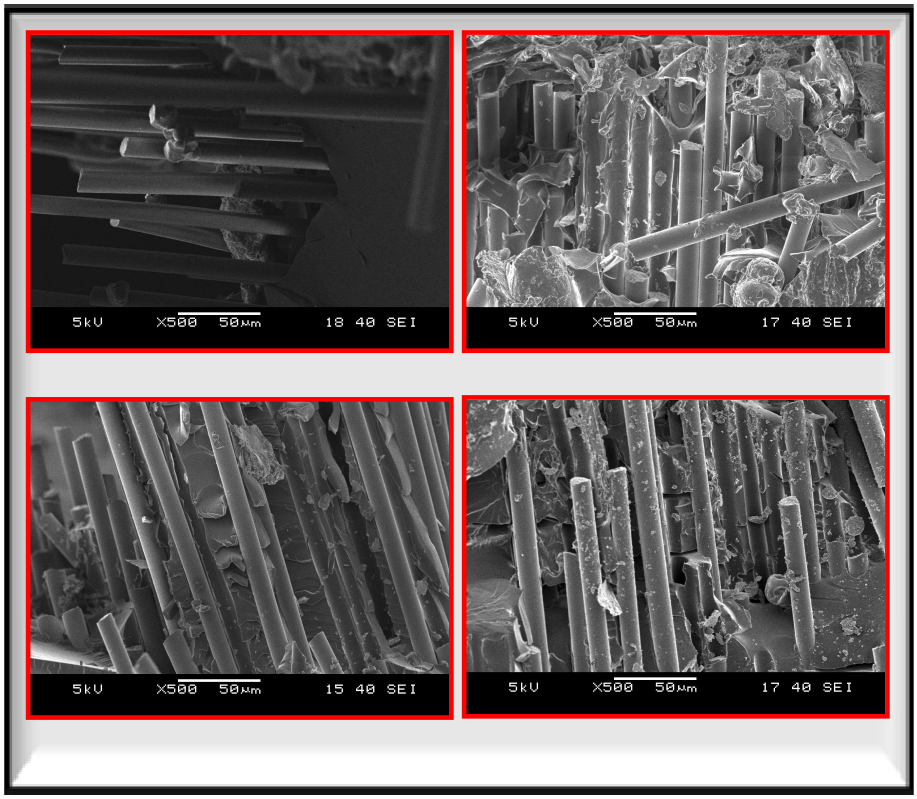

Figure 4.49 SEM micrographs of glass fiber/epoxy composite a) heat cleaned b) 30 W-15 min c) 60 W-15 min d) 90 W-15 min

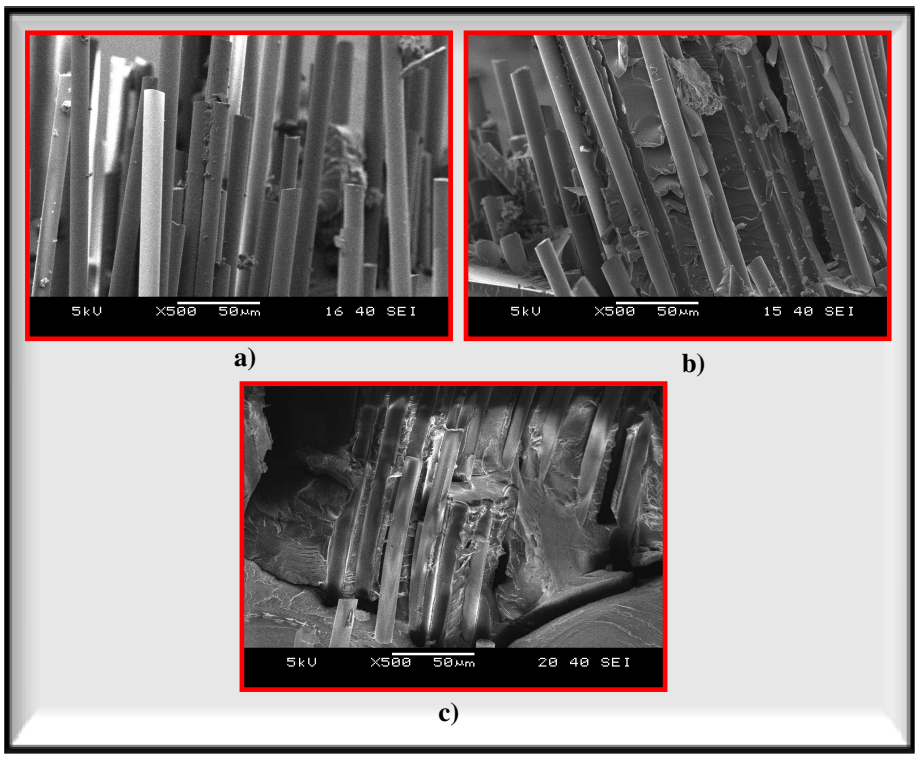

Figure 4.50 SEM micrographs of glass fiber/epoxy composite a) 5 min-60 W b) 15 min-60 W c) 30 min-60 W.

CHAPTER FIVE
CONCLUSIONS

5.1 Conclusions of the Thesis

In this study, fiber surface treatments were used to create a fiber/matrix interface possessing different characteristics. Glass fiber was used for experimental characterization and the glass fiber was subjected to wet chemical and plasma polymerization treatments by using (γ-glycidoxypropyltrimethoxysilane (γ-GPS)). Firstly, the structure of γ-glycidoxypropyltrimethoxysilane (γ-GPS) on glass substrates or glass fiber surfaces after wet chemical and plasma polymerization processes was analyzed. Then, the effects of silane and plasma polymerization treatments of glass fibers on mechanical properties of glass fiber/epoxy composites were investigated. From conducted experiments, several results obtained in this research are summarized as follows:

- Acid activation may increase the Si-OH surface content of the heat cleaned fiber and acid activation time affects the interaction level between glass fiber and hydrogen ions. When acid activation time increases, more Al may be leached out from glass fiber. Therefore, the surface content of Si-OH increases. It can be also that silanization time cause significant difference in terms of the interaction between glass fiber and silane coupling agent. However, the silane coating on the acid activated glass fibers did not improve the interlaminar shear strength, flexural strengths and the tensile strengths of the composite due to the fiber damage caused by HCl acid solution. On the other hand, the silane coating on the heat cleaned glass fibers has the beneficial effect on the adhesion between the fibers and the matrix. The presence of γ-GPS in the composite leads to increasing ILSS and flexural strength of the composite, which can be related to the effect of increased interfacial adhesion between glass fiber and polymer matrix.

- Different silane concentrations were used to modify the glass fiber surface. Based on the experimental results, it was found that the interlaminar shear strength, the flexural strength and the tensile strength increase with the increase of γ-GPS concentration in the range of 0.1–0.5%. The 0.5% γ-GPS silane treatment made the composite with the best mechanical properties (in terms of tensile, flexural and ILSS properties). 0.5% γ-GPS treated glass fiber composite when compared to the heat cleaned glass–epoxy composites exhibited an improvement of about 37% in tensile strength, about 78% in flexural strength and about 59% in ILSS. From SEM of tensile fracture surface, existence of fiber pull-out for heat-cleaned glass fiber composite is determined. However γ-GPS-treated glass fiber composites do not demonstrate any pull-outs, indicating good interfacial adhesion between the fiber and the epoxy.

- The effect of plasma power and plasma exposure time on the properties of plasma-polymerized glycidoxypropyltrimethoxysilane (PlzP-γ-GPS) deposited on glass substrate was investigated. From conducted experiments it is inferred that the surfaces of the glass substrates were successfully modified with γ-GPS by plasma polymerization. When plasma power increases from 30 to 60 W, Si/C ratio increases, it implies a more inorganic plasma polymer. It is also observed that enhanced power to 90 W exhibits a more organic character of plasma polymer. Si–C bonds may be broken with increasing plasma power, during plasma polymerization of γ-GPS onto glass substrate. The amount of Si–O bonds is greater than that of Si–C bonds at the studied plasma powers. Increasing of exposure time resulted in increase of inorganic character of PlzP-γ-GPS films on glass substrate.

- Plasma polymerization of γ-GPS on the surface of glass fibers was carried out successfully by using low frequency plasma generator and the plasma polymer thin films of γ-GPS on glass fibers were produced in order to improve interfacial adhesion of glass fiber reinforced epoxy composites. Deconvolution of XPS spectra of pp-glass fibers showed that relative concentrations of C-O, C-O-C (16.2 %) and C-C, C-H (74.6 %) groups was the

greatest values at 60 W for 30 min in the studied range. It is interesting to also note that the relative concentration of C-Si group (19.1%) at 60 W for 30 min was the lowest value among the C-Si groups. From SEM observations of pp-glass fibers it was observed that the glass fiber surfaces become rougher as a conclusion of plasma polymerization of glass fibers. The maximum ILSS value was obtained for exposure time of 30 min at 60 W. The ILSS value of heat cleaned glass reinforced epoxy composite increased by 110% after plasma polymerization of γ-GPS for 30 min at plasma power of 60 W. This indicates the greatest interfacial adhesion between glass fiber and epoxy matrix. SEM micrographs of fracture surfaces of pp-glass fiber reinforced epoxy composites were observed better adhesion between the fiber and the matrix.

5.2 Suggestions for the Future Studies

For future studies, in order to improve adhesion between glass fiber and epoxy matrix, the following studies can be performed:

- In this study, the ILSS increase with the increase of exposure time at 60 W in the range of 5–30 min. The maximum ILSS value was obtained for exposure time of 30 min at 60 W. For future studies, the effect of higher plasma exposure time on the properties of plasma-polymerized glycidoxypropyltrimethoxysilane (PlzP-γ-GPS) deposited on glass substrate may be investigated.

- Different silane coupling agents may be used to modify the glass fiber surface for wet chemical and plasma polymerization studies.

REFERENCES

Benzarti, K., Cangemi, L., & Dal Maso, F. (2001). Transverse properties of unidirectional glass/epoxy composites: influence of fibre surface treatments. *Composites Part A: Applied Science and Manufacturing, 32* (2), 197-206.

Berthelot, J. M. (1999). *Composite materials-Mechanical behavior and structural analysis.* Newyork: Springer-Verlag.

Biederman, H. (Ed.). (2004). *Plasma polymer films.* London: Imperial College Press.

Cai, S., Fang, J., & Yu, X. (1992). Plasma Polymerization of organosiloxanes. *Journal of Applied Polymer Science, 44* (1), 135-141.

Campbell, F. C. (2003). *Manufacturing processes for advanced composites.* Oxford: Elsevier Science.

Campbell, F.C. (2006). *Manufacturing technology for aerospace structural materials* (1 st ed.). The Netherlands: Elsevier Ltd.

Cech, V., Inagaki ,N., Vanek, J., Prikryl, R., Grycova, A., & Zemek, J. (2006). Plasma-polymerized versus polycondensed thin films of vinyltriethoxysilane. *Thin Solid Films, 502* (1–2), 181-187.

Cech, V., Prikryl, R., Balkova, R., Vanek, J., & Grycova, A. (2003). The influence of surface modifications of glass on glass fiber/polyester interphase properties. *Journal of Adhesion Science and Technology, 17* (10), 1299-1320.

Cech, V. (2007). Plasma-polymerized organosilicones as engineered interlayers in glass fiber/polyester composites. *Composite Interfaces, 14* (4), 321–334.

Cech, V., Prikryl, R., Balkova, R., Grycova, A., & Vanek, J. (2002). Plasma surface treatment and modification of glass fibers. *Composites Part A: Applied Science And Manufacturing, 33* (10), 1367–1372.

Cech, V., Studynka, J., Conte, N.,& Perina, V. (2007). Physico-chemical properties of plasma-polymerized tetravinylsilane. *Surface and Coatings Technology, 201* (9-11), 5512-5517.

Cokeliler, D., Erkut, S., Zemek, J., Biederman, H. & Mutlu, M. (2007). Modification of glass fibers to improve reinforcement: A plasma polymerization technique. *Dental Materials, 23* (3), 335–342.

Culler, S.R., Ishida, H., & Koenig, J.L. (1985). Structure of silane coupling agents adsorbed on silicon powder. *Journal of Colloid and Interface Science,106* (22), 334-346.

Daniel, I.M., & Ishai,O. (1994). *Engineering mechanics of composite materials* (1st ed.). Newyork: Oxford University Press.

Daniels, M.W., Sefcik, J., Francis, L.F., & McCormik, A.V. (1999). Reactions of a trifunctional silane coupling agent in the presence of colloidal silica sets in polar media. *Journal of Colloid and Interface Science, 219* (2), 351-356.

Denes, F., Nielsen, L.D., &Young, R.A. (1997). Cold plasma state—a new approach to improve surface adhesion in lignocellulosic-plastics composites. *Lignocellulosic-Plastic Composites,1,* 61–110.

DiBenedetto, A.T. (1985). Evaluation of fiber surface treatments in composite-materials. *Pure and Applied Chemistry, 57* (11), 1659-1665.

DiBenedetto, A.T. (2001). Tailoring of interfaces in glass fiber reinforced polymer composites: A review. *Materials Science and Engineering A, 302* (1), 74–82.

Feresenbet, E., Raghavan, D., & Holmes, G.A. (2003). The influence of silane coupling agent composition on the surface characterization of fiber and on fiber-matrix interfacial shear strength. *Journal of Adhesion, 79* (7), 643-665.

Gaur, S. & Vergason, G. (2000). Plasma polymerization: theory and practice. *43rd Annual -Technical Conference Proceedings,* 267-271.

González-Benito, J., Cabanelas, J.C., Aznar, A.J., Vigil, M.R., Bravo, J., & Baselga, J. (1996). Surface characterization of silanized glass fibers by labeling with environmentally sensitive fluorophores. *Journal of Applied Polymer Science, 62* (2), 375-384.

González-Benito, J. (2003). The nature of the structural gradient in epoxy curing at a glass fiber/epoxy matrix interface using FTIR imaging. *Journal of Colloid and Interface Science, 267* (2), 326-332.

González-Benito, J., Baselga, J., & Aznar, A.J. (1999). Microstructural and wettability study of surface pretreated glass fibres. *Journal of Materials Processing Technology*,92-93, 129-134.

Gulec, H.A., Sarıoglu, K., & Mutlu, M. (2006). Modification of food contacting surfaces by plasma polymerisation technique. Part I: Determination of hydrophilicity, hydrophobicity and surface free energy by contact angle method. *Journal of Food Engineering, 75* (2), 187–195.

Hamada, H., Fujihara, K., & Harada, A. (2000). The influence of sizing conditions on bending properties of continuous glass fiber reinforced polypropylene composites. *Composites Part A: Applied Science And Manufacturing, 31,* 979–990.

Hirai, Y., Hamada, H., & Kim, J. K. (1998). Impact response of woven glass fabric composites- I.Effect of fibre surface treatment. *Composite Science and Technology, 58,* 91-104.

Iler, R.K. (1979). *The chemistry of silica solubility, polymerization, colloid and surface properties, and biochemistry.* New York: Wiley.

Inagaki, N. (1996). *Plasma surface modification and plasma polymerization.* Lancaster Basel: Technomic Publishing Company.

Ishida, H., & Miller, J.D. (1984). Substrate effects on the chemisorbed and physisorbed layers of methacryl silane-modified particulate minerals. *Macromolecules, 17* (9), 1659-1666.

Ishida, H., & Koenig, J.L. (1978). Fourier transform infrared spectroscopic study of the structure of silane coupling agent on E-glass fiber. *Journal of Colloid and Interface Science, 64* (3), 565-576.

Iglesias, J.G., González-Benito, J., Aznar, A.J., Bravo, J., & Baselga, J. (2002). Effect of glass fiber surface treatments on mechanical strength of epoxy based composite materials. *Journal of Colloid and Interface Science., 250* (1), 251-260.

Jensen, R.E. (1999). *Investigation of waterborne epoxies for E-glass composites*. Doctoral Thesis. Blacksburg, Virginia.

Jokinen, A. E. E., Mikkola, P. J., Matisons, J. G., & Rosenholm, J. B. (1997). Treated glass fibers—Adsorption of an isocyanurate silane from CCl4. *Journal of Colloid and Interface Science, 196* (2), 207-214.

Jones, R. L., & Betz, D. (2004). The kinetics of corrosion of E-glass fibres in hydrochloric acid. *Journal of Materials Science, 39* (18), 5633-5637.

Jung, Y. C., & Bhushan, B. (2006). Contact angle, adhesion and friction properties of micro- and nanopatterned polymers for superhydrophobicity. *Nanotechnology, 17* (19), 4970-4980.

Kettle, A. P., Beck, A. J., O'Toole, L., Jones, F. R., & Short, R. D. (1997). Plasma polymerisation for molecular engineering of carbon-fibre surfaces for optimized composites. *Composites Science and Technology, 57* (8),1023–1032.

Kettle, A. P., Jones, F. R., Alexander, M. R, Short, R. D., Stollenwerk, M., Zabold, E., et al. (1998). Experimental evaluation of the interphase region in carbon fibre composites with plasma polymerised coatings. *Composites Part A: Applied Science And Manufacturing, 29* (3), 241–250.

Kim, J. K., & Mai, Y. W. (1998). *Engineered interfaces in fiber reinforced composites.* Oxford: Elsevier Science Ltd.

Kim, J. K., Sham, M. L., & Wu, J. S. (2001). Nanoscale characterisation of interphase in silane treated glass fibre composites. *Composites Part A: Applied Science And Manufacturing, 32* (5), 607-618.

Kollár, L. P., & Springer,G. S. (2003*). Mechanics of composite structures* (1 st ed.). USA: Cambridge University Press.

Lai, J. N., Sunderland, B., Xue, J. M., Yan, S., Zhao, W., Folkard, M., et al. (2006). Study on hydrophilicity of polymer surfaces improved by plasma treatment. *Applied Surface Science. 252* (10), 3375–3379.

Lenhart, J. L., Dunkers, J. P., Van Zanten, J. H., & Parnas, R. S. (2003). Characterization of sizing layers and buried polymer/sizing/substrate interfacial regions using a localized fluorescent probe. *Journal of Colloid and Interface Science, 257 (*2), 398–407.

Li, R., Ye, L., & Mai Y. W. (1997). Application of plasma technologies in fibre-reinforced polymer composites: a review of recent developments. *Composites Part A: Applied Science And Manufacturing, 28* (1), 73-86.

Lin, Y. S., Liao, Y. H., & Hu, C. H. (2009). Effects of N-2 addition on enhanced scratch resistance of flexible polycarbonate substrates by low temperature plasma-polymerized organo-silicon oxynitride. *Journal of Non-Crystalline Solids, 355* (3), 182–192.

Liu, Z., Zhao, F., & Jones, F. R. (2008). Optimising the interfacial response of glass fibre composites with a functional nanoscale plasma polymer coating. *Composites Science and Technology, 68* (15-16), 3161-3170.

Madhukar, M. S.,& Drzal, L. T. (1991). Fibre-matrix adhesion and its effect on composite mechanical properties: II. Longitudinal (0^o) and transverse (90^o)

tensile and flexure behavior of graphite/epoxy composites. *Journal of Composite Materials, 25* (8), 958-991.

Marks, D. J., & Jones, F. R. (2002). Plasma polymerised coatings for engineered interfaces for enhanced composite performance. *Composites Part A: Applied Science And Manufacturing, 33* (10), 1293–1302.

Matsuyama, H., Kariya, A., & Teramoto, M. (1994). Effect of siloxane chain lengths of monomers on characteristics of pervaporation membranes prepared by plasma polymerization. *Journal of Applied Polymer Science, 51* (4), 689-693.

Mazumdar, S. K. (2002). *Composites manufacturing- Materials, product, and process engineering.* Newyork: CRC Press.

Mehta, G., Drzal, L. T., Mohanty, A. K., & Misra, M. (2006). Effect of fiber surface treatment on the properties of biocomposites from nonwoven industrial hemp fiber mats and unsaturated polyester resin. *Journal of Applied Polymer Science, 99* (3), 1055-1068.

Mittal, K. L. (Ed.). (1992). *Silanes and other coupling agents*. The Netherlands: VSP.

Morales, J., Olayo, M. G., Cruz, G. J., Herrera-Franco, P., & Olayo, R. J. (2006). Plasma modification of cellulose fibers for composite materials. *Journal of Applied Polymer Science, 101* (6), 3821-3828.

Morra, M., Occhiello, E., & Garbassi, F. (1993). The effect of plasma-deposited siloxane coatings on the barrier properties of HDPE. *Journal of Applied Polymer Science, 48* (8),1331-1340.

Murphy, J. (2001). *Additives for plastics handbook* (2 nd ed.). Amsterdam: Elsevier.

Mwaikambo, L. Y., & Ansell, M. P. (2002). Chemical modification of hemp, sisal, jute, and kapok fibers by alkalization. *Journal of Applied Polymer Science, 84* (12), 2222-2234.

Nguyen, T., Byrd, E., Alshed, D., Aouadi K., & Chin, J. (1998). Water at the polymer/substrate interface and its role in the durability of polymer/glass fiber composites. *Durability of Fibre Reinforced Polymer (Frp) Composites For Construction (CDCC'98), 1st International Conference*, 451-462.

Nishiyama, N., Schick, R., & Ishida, H. (1991). Adsorption behavior of a silane coupling agent on colloidal silica studied by gel permeation chromatography. *Journal of Colloid and Interface Science, 143* (1), 146-156.

Norström, A. E. E., Mikkola, P. J., Matisons, J. G., & Rosenholm, J. B. (2000). Adsorption of an isocyanurate silane on E-glass fibers from ethanol and toluene. *Journal of Colloid And Interface Science, 232* (1), 149–155.

Noobut, W., & Koenig, J.L. (1999). Interfacial behavior of epoxy/E-glass fiber composites under wet-dry cycles by fourier transform infrared microspectroscopy. *Polymer Composites, 20* (1), 38-47.

Park, S. J., & Jin, J. S. (2003). Effect of silane coupling agent on mechanical interfacial properties of glass fiber-reinforced unsaturated polyester composites. *Journal of Polymer Science Part B-Polymer Physics,41* (1), 55-62.

Park, S. Y., & Kim, N. J. (1990). Mechanism and kinetics of organosilicon plasma polymerization. *Applied Polymer Symposia Series, 46,* 921-108.

Hsu, J. P. (Ed.). (1999). *Interfacial forces and fields: theory and applications*. New York: Dekker.

Park, S. J., & Jin, J. S. (2001). Effect of silane coupling agent on interphase and performance of glass fibers/unsaturated polyester composites. *Journal of Colloid and Interface Science, 242 (1),* 174-179.

Park, S. J., Jin, J. S., & Lee, J. R. (2000). Influence of silane coupling agents on the surface energetics of glass fibers and mechanical interfacial properties of glass fiber-reinforced composites. *Journal of Adhesion Science and Technology, 14* (13), 1677-1689.

Park, R., & Jang, J. (2004). Effect of surface treatment on the mechanical properties of glass fiber/vinylester composites, Journal of Applied Polymer Science, 91, 3730–3736.

Pavlidou, S., Krassa, K., & Papaspyrides, C. D. (2005). Woven glass fabric/polyester composites: Effect of interface tailoring on water absorption. *Journal of Applied Polymer Science, 98* (2), 843-851.

Piggott, M.R. (1997). Why interface testing by single-fibre methods can be misleading. Composites Science and Technology, 57 (8), 965-974.

Plueddemann, E. P. (Ed.). (1974*). Interfaces in polymer matrix composites.* New York: Academic Press.

Prikryl, R., Cech, V., Balkova, R., & Vanek, J. (2003). Functional interlayers in multiphase materials. Surface and Coatings Technology, 173 –174, 858–862.

Prikryl, R., Cech, V., Kripal, L., & Vanek, J. (2005). Adhesion of pp-VTES films to glass substrates and their durability in aqueous environments. *International Journal of Adhesion and Adhesives, 25* (2), 121-125.

Qiu, Q., & Kumosa, M. (1997). Corrosion of E-glass fibers in acidic environments. *Composites Science and Technology, 57* (5), 497-507.

Radeva, E., Tsankov, D., Bobev, K., & Spassov, L. (1993). Fourier-transform infrared analysis of hexamethyldisiloxane layers obtained in low frequency glow discharge. *Journal of Applied Polymer Science, 50* (1), 165-171.

Rot, K., Huskić, M., Makarovič, M., Ljubič Mlakar, T., & Žigon, M. (2001). Interfacial effects in glass fibre composites as a function of unsaturated polyester resin composition. Composites Part A: Applied Science And Manufacturing, 32 (3-4), 511-516.

Sakata, J., Yamamoto, M., & Hirai, M. (1986). Plasma polymerized membranes and gas permeability. *Journal of Applied Polymer Science, 31* (7), 1999–2006.

Saidpour, S. H., Richardson, M. O. W. (1997). Glass fibre coating for optimum mechanical properties of vinyl ester composites. *Composites Part A: Applied Science And Manufacturing. 28* (11), 97l-975.

Sheikh-Ahmad, J. Y. (2009). *Machining of polymer composites.* Newyork : Springer Science+Business Media.

Shih, G. C., & Ebert, L. J. (1986). Flexural failure mechanisms and global stress plane for unidirectional composites subjected to 4-point bending tests. *Composites, 17* (4), 309-320.

Shishoo, R. (Ed.). (2007). *Plasma technologies for textiles.* Cambridge: Woodhead Publishing Limited.

Sterman, S., & Bradley, H. B. (1961). A new interpretation of the glass-coupling agent surface through use of electron microscopy. *Polymer Engineering and Science, 1* (4), 224-233.

Tanaka, H., Kuraoka, K., Yamanaka, H., & Yazawa, T. J. (1997). Development and disappearance of microporous structure in acid treated E-glass fiber. *Journal of Non- Crystalline Solids, 215* (2–3), 262-270.

Tanoglu, M., McKnight, S. H., Palmese, G. R., & Gillespie, J. W. (2001). Dynamic stress/strain response of the interphase in polymer matrix composites. *Polymer Composites, 22* (5), 621-635.

Tanoglu, M., McKnight, S. H., Palmese, G. R., & Gillespie Jr., J. W. (2001). The effects of glass-fiber sizings on the strength and energy absorption of the fiber/matrix interphase under high loading rates. Composites Science and Technology, 61 (2), 205-220.

Vandenberg, E.T., Bertilsson, L., Liedberg, B., Uvdal, K., Erlandsson, R., Elwing, H., & Lundström, I. (1991). Structure of 3-aminopropyl triethoxy silane on silicon oxide. Journal of Colloid and Interface Science, 147, 103-118.

Van Der Voort, P., Gillis-D'Hamers, I., Vrancken, K. C., & Vansant, E. F. (1991). Effect of porosity on the distribution and reactivity of hydroxyl groups on the surface of silica gel**.** *Journal of the Chemical Society, Faraday Transactions, 87* (24), 3899-3905.

Vasiliev, N. V., & Morozov, E. V. (2007). *Advanced mechanics of composite materials,* The Netherlands: Elsevier Science Ltd.

Wang, T. W. H., Blum, F. D., & Dharani, L. R. (1999). Effect of interfacial mobility on flexural strength and fracture toughness of glass/epoxy laminates. *Journal of Materials Science, 34* (19), 4873-4882.

Xu, Z., Huang, Y., Zhang, C., Liu, L., Zhang, Y., & Wang, L. (2007). Effect of γ-ray irradiation grafting on the carbon fibers and interfacial adhesion of epoxy composites. *Composites Science and Technology, 67* (15,16), 3261–3270.

Yoshinaga, K., Yoshida, H., Yamamoto, Y., Takakura, K., & Komatsu, M. (1992). A convenient determination of surface hydroxyl group on silica-gel by conversion of silanol hydrogen to dimethylsilyl group with diffuse reflectance ftır spectroscopy . *Journal of Colloid and Interface Science, 153* (1), 207-211.

Yuan, X., Jayaraman K. & Bhattacharyya, D. (2004). Mechanical properties of plasma-treated sisal fibre-reinforced polypropylene composites. *Journal of Adhesion Science and Technology, 18* (9), 1027–1045.

Yuan, X., Jayaraman, K., & Bhattacharyya, D. (2004). Effects of plasma treatment in enhancing the performance of woodfibre-polypropylene composites, *Composites Part A: Applied Science And Manufacturing, 35* (12), 1363–1374.

Yue, C.Y., & Padmanabhan, K. (1999). Interfacial studies on surface modified Kevlar fibre epoxy matrix composites. *Composites Part B-Engineering, 30* (2), 205–217.

Zhandarov, S, & Mäder, E. (2005). Characterization of fiber/matrix interface strength: Applicability of different tests, approaches and parameters. *Composites Science And Technology, 65* (1), 149–160.

Zhao, F. M.,& Takeda, N. (2000). Effect of interfacial adhesion and statistical fiber strength on tensile strength of unidirectional glass fiber/epoxy composites. Part I: experiment results. *Composites Part A: Applied Science And Manufacturing, 31,*1203–1214.

Zhou, X. F., Wagner, H. D., & Nutt, S. R. (2001). Interfacial properties of polymer composites measured by push-out and fragmentation tests. *Composites Part A: Applied Science And Manufacturing, 32* (11), 1543-1551.

Zuri, L., Silverstein, M., & Narkis, M. (1996). Organic-inorganic character of plasma polymerized hexamethyldisiloxane. *Journal of Applied Polymer Science, 62* (12), 2147-2154.